การสังเคราะห์และสมบัติเชิงแสงของเอซา-โบดิพี-พอร์ไฟริน

นางสาวจริยา กาหยี



วิทยานิพนธ์นี้เป็นส่วนหนึ่งของการศึกษาตามหลักสูตรปริญญาวิทยาศาสตรมหาบัณฑิต
สาขาวิชาเคมี ภาควิชาเคมี
คณะวิทยาศาสตร์ จุฬาลงกรณ์มหาวิทยาลัย
ปีการศึกษา 2558

# SYNTHESIS AND OPTICAL PROPERTIES OF AZA-BODIPY-PORPHYRIN

Miss Jariya Kayee


A Thesis Submitted in Partial Fulfillment of the Requirements

for the Degree of Master of Science Program in Chemistry

Department of Chemistry

Faculty of Science

Chulalongkorn University

Academic Year 2015

| | |
|---|---|
| Thesis Title | SYNTHESIS AND OPTICAL PROPERTIES OF AZA-BODIPY-PORPHYRIN |
| By | Miss Jariya Kayee |
| Field of Study | Chemistry |
| Thesis Advisor | Assistant Professor Worawan Bhanthumnavin, Ph.D. |

Accepted by the Faculty of Science, Chulalongkorn University in Partial Fulfillment of the Requirements for the Master's Degree

.....Dean of the Faculty of Science
(Associate Professor Polkit Sangvanich, Ph.D.)

THESIS COMMITTEE

.....Chairman
(Associate Professor Vudhichai Parasuk, Ph.D.)

.....Thesis Advisor
(Assistant Professor Worawan Bhanthumnavin, Ph.D.)

.....Examiner
(Assistant Professor Yongsak Sritana-anant, Ph.D.)

.....External Examiner
(Assistant Professor Tienthong Thongpanchang, Ph.D.)

จริยา กาหยี : การสังเคราะห์และสมบัติเชิงแสงของเอซา-โบดิพี-พอร์ไฟริน (SYNTHESIS AND OPTICAL PROPERTIES OF AZA-BODIPY-PORPHYRIN) อ.ที่ปรึกษาวิทยานิพนธ์หลัก: ผศ. ดร.วรวรรณ พันธุมนาวิน, 75 หน้า.

ในงานวิจัยนี้ได้ทำการสังเคราะห์พอร์ไฟรินที่เชื่อมต่อกับโบดิพี โดยสามารถสังเคราะห์พอร์ไฟรินที่มีหมู่แอลไคน์อยู่ที่ตำแหน่งมีโซ (สาร 3) ซึ่งมีค่าการดูดกลืนแสงที่ดีในช่วง Soret หรือ B band ที่ความยาวคลื่น 451 นาโนเมตร และมีค่าการดูดกลืนแสงน้อยในช่วง Q band ที่ความยาวคลื่น 596 และ 641 นาโนเมตร เนื่องจากพอร์ไฟรินดูดกลืนแสงได้น้อยในช่วงแสงสีเขียว (500-600 นาโนเมตร) ในทางตรงกันข้ามพบว่าเอซา-โบดิพี (สาร 10) สามารถดูดกลืนแสงได้ดีในช่วงแสงสีเขียว (665 นาโนเมตร) ดังนั้นเมื่อทำการเชื่อมต่อพอร์ไฟริน (สาร 3) เข้ากับเอซา-โบดิพี (สาร10) จะได้ผลิตภัณฑ์ที่ช่วยเพิ่มการดูดกลืนแสงในช่วงดังกล่าวได้ โดยผลิตภัณฑ์ที่สังเคราะห์ขึ้น สามารถพิสูจน์เอกลักษณ์ทางโครงสร้างโดยอาศัยเทคนิคโปรตอนเอ็นเอ็มอาร์สเปกโทรสโกปี คาร์บอนเอ็นเอ็มอาร์สเปกโทรสโกปี มัลดิทอฟแมสสเปกโทรเมทรี และเทคนิคอินฟราเรดสเปกโทรสโกปี นอกจากนี้ยังได้ทำการวิเคราะห์สมบัติทางกายภาพเชิงแสง โดยเทคนิคยูวี-วิซิเบิลสเปกโทรสโกปี และเทคนิคฟลูออเรสเซนต์สเปกโทรสโกปี



ภาควิชา เคมี ลายมือชื่อนิสิต .....

สาขาวิชา เคมี ลายมือชื่อ อ.ที่ปรึกษาหลัก .....

ปีการศึกษา 2558

# # 5671920023 : MAJOR CHEMISTRY

KEYWORDS: AZA-BODIPY / PORPHYRIN / DYE SENSITIZED SOLAR CELL

JARIYA KAYEE: SYNTHESIS AND OPTICAL PROPERTIES OF AZA-BODIPY-PORPHYRIN. ADVISOR: ASST. PROF. WORAWAN BHANTHUMNAVIN, Ph.D., 75 pp.

In this work, a porphyrin-BODIPY conjugated system has been designed and synthesized. The *meso*-alkyne-linked porphyrin zinc complex precursor (3) has been successfully synthesized. The compound showed strong Soret or B band absorption at about 451 nm. Other absorptions are weak absorption bands (the Q band) at 596 and 641 nm. Due to the fact that porphyrin systems usually do not absorb light in the green region (500-600 nm), 2-Bromo-4,4-difluoro-1,7-bis(4-dodecyloxyphenyl)-3,5-diphenyl-4-bora-3a,4a,8-triaza-*s*-indacene (10) which can absorb light in the green region (665 nm) has been connected to the precursor 3 in order to increase absorbance in that region. All synthesized compounds were characterized by $^{1}$H NMR spectroscopy, $^{13}$C NMR spectroscopy, MALDI-TOF mass spectrometry and IR spectroscopy. Their photophysical properties were investigated by UV-visible spectroscopy and fluorescence spectroscopy.



Department: Chemistry Student's Signature .....

Field of Study: Chemistry Advisor's Signature .....

Academic Year: 2015

# ACKNOWLEDGEMENTS

I am heartily thankful to my advisor Assistant Professor Dr. Worawan Bhanthumnavin for kindness, invaluable guidance, excellent supervision, encouragement, personal friendship and support from the initial to the final stage enabling me to develop an understanding of my thesis. This research is impossible to succeed without her advice. In addition, sincere appreciation is also extended to Associate Professor Dr. Vudhichai Parasuk, Assistant Professor Dr. Yongsak Sritana-anant, and Assistant Professor Dr. Tienthong Thongpanchang, for acting as the chairman and examiners of my thesis committee, and for their valuable constructive comments and suggestions.

Furthermore, I would like to take this opportunity to express my appreciation to the Graduate School, Chulalongkorn University for granting me a financial support “Science Achievement Scholarship of Thailand (SAST)” to study and research during 2013-2015.

Finally, I also express my heartfelt gratitude towards my family who constantly present their love, care, understanding, encouragement, and overwhelming support throughout my life. This thesis would not have been possible without their supports.

**CONTENTS**

Page

Page

Page

# LIST OF FIGURES

**Figure** **Pages**

# LIST OF SCHEMES

**Scheme** **Pages**

# LIST OF TABLES

**Table** **Pages**

# LIST OF ABBREVIATIONS

| | |
|---|---|
| BuOH | butanol |
| cm | centimeter |
| $\delta$ | chemical shift |
| *J* | coupling constant |
| $^{o}C$ | degree celsius |
| $CDCl_3$ | deuterated chloroform |
| DCM | dichloromethane |
| d | doublet (NMR) |
| dd | doublet of doublet (NMR) |
| ddd | doublet of doublet of doublets (NMR) |
| DSSC | dye sensitized solar cell |
| EtOH | ethanol |
| EtOAc | ethyl acetate |
| g | gram |
| Hz | hertz |
| h | hour |
| m/z | mass per charge ratio |
| MALDI-TOF-MS | matrix assisted laser desorption ionization time-of-flight mass spectrometry |
| MHz | megahertz |
| MeOH | methanol |
| mg | milligram |

| | |
|---|---|
| mL | milliliter |
| mmol | millimole |
| min | minute |
| mol | mole |
| $[M]^+$ | molecular ion |
| m | multiplet (NMR) |
| nm | nanometer |
| NBS | *N*-bromosuccinimide |
| DIPEA | *N*,*N*-diisopropylethylamine |
| NMR | nuclear magnetic resonance |
| ppm | part per million |
| % | percent |
| rt | room temperature |
| s | singlet (NMR) |
| THF | tetrahydrofuran |
| TLC | thin layer chromatography |
| TEA | triethylamine |
| TMS | trimethylsilyl |
| t | triplet (NMR) |
| UV | ultraviolet |
| λ | wavelength |

# CHAPTER I

# INTRODUCTION

## 1.1 Porphyrins

Porphyrins belong to a class of naturally occurring planar aromatic macrocycles which compose of four pyrrole units connected to each other at the $\alpha$-carbon atoms with methine (=CH-) bridges. The structure of porphyrin is shown in **Figure 1.1**.

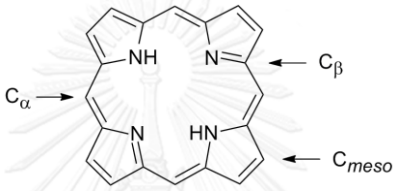


**Figure 1.1** The structure of porphyrin.

The word "porphyrin" is derived from a Greek word "porphura" which means purple [1]. On account of their large $\pi$-conjugated system, porphyrin typically has a very intense absorption band in the visible region. Moreover, these compounds always appear deeply colored. Although there is a total of 22 conjugated $\pi$-electrons inside the porphyrin macrocycle, only 18 electrons are found to actually participate in the delocalization pathway, which is consistent with Hückel's [4n+2] rule for aromaticity, where n = 4. The different 18 electrons delocalization pathways are shown in **Figure 1.2**.

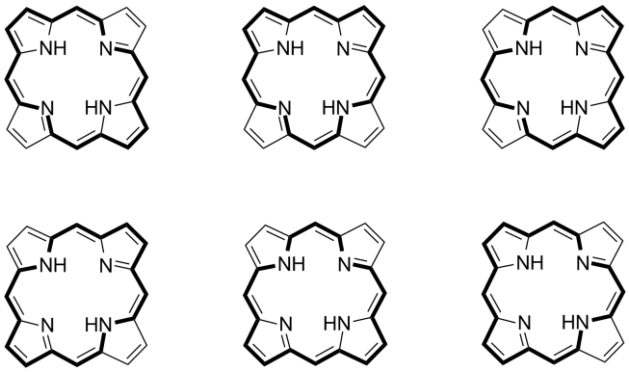


**Figure 1.2** The delocalization of porphyrins, the six possible canonical forms.

Porphyrin shows important roles in many biological systems. Complexes of many metal ions with various porphyrins are employed in specific purposes. Magnesium porphyrin complex is found in chlorophyll which is abundant in green plants as photosynthetic reaction centers which convert light energy into chemical energy while producing oxygen along the way. Iron porphyrin complexes are found in hemoglobin and cytochrome C which is responsible for oxygen transport and as a single electron transporter in a redox catalytic reaction [2], respectively (**Figure 1.3**) .

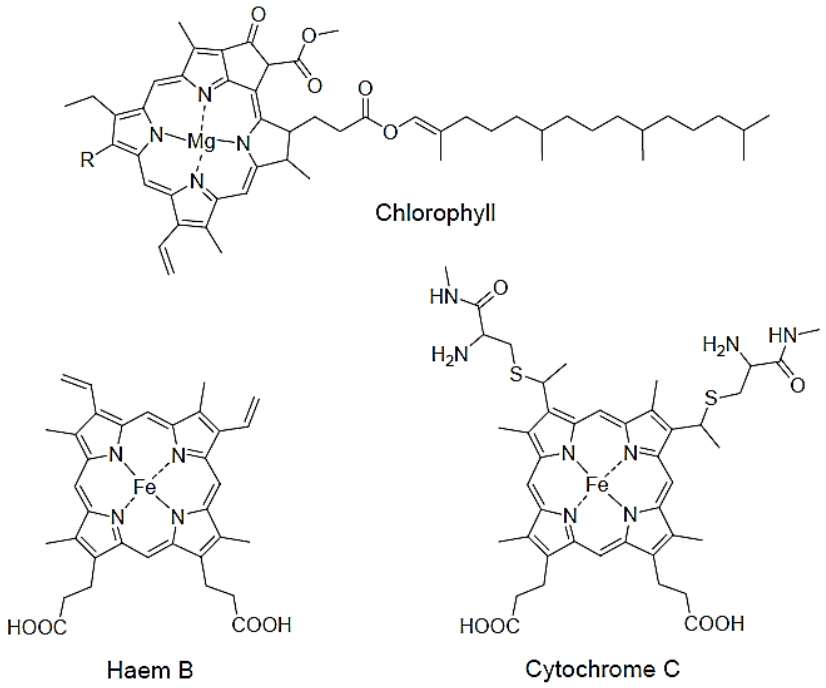


**Figure 1.3** Structures of some naturally occurring porphyrins.

### 1.1.1 Structure and nomenclature of porphyrin

Porphyrin is a tetrapyrrolic macrocyclic system consisting of all together four pyrrole units that are linked between their $\alpha$-positions *via* methane bridges. The first system of nomenclature for porphyrin was created by Hans Fischer. In this numbering system, the pyrrolic positions are numbered from 1 to 8 and the bridging positions named $\alpha$, $\beta$, $\gamma$, and $\delta$. Fischer's system is straightforward for naming simple porphyrins (**Figure 1.4**). However, as the complexity of a porphyrin derivative increases, the system becomes too complicated and naming can become contradictory. A new systematic nomenclature was introduced which numbered all the atoms in the

macrocycle and cut down on the number of trivial names. The inability of the Fischer's system to name the large number of synthetic and newly isolated porphyrin led to the adoption of a systematic nomenclature based on 1-24 numbering system which is developed by a joint commission on biochemical nomenclature, consisting of the International Union of Pure and Applied Chemistry (IUPAC) and the International Union of Biochemistry (IUB).

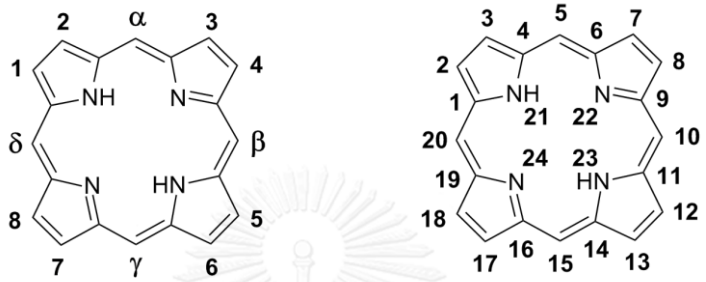


**Figure 1.4** Structure and nomenclature of porphyrin in Fischer's system relative to IUPAC system

The 1-24 numbering system is adopted for the porphyrin nucleus. The $\alpha$-positions are numbered 1, 4, 6, 9, 11, 14, 16, 19 and the $\beta$-positions are numbered 2, 3, 7, 8, 12, 13, 17, and 18, while the 5, 10, 15, and 20 positions have been referred to generically as "*meso*-position" (**Figure 1.4**). However, in order to avoid possible ambiguity with stereochemical designations, the use of these generic terms is discouraged.

### 1.1.2 Photophysical properties of porphyrin

Porphyrin and their related derivatives have an extensive system of delocalized $\pi$ electrons, hence these macrocyclic compounds display interesting and extraordinary photophysical properties, especially as shown in their UV-visible absorption and fluorescence emission spectra.

Normally, porphyrin and derivatives consist of a strong transition to the second excited state ($S_0 \rightarrow S_2$) called the Soret or B band at about 400 nm. Another

transition is from a weak transition to the first excited state ($S_0 \rightarrow S_1$), resulting in several absorption bands between 500-700 nm called the Q band (**Figure 1.5**) [3].

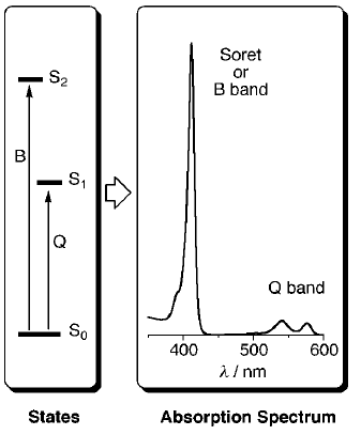


**Figure 1.5** The four Gouterman molecular orbitals explain the absorption spectra of simple porphyrins [3].

### 1.1.3 Synthesis of porphyrin

Porphyrin has been synthesized by various routes depending on the types of the substituents on the porphyrin ring. The routes employed generally become more elaborated as the number of different substituents increases. However, all of the synthetic routes of porphyrin can be divided into four fundamental types based on the number of pyrrolic subunits in starting materials: monopyrrolic, dipyrrolic, tripyrrolic, and tetrapyrrolic intermediates.

Monopyrrole tetramerization is the simplest synthetic strategy to porphyrins. Several methods relying on this strategy were discovered and developed in many ways. The easiest porphyrin to synthesize is tetraphenylporphyrin (TPP). One simply needs to react pyrrole with benzaldehyde under acidic conditions. The route was first reported by Rothemund [4, 5], who preferred to carry out the reaction in sealed glass tubes at high temperature (**Scheme 1.1**).

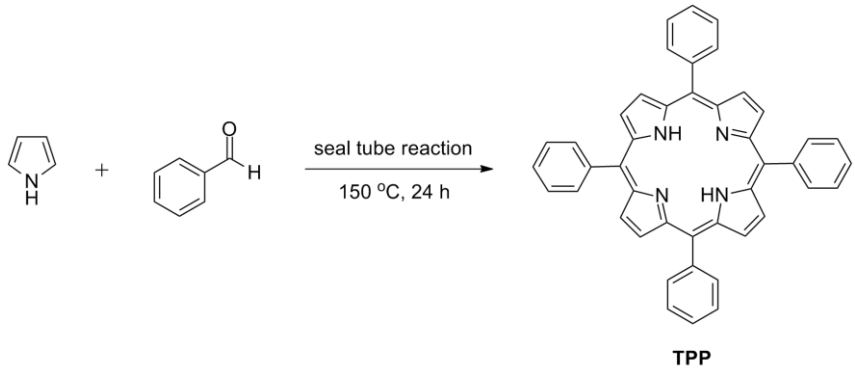


**Scheme 1.1** The synthetic route used to synthesize TPP by Rothemund.

Afterwards, a modification reported by Adler, Longo, and their coworkers [6] afforded the tetraphenylporphyrin (TPP) in 20-25% from a condensation of pyrrole and benzaldehyde in the presence of refluxing propionic acid instead.(**Scheme 1.2**).

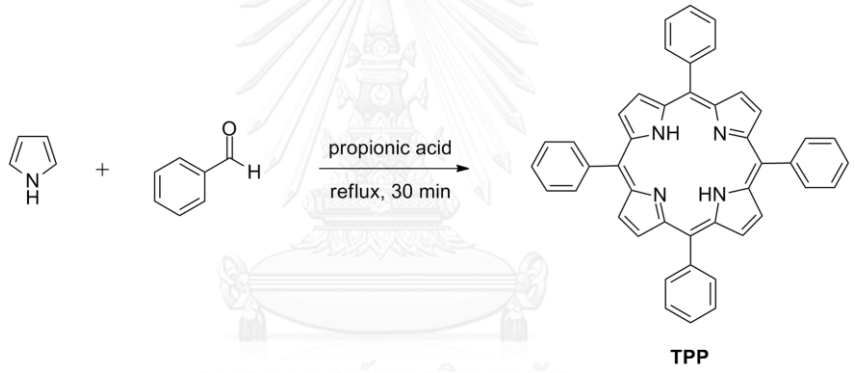


**Scheme 1.2** The synthetic route used to synthesize TPP by Adler, Longo and their coworkers.



The synthesis was finally optimized by Lindsey's group [7], which showed that excellent yields of a wide variety of tetraarylporphyrins can be afforded. The porphyrins can be obtained a two step reaction between aryl aldehydes and pyrrole. In the first step, the acid catalyst condensation reaction is carried out in the presence of a lewis acid catalyst, usually $BF_3{\cdot}OEt_2$ or TFA, to form tetraarylporphyrinogen. Following by the oxidation with a quinone derivative such as 2,3-dichloro-5,6-dicyanobenzoquinone (DDQ) in the second step (**Scheme 1.3**).

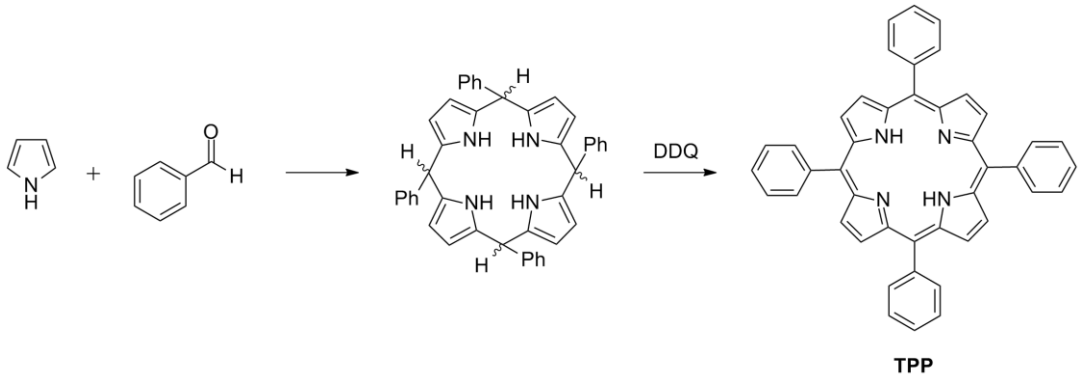


**Scheme 1.3** The synthetic route used to synthesize TPP by Lindsey's group.

### 1.2 Boron dipyrromethene or BODIPY

4,4-Difluoro-4-bora-3a,4a-diaza-*s*-indacene (boron dipyrromethene or BODIPY) dyes tend to show strong UV-absorption and emission near 500 nm, high fluorescence quantum yields, high molar extinction coefficients, and excellent photostability. BODIPY dyes are useful materials that have been proposed for applications in biological sensing [8, 9], fluorescent switches [10-12], chemosensors [13], and energy light harvesting [14, 15].

The IUPAC numbering system for BODIPY dyes as shown in **Figure 1.6**. The $\alpha$-positions are numbered 3, 5 and the $\beta$-positions are numbered 1, 2, 6 and 7, while the 8 position has been referred to generically as *meso*-position.

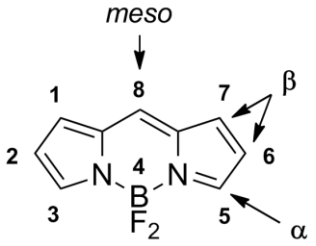


**Figure 1.6** The structure of boron dipyrromethene (BODIPY).

BODIPY dyes were first discovered in 1968 by Treibs and Kreuzer [16]. BODIPY has no substituents (**Scheme 1.4**). Afterward, Lindsey and co-workers [17] developed a route of BODIPY synthesis that bearing aryl substituent at the *meso*-position in

1996. In the recent times, the chemistry of BODIPYs has grown exponentially because of their excellent properties and their wide variety of applications.

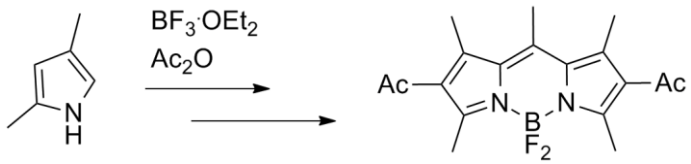


**Scheme 1.4** The synthetic route used to synthesize BODIPY by Treibs and Kreuzer.

Typically, BODIPY is formed from the complexation of a dipyrromethene ligand with a disubstituted boron moiety, usually in the form of $BF_2$, achieved using boron trifluoride diethyl etherate. The dipyrromethene ligand is formed from the linking of the $\alpha$-position of two pyrroles via a methane bridge.

### 1.3 Aza-dipyrromethene or aza-BODIPY

Aza-BODIPY is a structural analog of BODIPY (**Figure 1.7**). Replacement of the *meso* carbon in the BODIPY core by a nitrogen atom (two pyrrole rings linked via a nitrogen atom). Aza-BODIPYs are near-infrared fluorophores with remarkable spectral properties such as large fluorescent quantum yields above 700 nm and large extinction coefficients. Aza-BODIPY has also found applications as photosensitizers for photodynamic therapy [18, 19], NIR fluorescent probes, chemosensors [20-22] and dye sensitized solar cell [23-26].

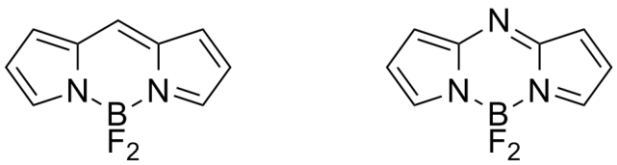


**Figure 1.7** The structure of BODIPY and aza-BODIPY.

### 1.3.1 Synthesis of azadipyrromethene

Aza-dipyrromethene (aza-DIPY) was first reported in the 1940's [27-29] but the $BF_2$ chelated aza-dipyrromethene (aza-BODIPY) was first synthesized by Boyer *et al*. in 1993 [30]. Symmetrically substituted aza-BODIPY with aryl groups can be synthesized by a four step synthetic route (**Scheme**) [18]. The first step, the aldol condensation reaction of benzaldehyde and acetophenone to produce 1,3-diphenyl-2-propen-1-one (chalcone). The second step is a Michael addition of nitromethane to chalcone with diethylamine (DEA) as a base to give the 1,3-diphenyl-4-nitrobutan-1-one nitromethane. Subsequent treatment with ammonium acetate in either ethanol or butanol yielded tetraphenylazadipyrromethene. Finally, the $BF_2$ chelated aza-dipyrromethene is readily produced with boron trifluoride etherate ($BF_3{\cdot}OEt_2$) using diisopropylethylamine (DIEA) as a base in dichloromethane.

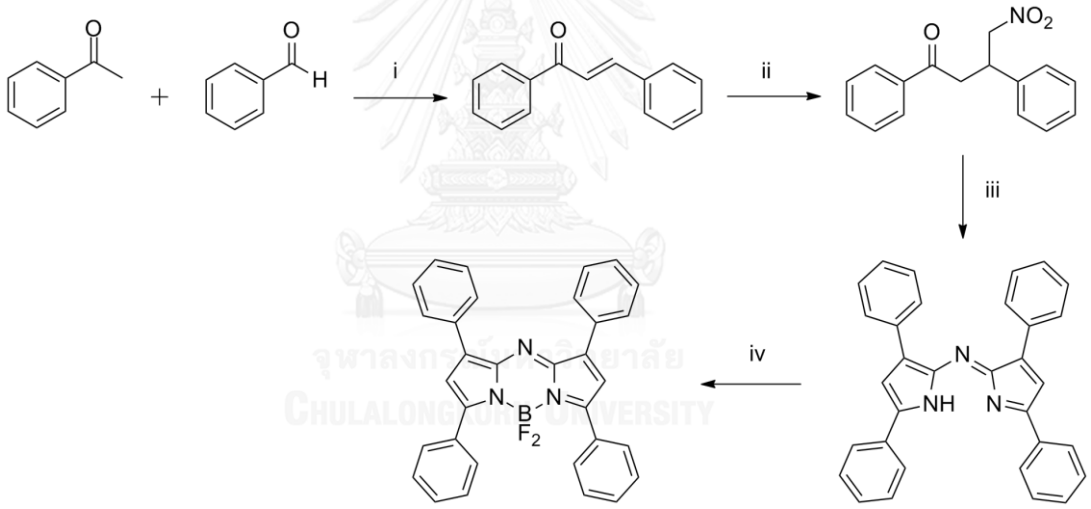


**Scheme 1.5** The synthetic route used to synthesize azadipyrromethene. Reagent and conditions: i) KOH, EtOH, rt, 24 h; ii) $CH_3NO_2$, diethylamine, MeOH, reflux, 24 h; iii) $NH_4OAc$, EtOH or BuOH, reflux, 1-48 h; iv) $BF_3{\cdot}OEt_2$, *N*,*N*-diisopropylethylamine, $CH_2Cl_2$, rt, 24 h.

### 1.3.2 Photophysical properties of azadipyrromethene

The absorption and emission properties of azadipyrromethene dyes can be geared towards longer wavelength if extension of the π-conjugation of the aza-BODIPY core is achieved. The absorption maxima of aza-BODIPY dyes span from 490 to 700 nm and their emission maxima span from 500 to 730 nm.

## 1.4 Dye sensitized solar cells (DSSCs)

The electricity generation capability of organic dyes have been known since late 1960s, the first attempt to converse of light into electricity from dye sensitized semiconductor film was from zinc oxide (ZnO) sensitized with Chlorophylls [31]. The first embodiment of Dye sensitized Solar Cell (DSSC) (**Figure 1.8**) was constructed by Gratzel *et al.* in 1988 [32].

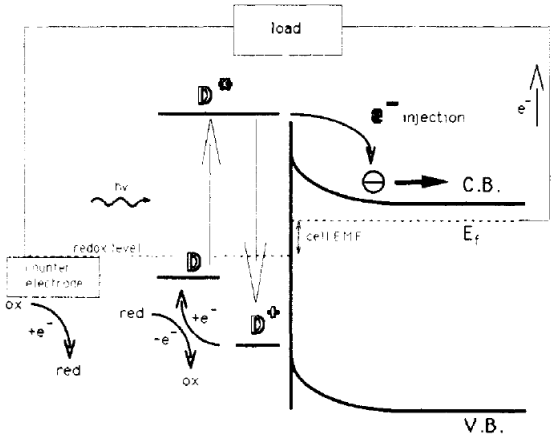


**Figure 1.8** Schematic illustration of a regenerative photoelectrochemical cell based on dye sensitization [32].

However, not until in 1991 the work of Grätzel and O'Regan [33], it was proven that DSSCs can be a feasible alternative energy source. It has one problem that is poor light harvesting (**Figure 1.9**).



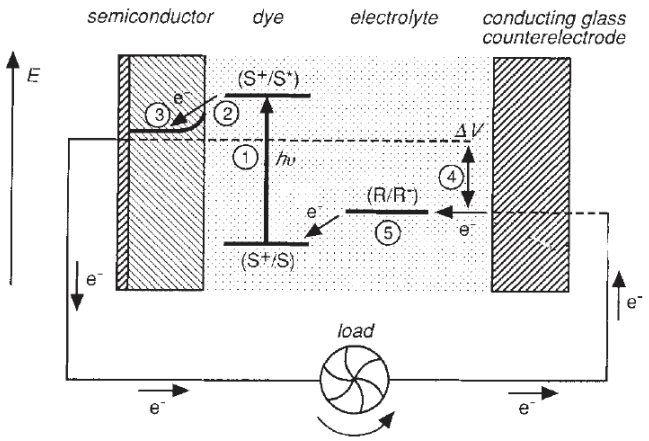


**Figure 1.9** Schematic representation of the principle of the dye-sensitized photovoltaic cell to indicate the electron energy level in the different phases.

In 2009, Greatzel and co-worker [34] have reported a new heteroleptic ruthenium sensitizer (**Figure 1.10**). This new dye exhibit an excellent light-harvesting capacity, greater than all of the heretofore-reported ruthenium dyes for DSSC that using a volatile liquid electrolyte exhibits an excellent conversion efficiency of 11.5%.

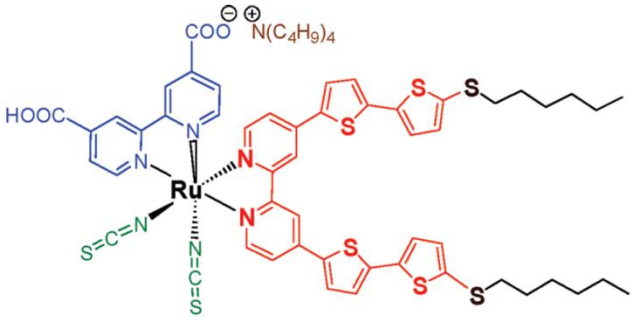


**Figure 1.10** The molecular structure of ruthenium complex.

Recently, Gratzel and co-worker [35] report mesoscopic solar cell that incorporate a Co-based electrolyte in conjunction with a custom synthesized donor-$\pi$-bridge-acceptor zinc porphyrin dyes as sensitizer (**Figure 1.11**) which lead to power conversion efficiency of 12.3%.

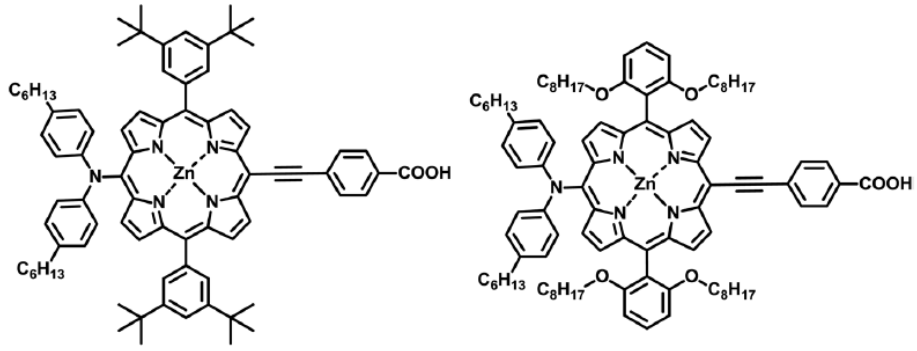


**Figure 1.11** The molecular structure of zinc porphyrin dyes.

## 1.5 Literature reviews

Porphyrin exhibits one strong Soret band and one or two Q band in 400-800 nm region. However, porphyrin exhibits poor absorption in the blue-green region (450-550 nm). One of the ways to improve the absorption properties of porphyrin in the blue-green region is linking them with chromophores that are strongly absorbing

in that region. Boron dipyrromethene (BODIPY) is highly fluorescent dyes with absorb strongly in blue-green region and has complementary properties with porphyrin.

Some of the BODIPY-porphyrin conjugates have also been incorporated into dye sensitized semiconductor solar cell to improve light harvesting ability of the photoelectrochemical cells. There are several reviews that treat exclusively either BODIPY or porphyrin.

Coutsolelos and co-workers [24] synthesized BODIPY-porphyrin, involving a cyanuric chloride bridging unit (**Figure 1.12**).

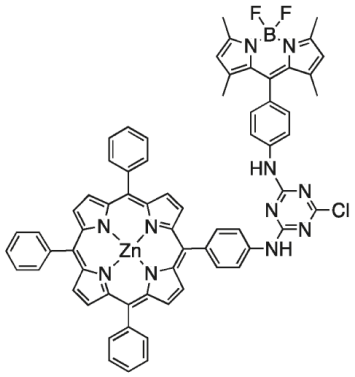


**Figure 1.12** The molecular structure of BODIPY porphyrin that linking via cyanuric chloride bridge.

The BODIPY unit increases the light-harvesting potential of the porphyrin chromophore excited state, as shown in the Jablonski diagram of **Figure 1.13**, excitation of BODIPY-based **π**- **π*** excited states is followed by energy transfer to the porphyrin-based singlet excited states. The energy transfer rates of BODIPY to porphyrin are faster than other BODIPY-porphyrin dyads with non-conjugated bridge.

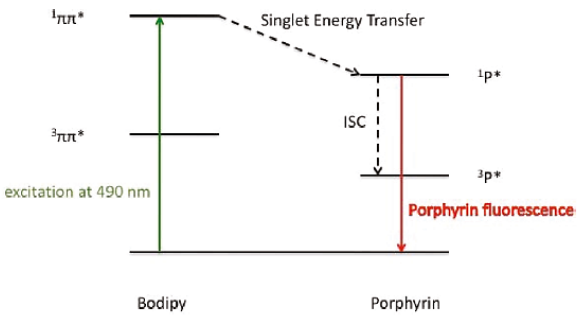


**Figure 1.13** Jablonski diagram relevant to the photophysics of BODIPY porphyrin that linking via cyanuric chloride bridge

Subsequently, Harvey and co-workers [36] synthesized *B*,*B*-diporphyrinbenzyloxy-BODIPY dyes (**Figure 1.14**) in high yields that exhibit good spectral overlap between the donor fluorescence (BODIPY) and acceptor absorption (porphyrin). The BODIPY dye as a good chromophore for the antenna and porphyrin as a good receptor.

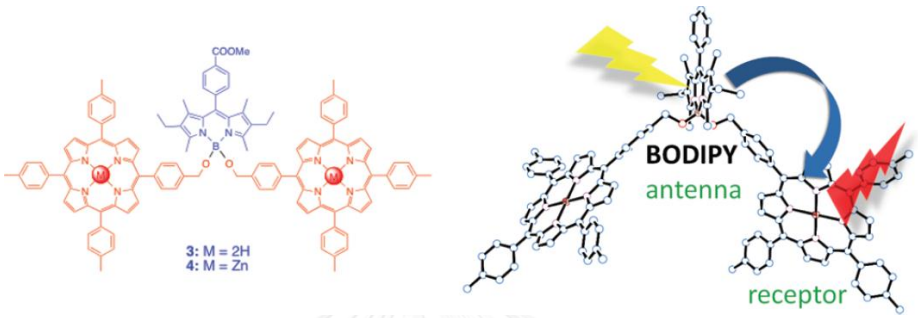


**Figure 1.14** The molecular structure of *B*,*B*-diporphyrinbenzyloxy-BODIPY dyes.

In 2011, the platinum benzoporphyrin connected to four units of BODIPY (Pt($^{BDP}$TPBP)) as show in **Figure 1.15** was synthesized by Thompson and co-workers [37].

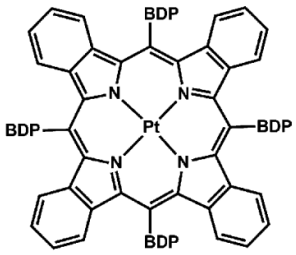


**Figure 1.15** The molecular structure of platinum benzoporphyrin bound to four BODIPY or Pt($^{BDP}$TPBP).

The UV-vis spectrum of Pt($^{BDP}$TPBP) complex was presented in **Figure 1.16**. The absorption spectra of Pt($^{BDP}$TPBP) complex is composite of platinum benzoporphyrin and BODIPY. Platinum benzoporphyrin exhibits the Soret band at 433 nm and Q band at 619 nm. Another one is BODIPY that exhibits a maximum wavelength at 514 nm.

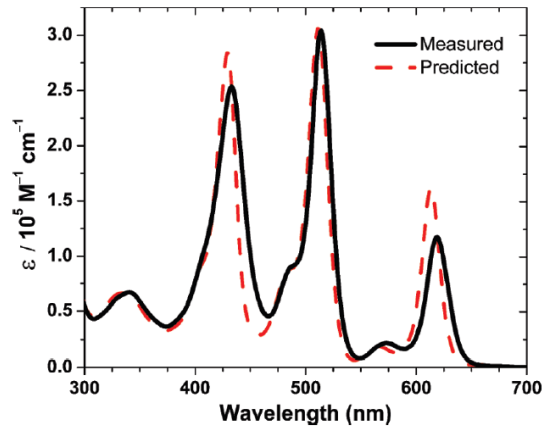


**Figure 1.16** The UV-vis spectrum of Pt($^{BDP}$TPBP).

In addition, Lee and Hupp [15] synthesized a zinc porphyrin-BODIPY dyad as shown in **Figure 1.17**. On the basis of absorption and fluorescence excitation, the spectra exhibited efficient energy transfer from the BODIPY to the zinc porphyrin.

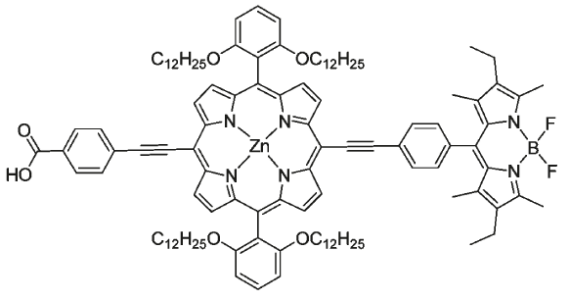


**Figure 1.17** The molecular structure of a zinc porphyrin-BODIPY.

The absorption spectra as shown in **Figure 1.18**. The BODIPY exhibits a maximum wavelength at 528 nm (black dash line), zinc porphyrin exhibits a Soret band at 457 nm and Q band at 586, 648 nm (blue dash line), and zinc porphyrin-BODIPY exhibits coverage absorption of zinc porphyrin and BODIPY (red solid line). In zinc porphyrin-BODIPY, BODIPY can act as an antenna light harvesting molecule to fill out of blue-green region of the spectrum where porphyrin does not absorb.

Moreover, the zinc porphyrin-BODIPY was applied to dye sensitized solar cell (DSSC) with improved power conversion efficiency ($\eta$ = 1.55%) compared to zinc porphyrin ($\eta$ = 0.84%).

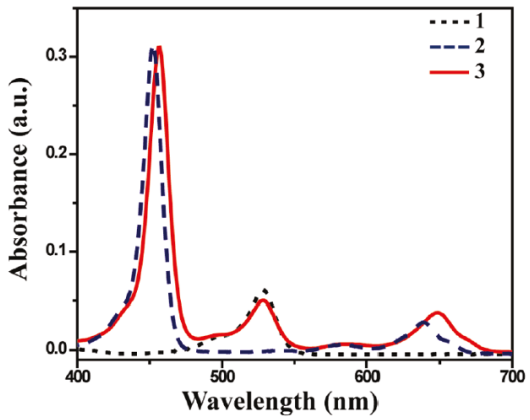


**Figure 1.18** The absorption spectra of BODIPY, zinc porphyrin, and zinc porphyrin-BODIPY.

It can be anticipated that a link between the porphyrin unit and aza-BODIPY units will yield compounds with UV-VIS absorption in a wider spectral range with relatively good molar absorptivity.

## 1.6 Objectives

In light of the aforementioned ideas, this research is aimed to synthesize aza-BODIPY-porphyrin systems, the general structure of which is illustrated in **Figure 1.19**. The structure consists of two light absorbing chromophores, namely the porphyrin core and the aza-BODIPY core linked by alkynyl bridges. One of the substituents on the porphyrin ring is a carboxyl group aimed to be used as an anchor to the $TiO_2$ surface of the DSSC system. All of the synthesized aza-BODIPY-porphyrin will be characterized by $^1$H NMR spectroscopy and MALDI-TOF mass spectrometry. Moreover, UV-visible absorption spectroscopy and fluorescence spectroscopy are also used to investigate their photophysical properties.

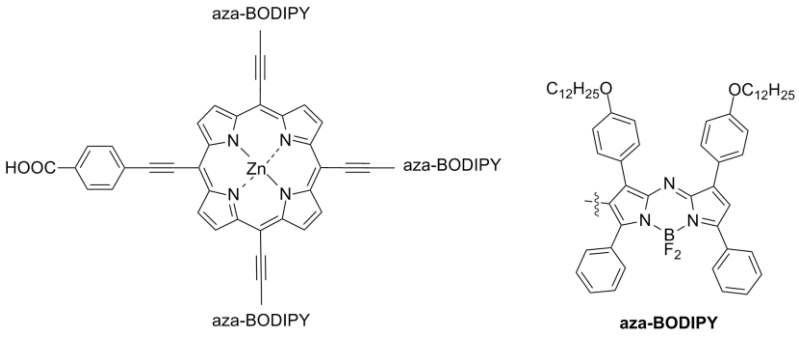


**Figure 1.19** The general structure of target molecule

# CHAPTER II

# EXPERIMENTAL

## 2.1 Materials and Chemicals

All reactions were performed in oven-dried glassware. The progress of the reactions and separation techniques of products by column chromatography were monitored by thin layer chromatography (TLC) performed on Merck D.C. silica gel 60 $F_{254}$ 0.2 mm precoated aluminium sheets and visualized using UV light (254 nm) or by dipping in a solution of potassium permanganate. Column chromatography was performed on Merck 70-230 mesh ASTM silica gel.

Solvents for reaction set ups including acetonitrile, 1-butanol, dichloromethane, 1,2-dichloroethane, ethanol, tetrahydrofuran (THF), and methanol were AR grade. Solvent used for extraction and column chromatography purification including dichloromethane, ethyl acetate, hexanes were commercial grade and were distilled before use.

All chemicals used in the reactions were reagent grade and were used as received without further purification. They were purchased from the following vendors:

- Aldrich Chemical Co., Inc. (Milwaukee, Wisconsin, USA): pyrrole, boron trifluoride diethyl etherate, 2,3-dichloro-5,6-dicyano-*p*-benzoquinone, 4-iodobenzoic acid, tris(dibenzylideneacetone)dipalladium (0)

- Carlo Erba Reagenti (Milan, Italy): potassium carbonate, potassium hydroxide, sodium chloride, sodium hydrogen carbonate, triethylamine, dichloroethane

- Fluka Chemical Corp. (Buchs, Switzerland): 1-bromododecane, ammonium acetate

- Labscan Asia Co., Ltd. (Bangkok, Thailand): acetonitrile, butanol, dichloromethane, ethyl acetate, chloroform, hexanes, acetone, tetrahydrofuran, *N*,*N*-dimethylformamide

- Merck Co., Ltd. (Darmstadt, Germany) : methanol, ethanol

- Sigma-Aldrich Chemical Co., Inc. (Steinheim, Germany) : acetophenone, nitromethane, diisopropylamine, zinc acetate dihydrate, tetrabutylammonium fluoride, copper(I) iodide, triphenylarsine, triphenylphosphine

- Tokyo Chemical Industry Co., Ltd. (Japan) : 3-trimethylsilylpropynal

- Acros Organic (New Jersey, USA) : 4-hydroxybenzaldehyde, *N*-bromosuccinimide

- Panreac Quimica Slu. (Barcelona, Spain) : magnesium sulfate

**2.2 Instruments and Equipments**

The weight of all chemical substances was determined on a Mettler Toledo AB204-S or a Precisa XT 220A electrical balance. Evaporation of solvents was carried out on a Büchi Rotavapor R-200 rotary evaporator equipped with a Büchi Heating Bath B-490, and a Büchi Recirculating Chiller B-740.

All reported $^{1}$H NMR data were recorded on a Varian Mercury NMR spectrometer at 400 MHz. $^{13}$C NMR and 2D NMR data were recorded on a Bruker NMR spectrometer at 100 MHz. The spectra were taken in chloroform-D. The chemical shifts ($\delta$) are reported in parts per million (ppm). Coupling constants (*J*) are proton-proton coupling and were reported in hertz (Hz). Multiplicities were abbreviated as followed: s = singlet, d = doublet, dd = doublet of doublet, t = triplet, m = multiplet and br = broad.

Mass spectroscopic data were obtained on a Bruker Microflex Matrix Assisted Laser Desorption Ionization Time-of-Flight Mass Spectrometer (MALDI-TOF-MS). The instrument was equipped with a nitrogen laser to desorb and ionize the samples. A stainless steel target was used as the substrate on which the samples were deposited. Samples were prepared as solutions in micromolar concentration in THF.

The FT-IR spectroscopic data were recorded on a Nicolet 6700 FT-IR spectrometer.

UV-visible spectroscopic data were measured in a 1 cm path length quartz cell using a Varian Cary 100 Bio UV-Visible Spectrophotometer. The deuterium and the visible lamps were used as light sources in this instrument. Fluorescence emission spectra were acquired using a Varian Cary Eclipse Fluorescence Spectrophotometer. The light source is a pulsed xenon lamp and the detector is a photomultiplier tube.

### 2.3 Synthesis of Porphyrin

The synthesis of [5,10,15,20-ethynylporphinato] zinc(II) (**3**) was conducted in 3 steps as shown in **Scheme 2.1**. First, pyrrole was reacted with aldehyde of 3-trimethylsilylpropynal *via* condensation. Next, the metallation was performed by using zinc (II) acetate, followed by desilylation.

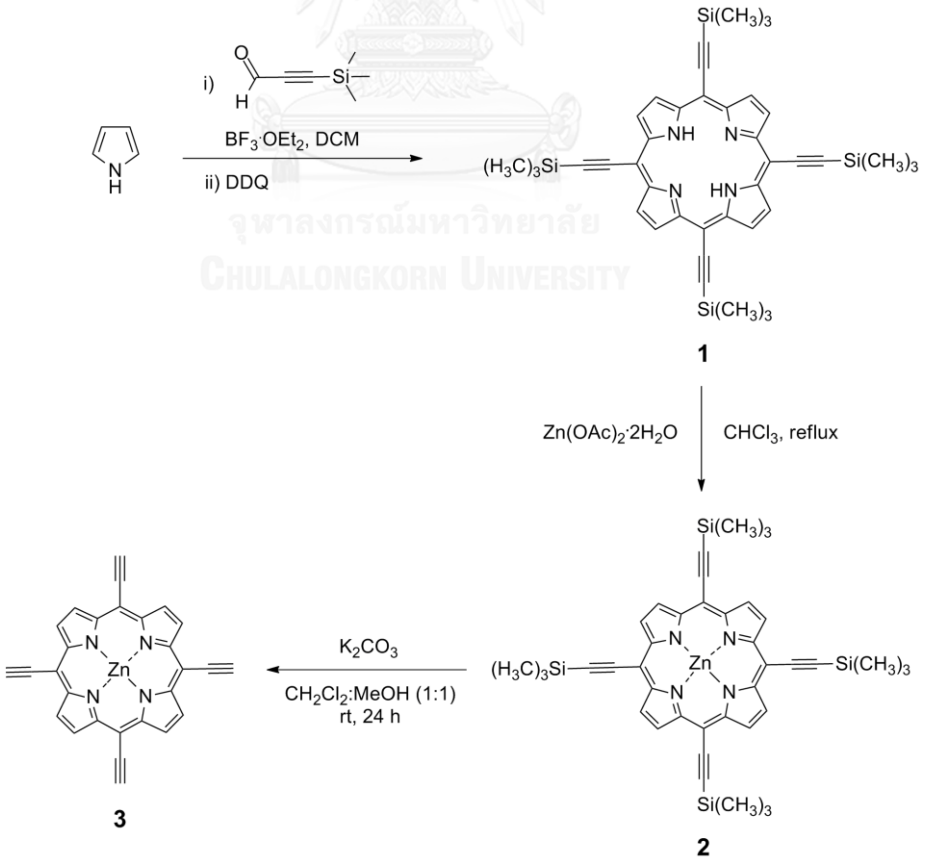


**Scheme 2.1** Synthetic route of [5,10,15,20-ethynylporphinato] zinc(II) (**3**)

### 2.3.1 Synthesis of 5,10,15,20-trimethylsilylethynylporphyrin (1)

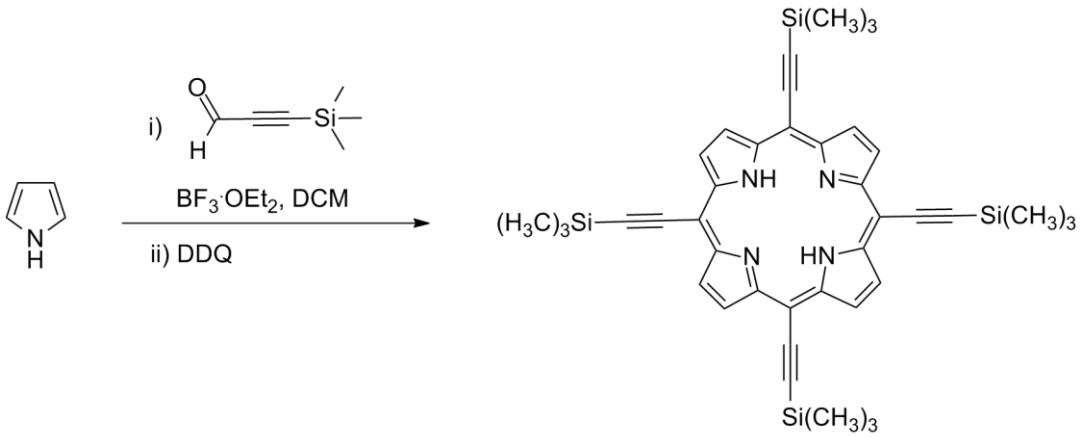


**1**

A method used was modified from that of Lee and Hupp's [15]. Pyrrole (0.07 mL, 1mmol) and 3-trimethylsilylpropynal (0.11 mL, 1 mmol) were dissolved in dichloromethane (60 mL). The reaction mixture was treated with boron trifluoride diethyl etherate (0.06 mL, 0.5 mmol) then cooled to 0 $^{\circ}$C. The ice bath was removed and the mixture was warm up to rt over 3 h. 2,3-Dichloro-5,6-dicyano-*p*-benzoquinone (0.2270 g, 1 mmol) in 2 mL of tetrahydrofuran was then added with continuous stirring for an additional 2 h. The reaction was then quenched by an addition of triethylamine and the stirring continued for an additional 30 min. The solution was concentrated under vacuum and passed through a short silica column using dichloromethane as eluent. The solvent was removed under reduced pressure to give 5,10,15,20-trimethylsilylethynylporphyrin (**1**) (31.7 mg, 5%) as a deep green solid. UV/vis (THF): $\lambda_{max}$ = 450, 566, 605, 648, 711 nm. Fluorescence (THF): $\lambda_{max}$ = 713, 798 nm. $^{1}$H NMR (400 MHz, $CDCl_3$) $\delta$ 7.10 (s, 8H), 1.25 (s, 36H). MALDI-TOF-MS : *m/z* $[M]^+$ calcd. for $C_{40}H_{46}N_4Si_4$: 695.162, Found: 695.598.

### 2.3.2 Synthesis of [5,10,15,20-trimethylsilylethynylporphinato] zinc(II) (2)

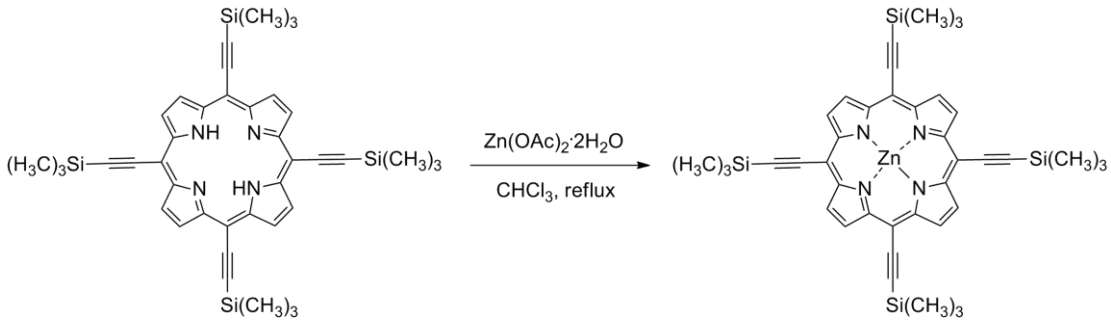


**1** **2**

Zinc acetate dihydrate (11 mg, 0.05 mmol) in 1 mL of methanol was added to 5,10,15,20-trimethylsilylethynylporphyrin (**1**) (7.3 mg, 0.01 mmol) in 2 mL of chloroform. The reaction mixture was refluxed for 2 h, cooled to rt and extracted with deionized water (3×15 mL). The combined organic layers were dried over magnesium sulfate. The solvent was removed under reduced pressure to give [5,10,15,20-trimethylsilylethynylporphinato] zinc(II) (**2**) (4.6 mg, 58%) as a green solid. This method was modified from that of Lee and Hupp's [15]. UV/vis (THF): $\lambda_{max}$ = 457, 599, 645 nm. Fluorescence (THF): $\lambda_{max}$ = 661, 728 nm. $^{1}$H NMR (400 MHz, $CDCl_3$) $\delta$ 7.19 (s, 8H), 1.18 (s, 36H). MALDI-TOF-MS : *m/z* $[M]^+$ calcd. for $C_{40}H_{44}N_4Si_4Zn$: 758.536, Found: 757.547.

### 2.3.3 Synthesis of [5,10,15,20-ethynylporphinato] zinc(II) (3)

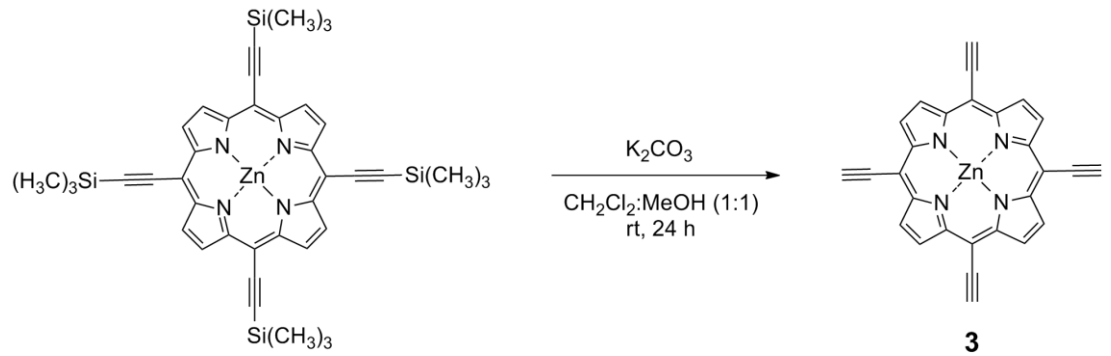


**2** **3**

[5,10,15,20-Ethynylporphinato] zinc(II) (**2**) (7.6 mg, 0.01 mmol) and potassium carbonate (7.0 mg, 0.05 mmol) were dissolved in 10 mL of dichloromethane/methanol (1:1). The reaction mixture was stirred for 24 h at rt. The precipitates were then filtered off and washed with deionized water. Dissolution from tetrahydrofuran gave [5,10,15,20-ethynylporphinato] zinc(II) (**3**) (3.2 mg, 68%) as a dark green solid. UV/vis (THF): $\lambda_{max}$ = 459, 598, 645 nm. $^1$H NMR (400 MHz, $CDCl_3$) $\delta$ 6.98 (s, 8H), 5.02 (s, 4H). MALDI-TOF-MS : m/z $[M]^+$ calcd. for $C_{28}H_{12}N_4Zn$: 469.812, Found: 467.509.

### 2.4 Synthesis of aza-boron-dipyrromethene (aza-BODIPY)

The synthesis of aza-boron-dipyrromethene (**10**) was conducted in 6 steps as shown in **Scheme 2.2**. First step was the Williamson ether synthesis of 4-hydroxybenzaldehyde. Next, aldol condensation and Michael addition were performed, respectively. Aza-dipyrromethene formation was carried out, followed by complexation with boron trifluoride diethyl etherate. Finally, the product (10) was obtained after bromination.

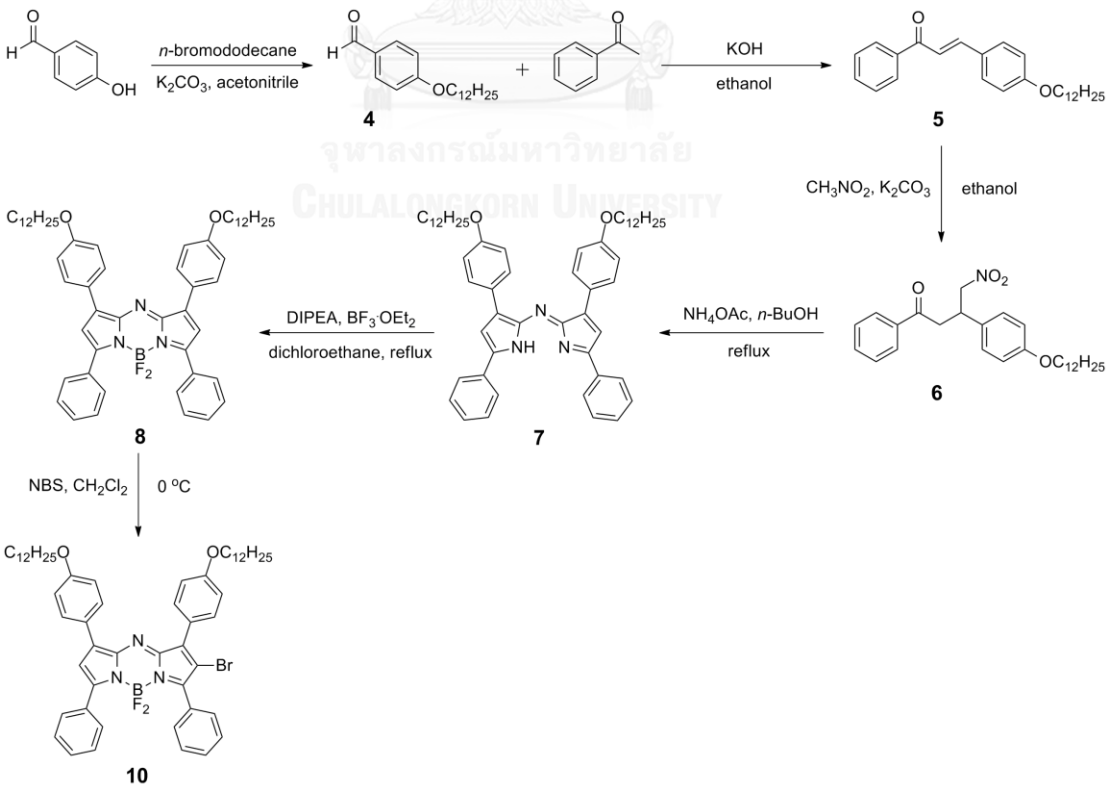


**Scheme 2.2** Synthetic route of aza-boron-dipyrromethene (**10**)

### 2.4.1 Synthesis of 4-(dodecyloxy)benzaldehyde (4)

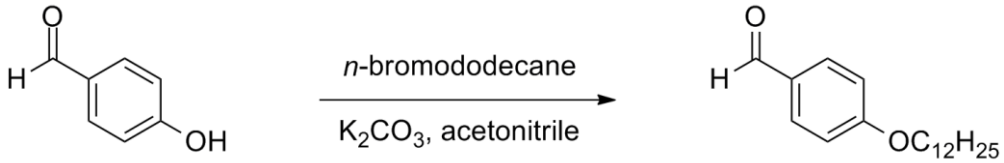


**4**

A method used was modified from that of Gresser's [38]. 1-Bromododecane (3.6 mL, 15 mmol) was added to a mixture of 4-hydroxybenzaldehyde (1.2212 g, 10 mmol) and $K_2CO_3$ (2.073 g, 15 mmol) in acetonitrile 20 mL. The reaction mixture was refluxed for 6 h, then quenched by addition of deionized water. The mixture was then extracted with ethyl acetate (3×30 mL). The combined organic layers were dried over magnesium sulfate. The solvent was removed under reduced pressure. The crude product was purified by silica-gel column chromatography (hexanes/ethyl acetate (4:1)) to give 4-(dodecyloxy) benzaldehyde (**4**) (2.7565 g, 95%) as a white crystalline solid. $^{1}$H NMR (400 MHz, $CDCl_3$) $\delta$ 9.90 (s, 1H), 7.85 (d, *J* = 8.6 Hz, 2H), 7.01 (d, *J* = 8.6 Hz, 2H), 4.06 (t, *J* = 6.5 Hz, 2H), 1.89 – 1.77 (m, 2H), 1.54 – 1.20 (m, 18H), 0.90 (t, *J* = 6.6 Hz, 3H). $^{13}$C NMR (100 MHz, $CDCl_3$) $\delta$ 190.73, 164.29, 131.95, 129.81, 114.77, 68.45, 31.90, 29.63, 29.61, 29.56, 29.52, 29.32, 29.05, 26.10, 25.95, 22.66, 14.07.

### 2.4.2 Synthesis of 3-(4-(dodecyloxy)phenyl)-1-phenylprop-2-en-1-one (5)

To a solution of 4-(dodecyloxy)benzaldehyde (**4**) (2.9044g, 10 mmol) and acetophenone (2 mL, 17 mmol) in 10 mL of ethanol was added a solution of potassium hydroxide (0.0393 g, 0.7 mmol) in 1 mL of deionized water. After stirring for 24 h, the precipitates were filtered off and washed with ethanol.

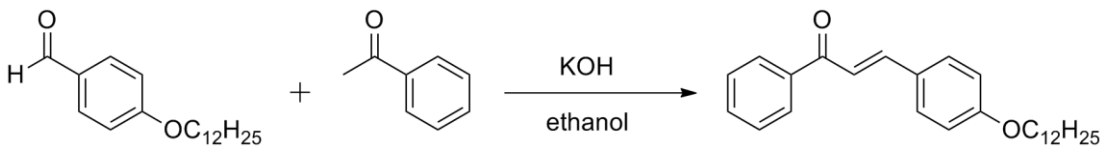


**4** **5**

Recrystallization from ethanol gave 3-(4-(dodecyloxy)phenyl)-1-phenylprop-2-en-1-one (**5**) (3.3861 g, 86%) as yellow crystaline solid. This method was modified from that of Gresser's [38]. mp = 71-72 $^{o}$C. UV/vis (ethyl acetate): $\lambda_{max}$ = 342 nm. $^{1}$H NMR (400 MHz, $CDCl_3$) $\delta$ 8.03 (d, *J* = 7.3 Hz, 2H), 7.81 (d, *J* = 15.6 Hz, 1H), 7.62 (d, 2H), 7.58 (t, 1H), 7.52 (t, *J* = 7.4 Hz, 2H), 7.43 (d, *J* = 15.6 Hz, 1H), 6.95 (d, *J* = 8.7 Hz, 2H), 4.03 (t, *J* = 6.6 Hz, 2H), 1.88 – 1.77 (m, 2H), 1.53 – 1.20 (m, 18H), 0.91 (t, *J* = 6.7 Hz, 3H). $^{13}$C NMR (100 MHz, $CDCl_3$) $\delta$ 190.62, 161.37, 144.82, 138.62, 132.48, 130.21, 128.54, 128.41, 127.43, 119.70, 114.96, 68.24, 31.91, 29.64, 29.62, 29.58, 29.55, 29.36, 29.33, 29.16, 26.00, 22.67, 14.08. MS (MALDI-TOF): *m/z* $[M]^+$ calcd. for $C_{27}H_{36}O_2$: 392.574, Found: 391.405.

### 2.4.3 Synthesis of 3-(4-(dodecyloxy)phenyl)-4-nitro-1-phenylbutan-1-one (6)

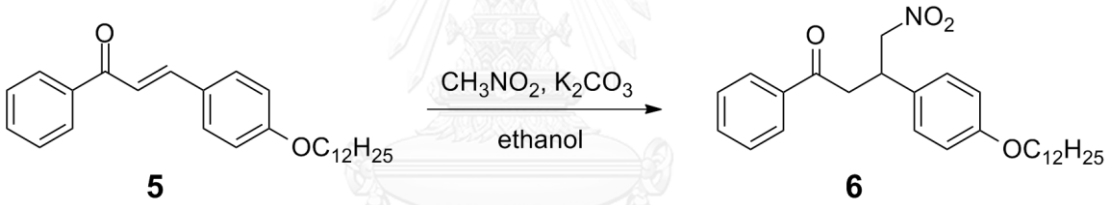


**5** **6**

3-(4-(Dodecyloxy)phenyl)-1-phenylprop-2-en-1-one (**5**) (5.8973 g, 15 mmol), nitromethane (4.0 mL, 75 mmol), and potassium carbonate (0.02 mmol) were dissolved in ethanol (15 mL). The reaction mixture was refluxed for 6 h. After being cooled to rt, solvent was removed under reduced pressure. Oily residue was dissolved in ethyl acetate and extracted with deionized water (3×30mL). The combined organic layers were washed with brine and dried over magnesium sulfate. The solvent was removed under reduced pressure to give 3-(4-(dodecyloxy)phenyl)-4-nitro-1-phenylbutan-1-one (**6**) (6.5356 g, 96%) as a yellowish brown oil. This method was modified from that of Gresser's [38]. mp. = 59-61 $^{o}$C. UV/vis (ethyl acetate): $\lambda_{max}$ = 231, 244 nm. $^{1}$H NMR (400 MHz, $CDCl_3$) $\delta$ 7.94 (d, *J* = 7.5 Hz, 2H), 7.60 (t, *J* = 7.4 Hz, 1H), 7.48 (t, *J* = 7.7 Hz, 2H), 7.20 (d, *J* = 8.6 Hz, 2H), 6.87 (d, *J* = 8.6 Hz, 2H), 4.74 (ddd, *J* = 20.2, 12.3, 7.3 Hz, 2H), 4.24 – 4.12 (m, 1H), 3.93 (t, *J* = 6.5 Hz, 2H),

3.51 – 3.37 (m, 2H), 1.83 – 1.72 (m, 2H), 1.51 – 1.19 (m, 18H), 0.91 (t, *J* = 6.7 Hz, 3H). $^{13}$C NMR (100 MHz, $CDCl_3$) δ 197.00, 158.73, 136.52, 133.47, 130.77, 128.71, 128.44, 128.02, 115.01, 79.86, 68.05, 41.70, 38.70, 31.90, 29.64, 29.62, 29.58, 29.56, 29.38, 29.32, 29.25, 26.03, 22.67, 14.08.

### 2.4.4 Synthesis of 3-(4-(dodecyloxy)phenyl)-*N*-(3-(4-(dodecyloxy) phenyl)-5-phenyl-2*H*-pyrrol-2-ylidene)-5-phenyl-1*H*-pyrrol-2-amine (7)

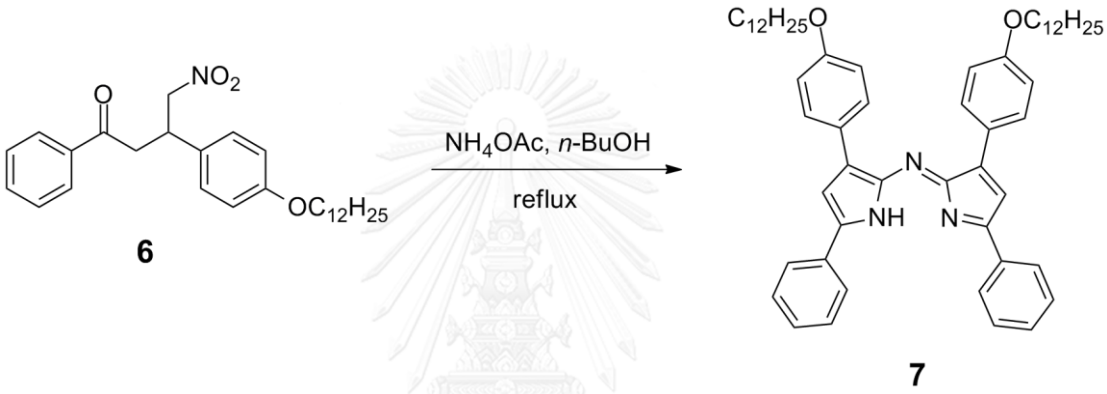


**6** **7**

A method used was modified from that of Gorman's [18]. 3-(4-(Dodecyloxy) phenyl)-4-nitro-1-phenylbutan-1-one (**6**) (0.9210 g, 2 mmol) and ammonium acetate (3.1129 g, 40 mmol) were dissolved in 200 mL of 1-butanol. The reaction mixture was refluxed for 24 h. After being cooled to rt, solvent was removed under reduced pressure. The reaction mixture was diluted with deionized water and extracted with dichloromethane (3×30mL). The combined organic layers were washed with deionized water and brine then dried over magnesium sulfate. The solvent was removed under reduced pressure. The crude product was purified by silica-gel column chromatography (hexanes/dichloromethane (1:1)) to give 3-(4-(dodecyloxy)phenyl)-*N*-(3-(4-(dodecyloxy)phenyl)-5-phenyl-*2H*-pyrrol-2-ylidene)-5-phenyl-*1H*-pyrrol-2-amine (**7**) (0.2264 g, 14%) as a shiny dark blue solid. Mp: 185-187 $^{o}$C. UV/vis (ethyl acetate): $\lambda_{max}$ = 608 nm. $^{1}$H NMR (400 MHz, $CDCl_3$) δ 8.02 (d, *J* = 8.8 Hz, 2H), 7.94 (d, *J* = 7.3 Hz, 2H), 7.52 (t, *J* = 7.5 Hz, 2H), 7.45 (t, *J* = 7.3 Hz, 1H), 7.10 (s, 1H), 6.95 (d, *J* = 8.8 Hz, 2H), 4.03 (t, *J* = 6.6 Hz, 2H), 1.83 (dd, *J* = 14.5, 6.8 Hz, 2H), 1.38

(d, *J* = 89.7 Hz, 18H), 0.88 (t, *J* = 6.5 Hz, 3H). $^{13}$C NMR (100 MHz, $CDCl_3$) δ 159.37, 154.94, 149.57, 142.46, 132.44, 130.37, 129.86, 129.09, 126.52, 125.07, 114.42, 113.45, 68.18, 32.24, 31.95, 29.71, 29.66, 29.49, 29.37, 26.43, 26.13, 23.43, 22.71, 14.11. MS (MALDI-TOF): *m/z* $[M]^+$ calcd. for $C_{56}H_{71}N_3O_2$: 818.182, Found: 818.209.

### 2.4.5 Synthesis of 4,4-difluoro-1,7-bis(4-dodecyloxyphenyl)-3,5-diphenyl-4-bora-3a,4a,8-triaza-*s*-indacene (8)

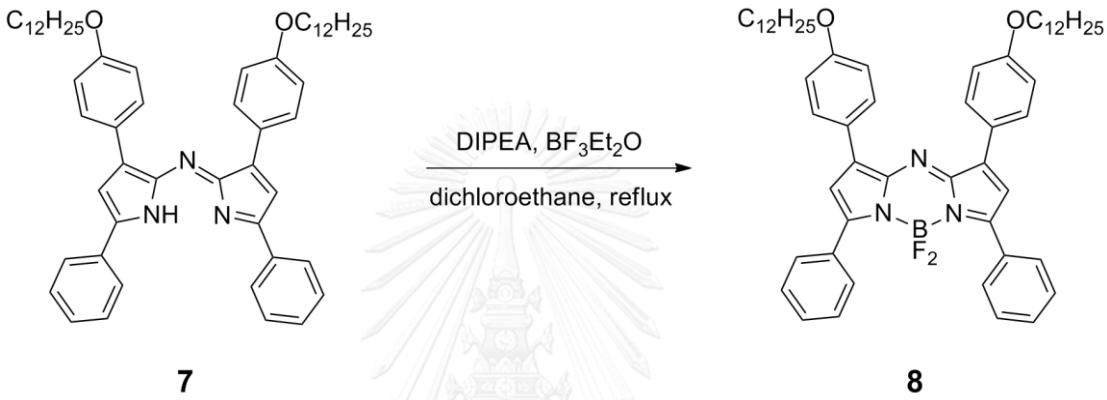


**7** **8**

3-(4-(Dodecyloxy)phenyl)-*N*-(3-(4-(dodecyloxy)phenyl)-5-phenyl-2*H*-pyrrol-2-ylidene)-5-phenyl-1*H*-pyrrol-2-amine (**7**) (0.5115 g, 0.6 mmol) and diisopropylamine (0.5 mL, 3.6 mmol) were dissolved in 10 mL of dichloroethane. After stirring at rt for 1 h, boron trifluoride diethyl etherate (0.37 mL, 3.0 mmol) was added and the resulting mixture was refluxed until starting material was completely converted to the corresponding product (checked with TLC). After being cooled to rt, the reaction mixture was diluted with deionized water and extracted with dichloromethane (3×30mL). The combined organic layers were dried over magnesium sulfate. The solvent was removed under reduced pressure. The crude product was purified by silica-gel column chromatography (hexanes/dichloromethane (3:2)) to give 4,4-difluoro-1,7-bis(4-dodecyloxyphenyl)-3,5-diphenyl-4-bora-3a,4a,8-triaza-*s*-indacene (**8**) (0.2630 g, 49%) as a dark blue shiny solid. This method was modified from that of Gorman's [18]. UV/vis (ethyl acetate): $\lambda_{max}$ = 665 nm. Fluorescence (ethyl acetate): $\lambda_{max}$ = 716 nm. $^1$H NMR (400 MHz, $CDCl_3$) δ 8.12 – 8.01 (m, 4H), 7.49 (d, *J* = 4.5 Hz, 3H), 6.98 (d, *J* = 8.7 Hz, 2H), 6.90 (s, 1H), 4.04 (t, *J* = 6.5 Hz, 2H), 1.88 – 1.77 (m, 2H),

1.58 – 1.17 (m, 18H), 0.88 (t, *J* = 6.6 Hz, 3H). $^{13}$C NMR (100 MHz, $CDCl_3$) δ 160.63, 159.03, 145.48, 143.82, 131.95, 130.90, 130.57, 129.51, 128.49, 125.19, 117.39, 114.78, 68.26, 71.94, 29.70, 29.67, 29.64, 29.62, 29.46, 29.37, 29.30, 26.09, 22.70, 14.11. MS (MALDI-TOF): *m/z* $[M]^+$ calcd for $C_{56}H_{70}N_3O_2BF_2$: 865.982, Found: 866.755.

### 2.4.6 Synthesis of 2,6-bromo-4,4-difluoro-1,7-bis(4-dodecyloxyphenyl)-3,5-diphenyl-4-bora-3a,4a,8-triaza-*s*-indacene (9)

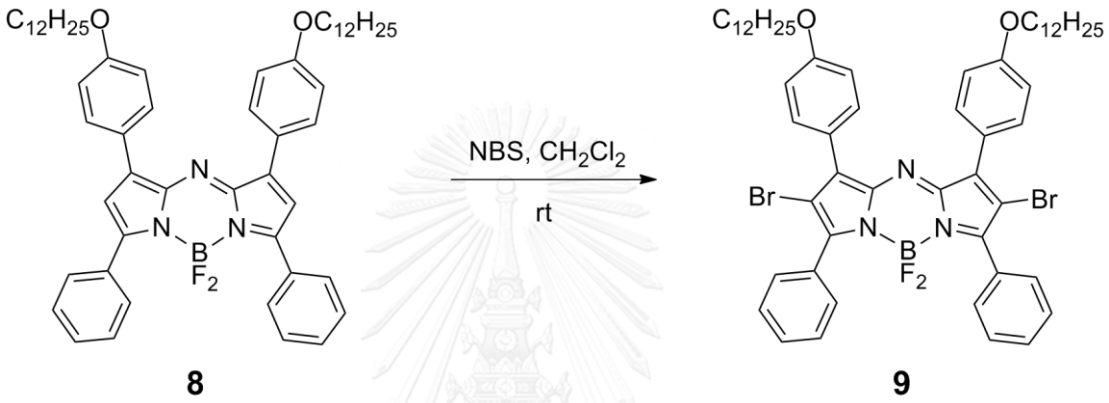


**8** **9**

A method used was modified from that of Karatay's [39]. 4,4-Difluoro-1,7-bis(4-dodecyloxyphenyl)-3,5-diphenyl-4-bora-3a,4a,8-triaza-*s*-indacene (**8**) (0.098 g, 0.1 mmol) in 5 mL of dichloromethane. Then *N*-bromosuccinimide (0.036 g, 0.2 mmol) was added. After stirring for 30 min, the reaction was quenched with sodium hydrogen carbonate and washed two times with sodium hydroxide. An organic layer was dried with magnesium sulfate and concentrated to give the crude product. Purification by silica-gel column chromatography (dichloromethane/hexanes (1:1) gave 2,6-bromo-4,4-difluoro-1,7-bis(4-dodecyloxyphenyl)-3,5-diphenyl-4-bora-3a,4a,8-triaza-*s*-indacene (**9**) (0.079 g, 68%) as a shiny dark purplish blue solid. UV/vis (ethyl acetate): $\lambda_{max}$ = 651 nm. Fluorescence (ethyl acetate): $\lambda_{max}$ = 711 nm. $^1$H NMR (400 MHz, $CDCl_3$) δ 7.95 (d, *J* = 8.5 Hz, 2H), 7.76 – 7.69 (d, 2H), 7.48 (m, 3H), 6.99 (d, *J* = 10.8 Hz, 2H), 4.06 (t, *J* = 6.5 Hz, 2H), 1.93 – 1.78 (m, 2H), 1.55 – 1.21 (m, 18H), 0.91 (t, *J* = 6.6 Hz, 3H). $^{13}$C NMR (100 MHz, $CDCl_3$) δ 160.65, 157.97, 144.16, 142.44, 132.44, 130.58, 130.27, 129.69, 127.90, 123.23, 114.21, 106.52, 68.22, 31.93, 30.89, 29.69, 29.65, 29.63, 29.61, 29.43, 29.36, 29.23, 26.06, 22.69, 14.10.

### 2.4.7 Synthesis of 2-bromo-4,4-difluoro-1,7-bis(4-dodecyloxyphenyl)-3,5-diphenyl-4-bora-3a,4a,8-triaza-*s*-indacene (10)

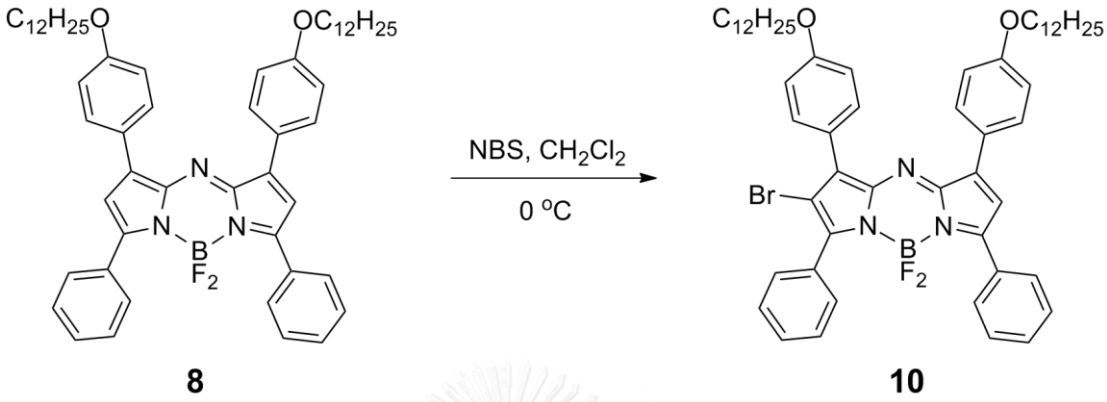


**8** **10**

4,4-Difluoro-1,7-bis(4-dodecyloxyphenyl)-3,5-diphenyl-4-bora-3a,4a,8-triaza-*s*-indacene (**8**) (29.8 mg, 0.03 mmol) in 5 mL of dichloromethane at 0°C and *N*-bromosuccinimide (6.23 mg, 0.03 mmol) were slowly added to the reaction. The reaction mixture was stirred at 0°C for 30 min and stirring was continued for 1 h at rt. The reaction was then quenched by addition of sodium hydrogen carbonate and washed with sodium hydroxide (2×15 mL). The combined organic layers were dried over magnesium sulfate. The solvent was removed under reduced pressure. The crude product was purified by silica-gel column chromatography (hexanes/ dichloromethane (1:1)) to give 2-bromo-4,4-difluoro-1,7-bis(4-dodecyloxyphenyl)-3,5-diphenyl-4-bora-3a,4a,8-triaza-*s*-indacene (**9**) (22.4 mg, 69%) as a shiny dark purplish blue solid. $^{1}$H NMR (400 MHz, $CDCl_3$) δ 8.07 (d, *J* = 8.8 Hz, 2H), 7.98 (d, *J* = 8.0 Hz, 2H), 7.92 (d, *J* = 8.8 Hz, 2H), 7.74 (d, *J* = 3.7 Hz, 2H), 7.51 – 7.47 (m, 3H), 7.45 (d, *J* = 6.9 Hz, 3H), 7.04 (d, *J* = 8.8 Hz, 2H), 6.96 (s, 1H), 6.92 (d, *J* = 8.9 Hz, 2H), 4.07 (t, *J* = 6.6 Hz, 2H), 4.02 (d, *J* = 6.5 Hz, 2H), 1.91 – 1.77 (m, 4H), 1.49 (s, 4H), 1.30 (t, *J* = 25.0 Hz, 32H), 0.88 (t, *J* = 6.7 Hz, 6H). $^{13}$C NMR (100 MHz, $CDCl_3$) δ 161.13, 160.27, 132.46, 132.39, 131.36, 131.06, 130.47, 130.36, 130.29, 130.07, 129.64, 128.64, 127.92, 127.84, 124.46, 123.86, 117.87, 114.86, 114.23, 114.17, 68.25, 31.94, 29.71, 29.67, 29.63, 29.46, 29.43, 29.37, 29.30, 29.24, 29.12, 26.12, 26.06, 22.70, 14.12. MS (MALDI-TOF): *m/z* $[M]^+$ calcd for $C_{56}H_{69}N_3O_2BF_2Br$: 944.878, Found: 945.503.

**2.5 Synthesis of aza-BODIPY-porphyrin (11)**

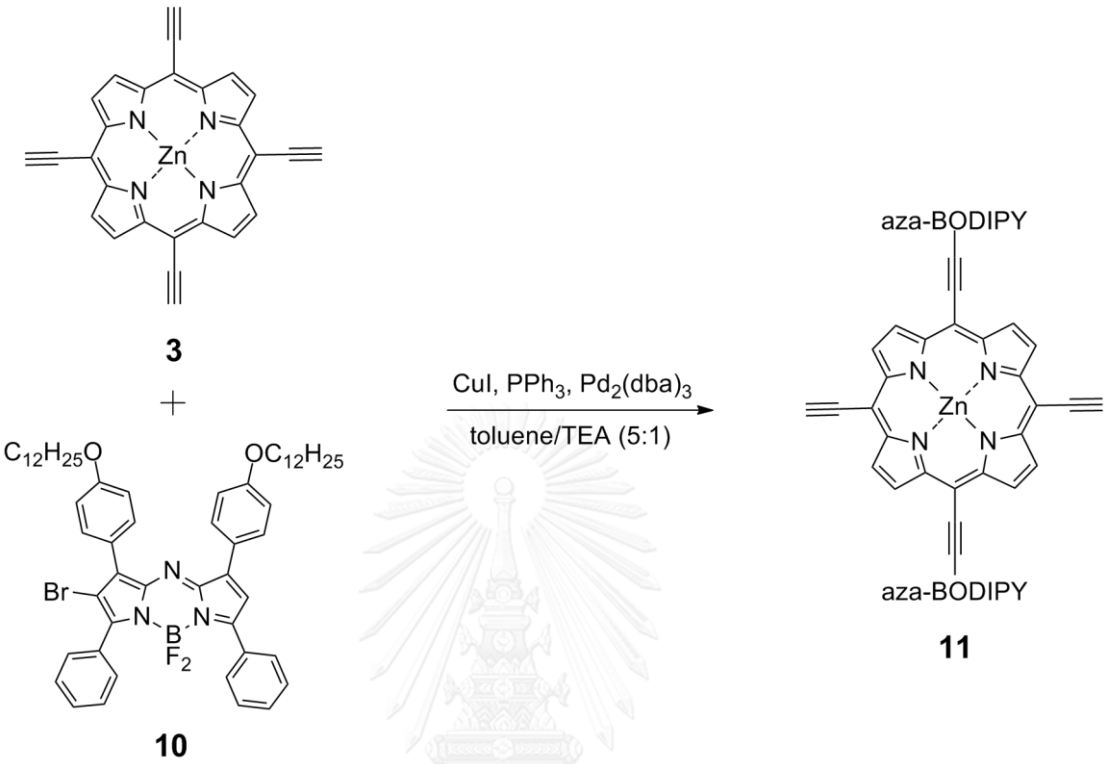


To a solution of [5,10,15,20-ethynylporphinato] zinc(II) (**3**) (3.1 mg, 0.007 mmol) a solution of 2-bromo-4,4-difluoro-1,7-bis(4-dodecyloxyphenyl)-3,5-diphenyl-4-bora-3a,4a,8-triaza-*s*-indacene (**10**) (18.7 mg, 0.02 mmol), CuI (2.5 mg, 0.01 mmol), and $PPh_3$ (6.9 mg, 0.03 mmol) in 10 mL of TEA/toluene (1:5) was added under $N_2$. Then $Pd_2(dba)_3$ (6.0 mg, 0.007 mmol) was added and stirred for 12 h at 60-70 $^{o}$C. After being cooled to rt, solvent was removed under reduced pressure. The crude product was purified by silica-gel column chromatography (hexanes/dichloromethane (1:1)) to give aza-BODIPY-porphyrin (**11**) as an aquamarine solid. This method was modified from reference [15]. UV/vis (THF): $\lambda_{max}$ = 425, 453, 666 nm.

# CHAPTER III
# RESULTS AND DISCUSSION

## 3.1 Concept of Molecular Design

It is well known that porphyrins and their metal complexes can be utilized as materials in various applications, for example as photodynamic therapeutic agents, molecular sensors and as dye in dye-sensitized solar cells. However, porphyrins display strong absorption around 400 nm and weak absorption around 500-700 nm. One of the most interesting ways to tune their optical properties is the increase of the absorption around 500-700 nm of porphyrin by connecting the porphyrin ring with aza-BODIPY.

Owing to this reason, this research is aimed to synthesize novel aza-BODIPY-porphyrin which exhibit stronger absorption around 500-700 nm. In addition, in order to expand the application of the target compound as a dye for dye-sensitized solar cell, we aimed to synthesize aza-BODIPY-porphyrin system connected with one or two carboxylic group(s). The structure of target molecules is presented in **Figure 3.1**.



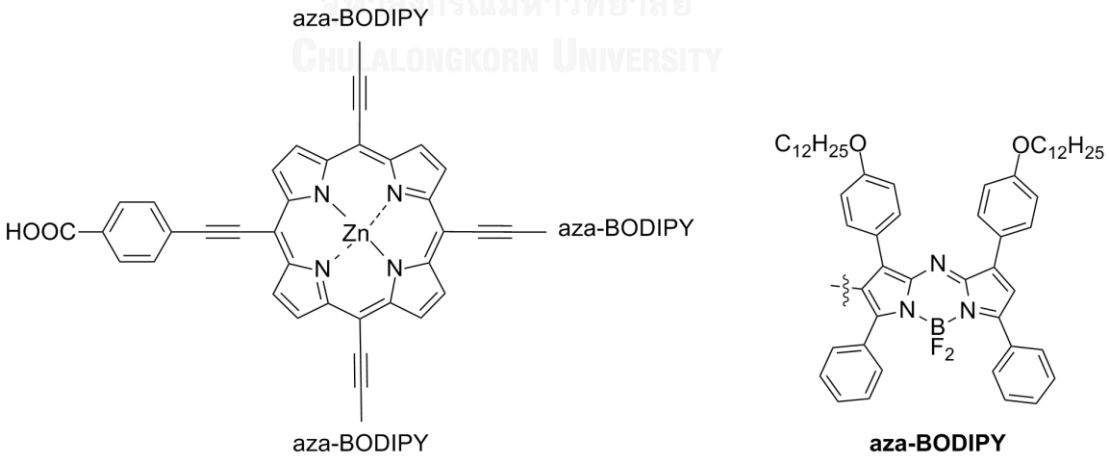


**Figure 3.1** The structure of target molecule

As shown in **Figure 3.1**, there are four parts in the structure including :

- Porphyrin : porphyrin exhibits strong absorption around 400 nm (Soret band) and weak absorption around 500-700 nm (Q band).
- Aza-BODIPY : aza-BODIPYs exhibit strong absorption around 500-700 nm.
- Alkyne linkers : alkyne moieties are linked directly at the remaining *meso*-position of porphyrin rings in order to extend the π-conjugated systems.
- Carboxylic group : carboxylic group which can anchor to $TiO_2$ surface for dye-sensitized solar cells (DSSCs)

The synthesis of porphyrin was conducted in 4 steps as shown in **Scheme 3.1**.

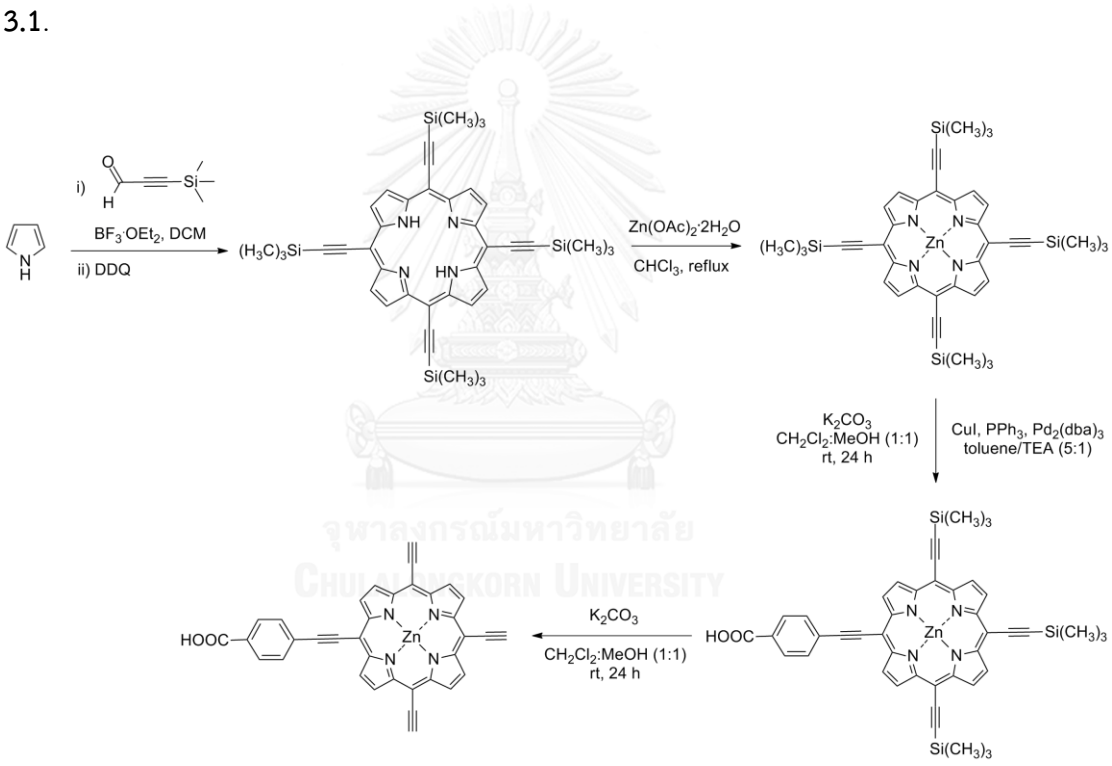


**Scheme 3.1** Synthetic route of porphyrin

The synthesis of brominated aza-boron-dipyrromethene was conducted in 6 steps as shown in **Scheme 3.2**.

Finally, the aza-BODIPY-porphyrin was synthesized *via* Pd (0) catalyzed Sonogashira coupling as shown in **Scheme 3.3**.

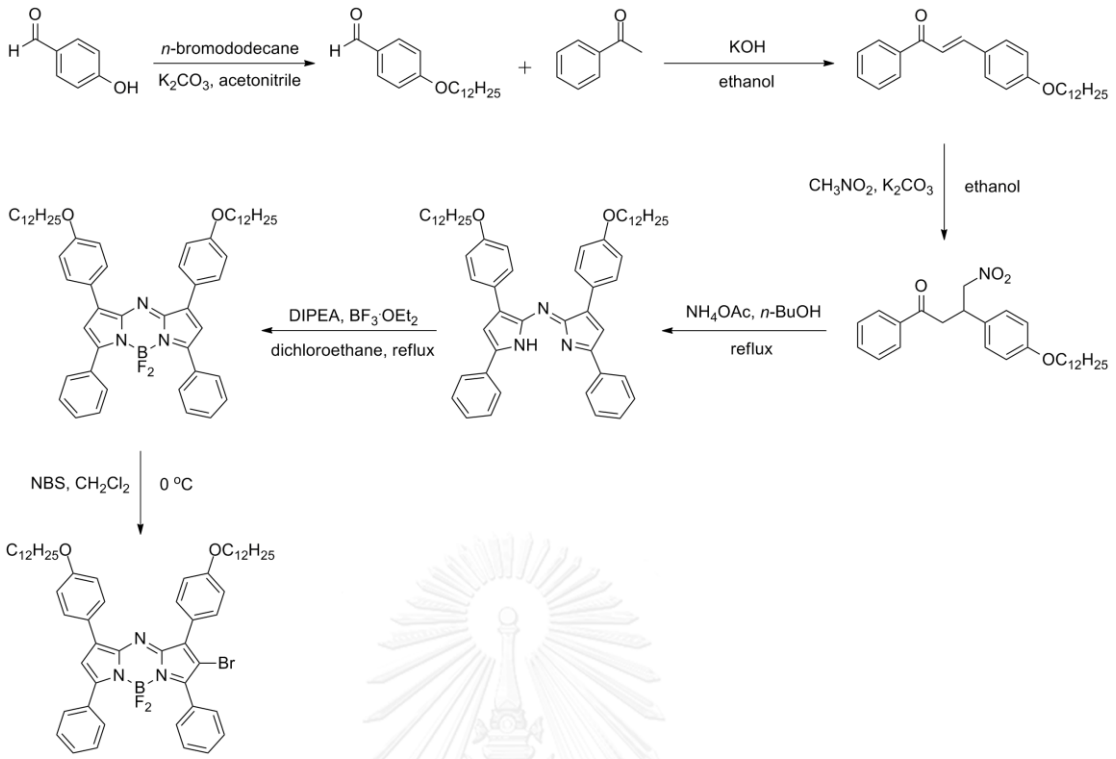


**Scheme 3.2** Synthetic route of brominated aza-boron-dipyrromethene

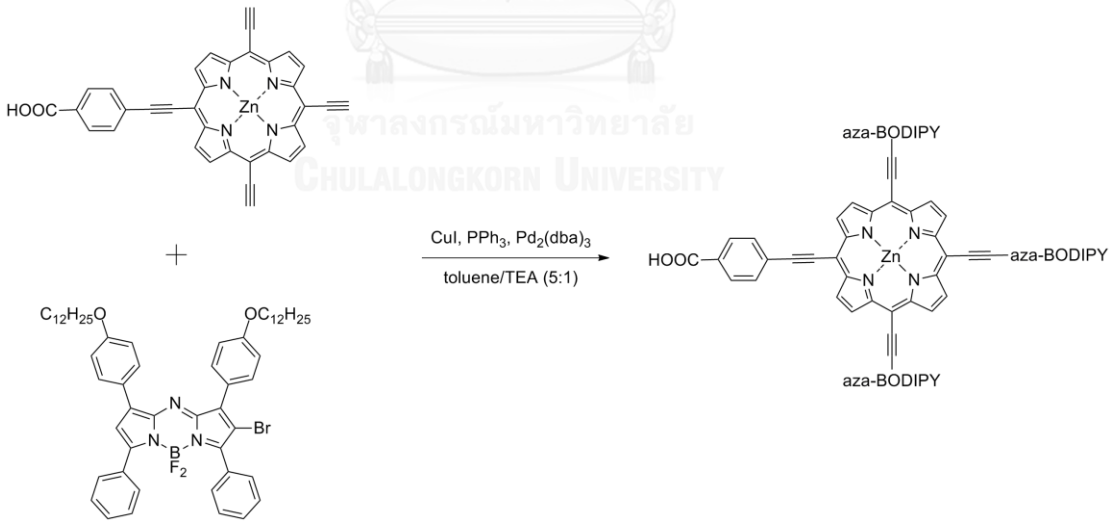


**Scheme 3.3** Synthetic route of aza-BODIPY-porphyrin

## 3.2 Synthesis of Porphyrin

### 3.2.1 Synthesis of 5,10,15,20-trimethylsilylethynylporphyrin (1)

Synthesis of porphyrin (**1**) was carried out from a reaction of pyrrole with 3-trimethylsilylpropynal in the presence of $BF_3 \cdot OEt_2$ as catalyst followed by oxidation with DDQ. A workup through a short plug of silica gel gave 5,10,15,20-trimethylsilyl ethynylporphyrin (**1**). Two preparation conditions have been applied in the synthesis of compound **1** as shown in **Table 3.1**.

**Table 3.1** Effect of pyrrole:3-trimethylsilylpropynal:$BF_3 \cdot OEt_2$ ratio on the yield of porphyrin (**1**)

| entry | ratio of pyrrole: 3-trimethylsilylpropynal:$BF_3 \cdot OEt_2$ | $CH_2Cl_2$ (mL) | yield (%) |
|---|---|---|---|
| 1 | 1 : 1 : 1 | 60 | 1 |
| 2 | 1 : 1 : 0.5 | 60 | 5 |



The effect of pyrrole : 3-trimethylsilylpropynal : $BF_3 \cdot OEt_2$ ratio on the yield of porphyrin was also examined and summarized in **Table 3.1**. The ratio of pyrrole : 3-trimethylsilylpropynal : $BF_3 \cdot OEt_2$ was varied from 1:1:1 to 1:1:0.5. These results indicated that upon decreasing $BF_3 \cdot OEt_2$ from 1 equivalent to 0.5 equivalent gave product in 5%.

MALDI-TOF analysis was used to confirm the structure of 5,10,15,20-trimethylsilyl ethynylporphyrin (**1**) with the molecular ion peak found at 945.503 which was consistent with calculated exact mass of 944.878 (**Figure 3.2**).

The product was analyzed by UV-visible spectroscopy (**Figure 3.3**). The result showed characteristic absorption peaks of porphyrin including a strong Soret band at 450 nm and four Q band peaks at 566, 605, 648 and 711 nm.

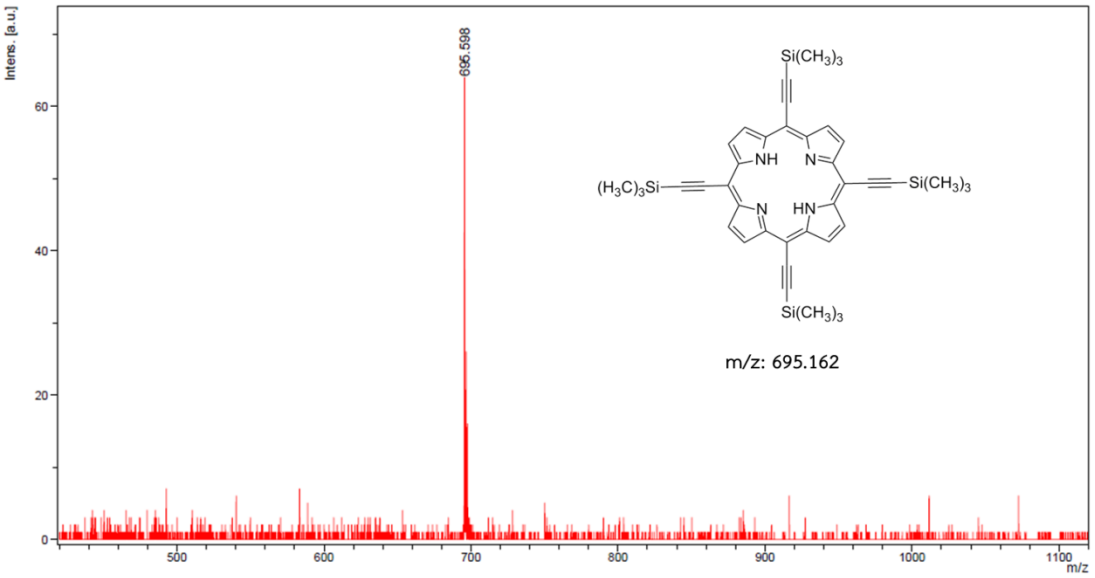


**Figure 3.2** The MALDI-TOF mass spectrum of 5,10,15,20-trimethylsilylethynyl porphyrin (**1**)

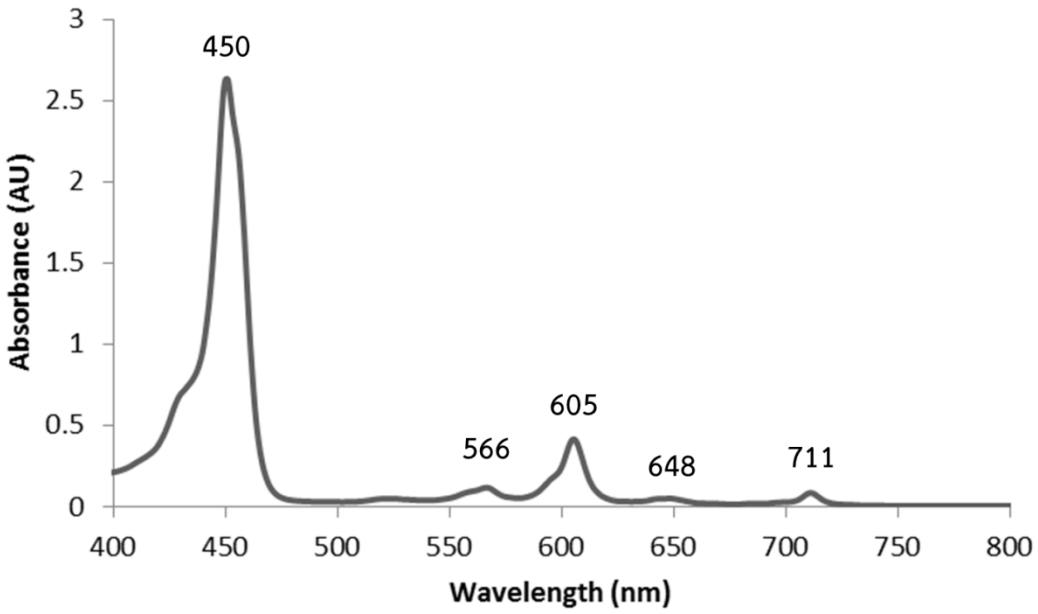


**Figure 3.3** The UV-visible spectrum of 5,10,15,20-trimethylsilyl ethynylporphyrin (**1**)

### 3.2.2 Synthesis of [5,10,15,20-trimethylsilylethynylporphinato] zinc(II) (2)

The synthesis of [5,10,15,20-trimethylsilylethynylporphinato] zinc(II) (**2**) using a 5 equivalents of $Zn(OAc)_2{\cdot}2H_2O$ in methanol was carried out in a boiling $CHCl_3$

solution of 5,10,15,20-trimethylsilylethynylporphyrin. Within 1 hour, the metallation of zinc(II) ion into the core of porphyrin ring as monitored by the MALDI-TOF mass spectrometry (**Figure 3.4**). Then the resulting solution was extracted with deionized water to remove $Zn(OAc)_2 \cdot 2H_2O$, green solid was obtained in 58% yield. The MALDI-TOF mass spectrum showed the molecular ion peak at 757.757 which was similar to calculated exact mass of 758.536.

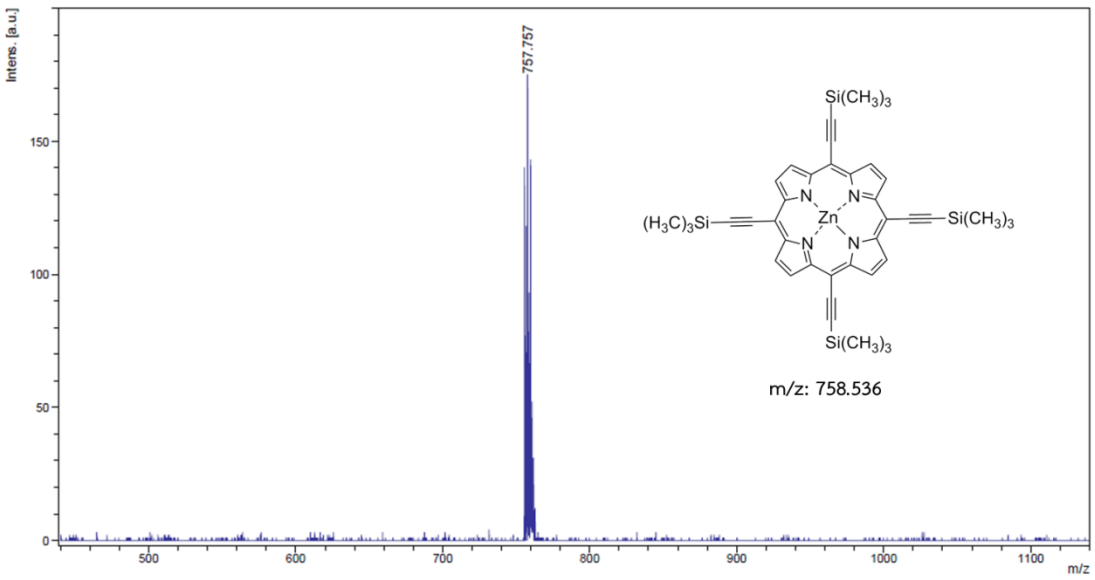


**Figure 3.4** The MALDI-TOF mass spectrum of 5,10,15,20-trimethylsilylethynyl porphinato zinc(II) (**2**)

The product was analyzed by UV-visible spectroscopy (**Figure 3.5**). The result showed characteristic absorption peaks of metal-porphyrin including a strong Soret band at 462 nm and two Q band peaks at 606 and 654 nm.

The product was comfirmed by IR spectroscopy. The IR spectra of 5,10,15,20-trimethylsilylethynylporphyrin (**1**) and [5,10,15,20-trimethylsilylethynylporphinato] zinc(II) (**2**) are compared in **Figure 3.6**. The N-H stretching which appeared at 3647.53 $cm^{-1}$ in the spectra of compound **1** is indicative of the porphyrin is its free-based form. This absorption is no longer present in the spectrum of the zinc-porphyrin complex (compound **2**).

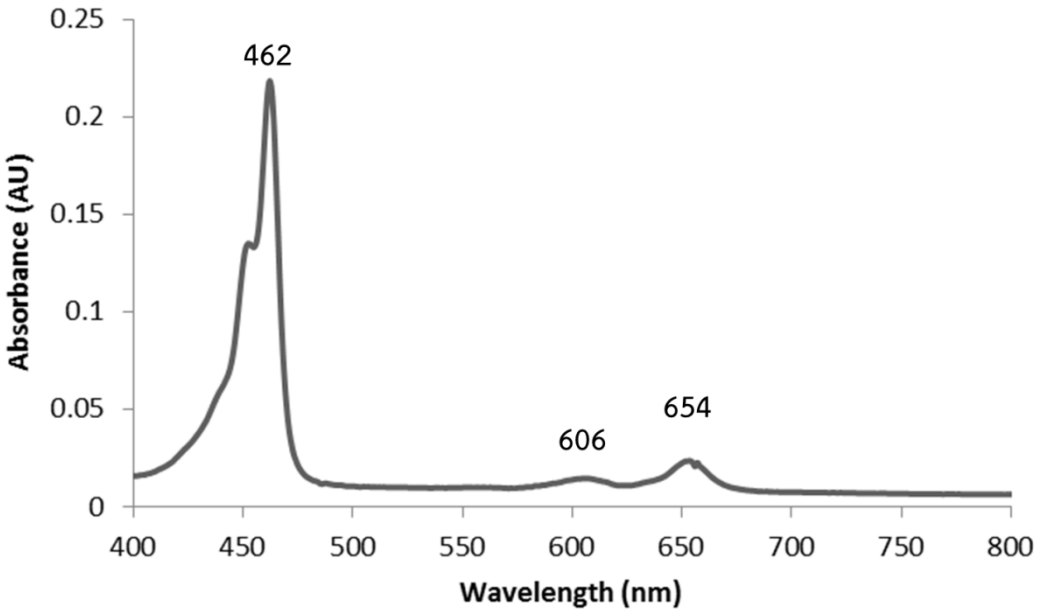


**Figure 3.5** The UV-visible spectrum of 5,10,15,20-trimethylsilylethynyl porphinato zinc(II) (**2**)

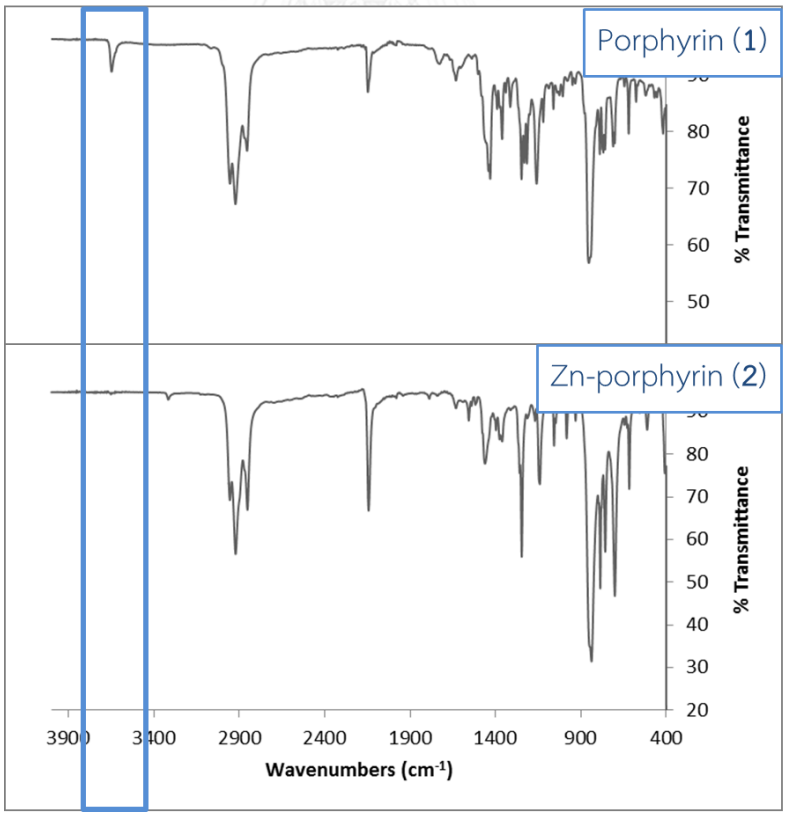


**Figure 3.6** The IR spectrum of 5,10,15,20-trimethylsilylethynylporphyrin (**1**) and [5,10,15,20-trimethylsilylethynylporphinato] zinc(II) (**2**)

### 3.2.3 Synthesis of [5,10,15,20-ethynylporphinato] zinc(II) (3)

Deprotection of trimethylsilyl group in zinc-porphyrin (**2**) with TBAF in THF did not occur and core porphyrin was broken. After that, changing TBAF to $K_2CO_3$ and deprotect of trimethylsilyl group for four groups.

The terminal alkyne zinc complex **3** was prepared by the deprotection of all trimethylsilyl groups of the porphyrin zinc (**2**) with potassium carbonate in dichloromethane/methanol (1:1). After workup by deionized water the product was obtained as a dark green solid. The product was then characterized by MALDI-TOF mass spectrometry (**Figure 3.7**). A molecular ion peak was found at 467.509 which was consistent with calculated exact mass of 469.80.

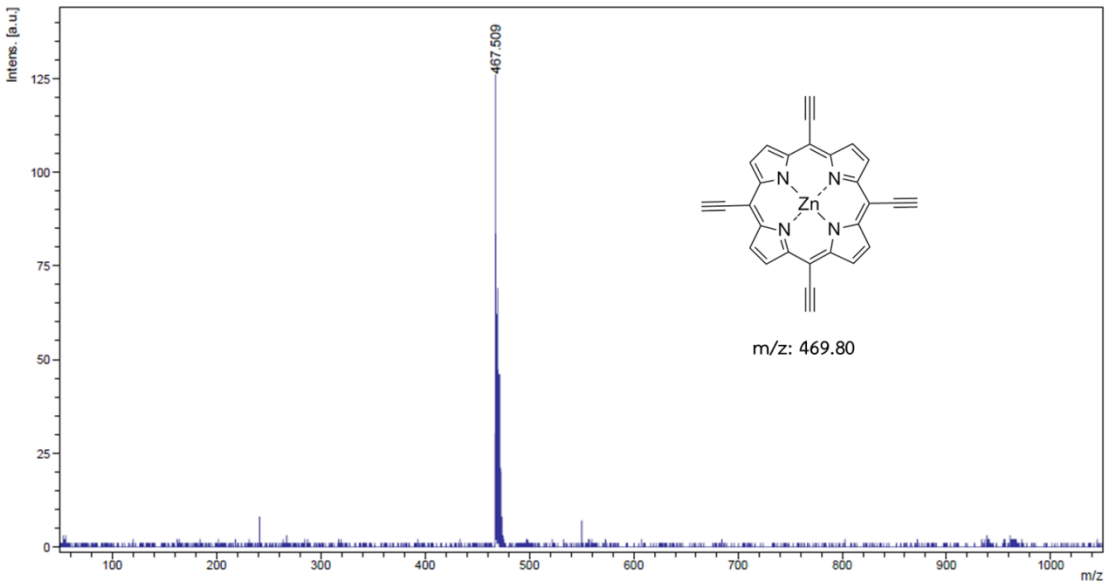


**Figure 3.7** The MALDI-TOF mass spectrum of [5,10,15,20-ethynylporphinato] zinc(II) (**3**)

## 3.3 Synthesis of aza-boron-dipyrromethene (aza-BODIPY)

### 3.3.1 Synthesis of 4-(dodecyloxy)benzaldehyde (4)

The synthesis of 4-(dodecyloxy)benzaldehyde (**4**) from 4-hydroxy benzaldehyde and 1-bromododecane was carried out in acetonitrile in the presence of potassium carbonate. The reaction mixture was refluxed for 6 h. After a workup, the crude product was further purified by column chromatography using

hexanes:ethyl acetate at 4:1 eluent. The product was obtained in nearly quantitative yield (95%) and was characterized by $^{1}$H NMR spectroscopy.

The $^{1}$H NMR spectrum exhibited signals of protons corresponding to the structure of 4-(dodecyloxy)benzaldehyde (**4**) as shown in **Figure 3.8**. The signal of proton of the aldehyde group was observed as a singlet peak at δ 9.90 ppm. There were 2 sets of signal in the aromatic region. The first doublet signal at δ 7.85 ppm indicated the protons ortho to the aldehyde group. The other doublet signal at δ 7.01 ppm was that of the protons ortho to the long chain alkoxy group. Moreover, the signals of proton in the dodecyloxy side chain groups were observed at δ 4.06 (d), 1.89 – 1.77 (e), 1.54 – 1.20 (f) and 0.90 ppm (g).

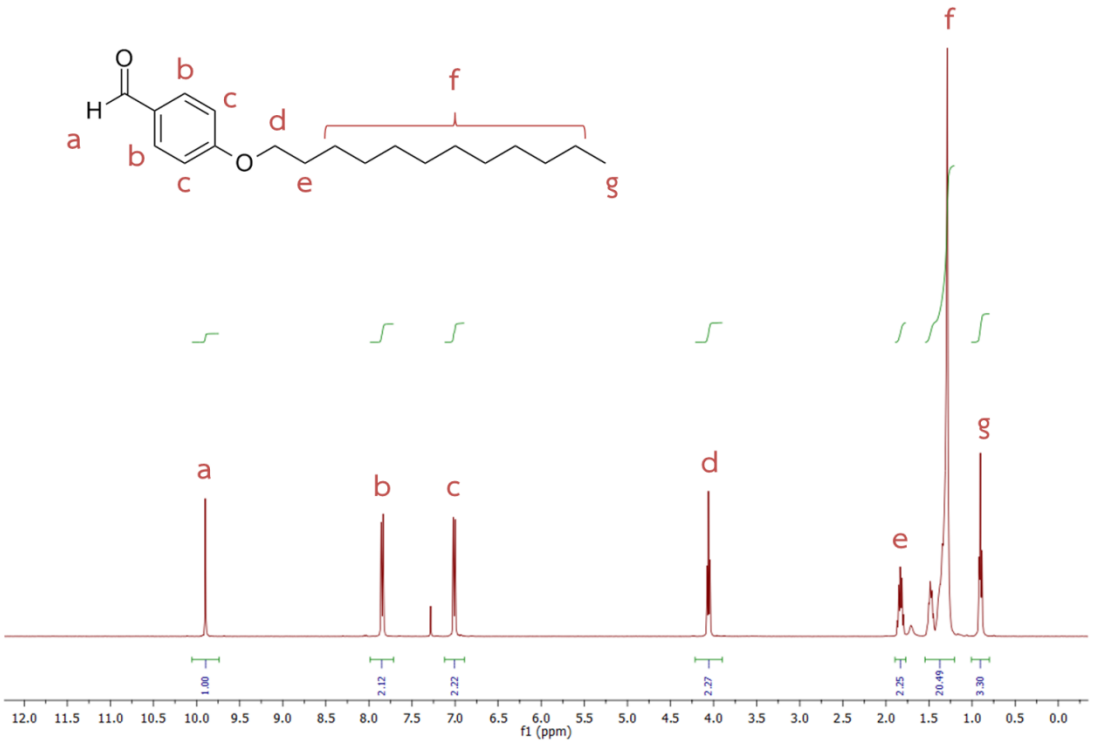


**Figure 3.8** The $^{1}$H NMR spectrum of 4-(dodecyloxy)benzaldehyde (**4**)

### 3.3.2 Synthesis of 3-(4-(dodecyloxy)phenyl)-1-phenylprop-2-en-1-one (5)

3-(4-(Dodecyloxy)phenyl)-1-phenylprop-2-en-1-one (**5**) was synthesized readily from aldol condensation of 4-(dodecyloxy)benzaldehyde (**4**) and acetophenone in ethanol. The solution of **4** and **5** was added to a solution of potassium hydroxide in

deionized water and stirred for 24 h. The product was obtained through recrystallization from ethanol in good yield (86%). The structure of the product was confirmed by $^{1}$H NMR spectroscopy as shown in **Figure 3.9**. There were 5 signals in the aromatic region which were observed at chemical shifts ranging from $\delta$ 6.95 to 8.03 ppm. The signals of protons in alkene group (alkenyl hydrogens) were observed at $\delta$ 7.43 and 7.81 ppm. The alkenyl hydrogens indicated *trans* isomer with the coupling constant of 15.6 Hz. Moreover, the signals of proton in dodecyloxy side chain groups were found at similar positions to that of 4-(dodecyloxy)benzaldehyde (**4**).

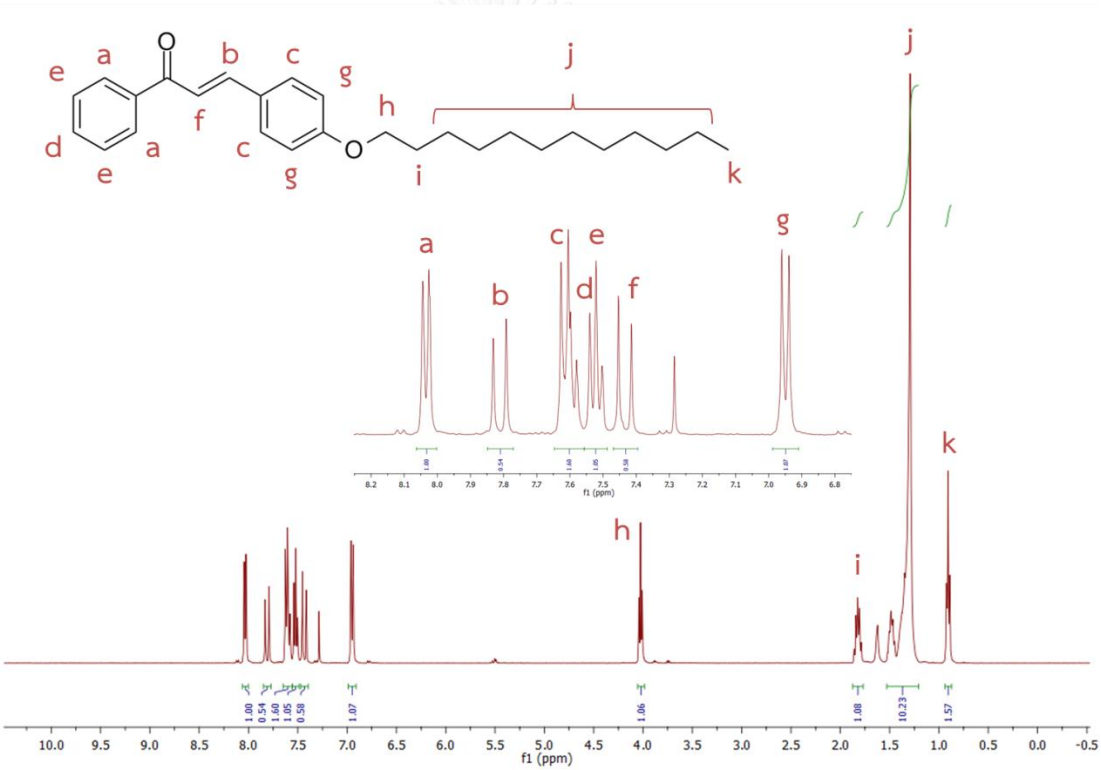


**Figure 3.9** The $^{1}$H NMR spectrum of 3-(4-(dodecyloxy)phenyl)-1-phenylprop-2-en-1-one (**5**)

### 3.3.3 Synthesis of 3-(4-(dodecyloxy)phenyl)-4-nitro-1-phenylbutan-1-one (3)

3-(4-(dodecyloxy)phenyl)-4-nitro-1-phenylbutan-1-one (**6**) was synthesized from aza-michael addition of 3-(4-(dodecyloxy)phenyl)-1-phenylprop-2-en-1-one (**5**) with nitromethane (the mechanism shown in **Figure 3.10**). The reaction mixture was

refluxed for 6 h. After a workup, the product was obtained in nearly quantitative yield (96%), and was used in the next step without further purification.

The $^{1}$H NMR spectrum of 3-(4-(dodecyloxy)phenyl)-4-nitro-1-phenylbutan-1-one (**6**) was shown in **Figure 3.11**. There were 5 signals in the aromatic region which were observed at chemical shifts ranging from δ 6.87 to 7.94 ppm. The signals of proton in $CH_2$ group (f and i positions) were observed a doublet of doublet of doublets (ddd) at 4.74 and 3.44 ppm respectively. The stereogenic carbon at position g appeared as a pentet at 4.19 ppm. Moreover, the signals of proton in dodecyloxy side chain groups were found at similar positions to that of 4-(dodecyloxy)benzaldehyde (**4**).

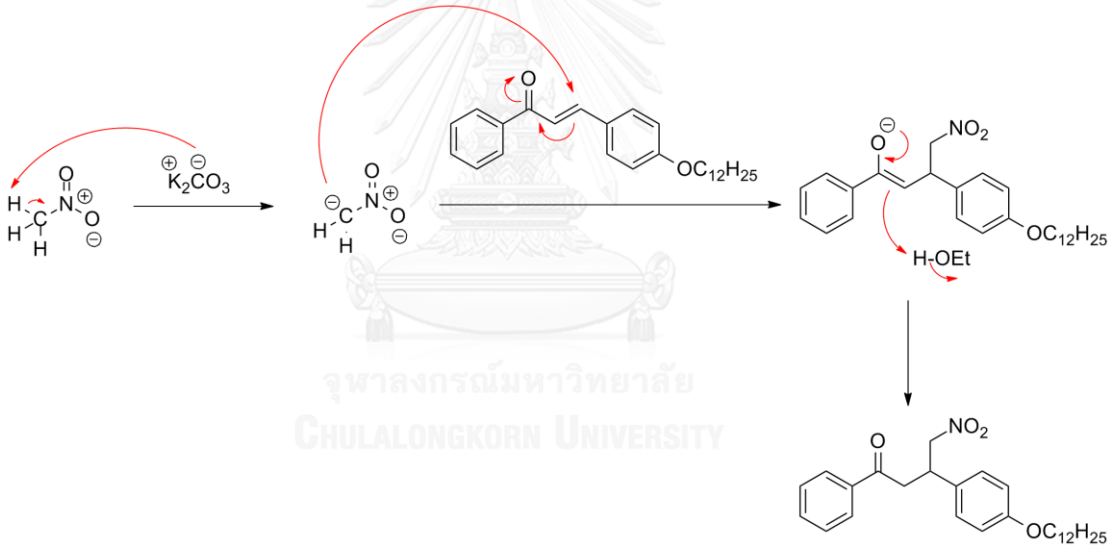


**Figure 3.10** The mechanism of Michael addition reaction

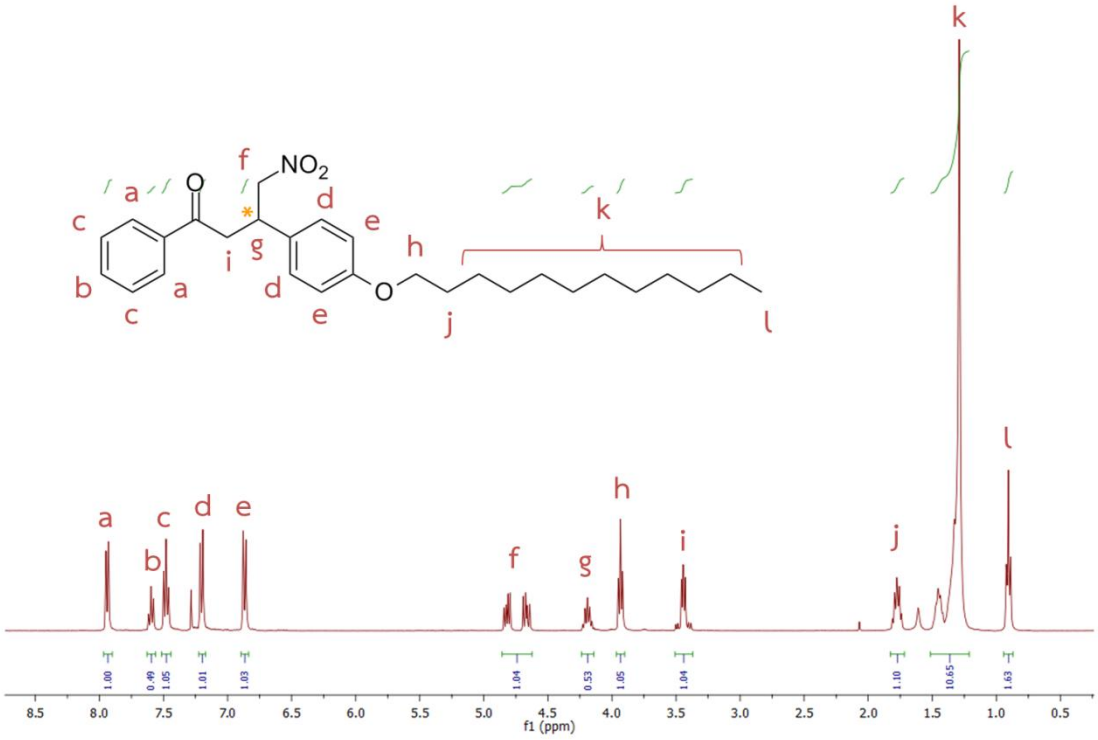


**Figure 3.11** The $^{1}$H NMR spectrum of 3-(4-(dodecyloxy)phenyl)-4-nitro-1-phenylbutan-1-one (**6**)

### 3.3.4 Synthesis of 3-(4-(dodecyloxy)phenyl)-*N*-(3-(4-(dodecyloxy)phenyl) 5-phenyl-2*H*-pyrrol-2-ylidene)-5-phenyl-1*H*-pyrrol-2-amine (7)

Compound **6** was then put together to assemble the aza-dipyyromethene core. 3-(4-(Dodecyloxy)phenyl)-*N*-(3-(4-(dodecyloxy)phenyl)-5-phenyl-2*H*-pyrrol-2-ylidene)-5-phenyl-1*H*-pyrrol-2-amine (**7**) was assembled from a refluxing reaction of 3-(4-(dodecyloxy)phenyl)-4-nitro-1-phenylbutan-1-one (**6**) and ammonium acetate in 1-butanol in 24 h (the mechanism as shown in **Figure 3.12**). Although the starting material was completely converted to the corresponding product (checked with TLC) in 8 h, the product was obtained in only 14% yield after silica-gel column chromatography (hexanes:dichloromethane at 1:1).

The product **7** was characterized by $^{1}$H NMR spectroscopy (**Figure 3.13**). There were 5 signals in aromatic region which were observed at chemical shifts ranging from δ 6.95 to 8.02 ppm. Since the structure of aza-dipyrromethane is symmetrical

NMR signals of equivalent protons appear at the same position. The signals of protons in aza-dipyrromethane core were observed as singlet protons at δ 7.10 ppm. Moreover, the signals of proton in dodecyloxy side chain groups were found at similar positions to that of 4-(dodecyloxy)benzaldehyde (**4**).

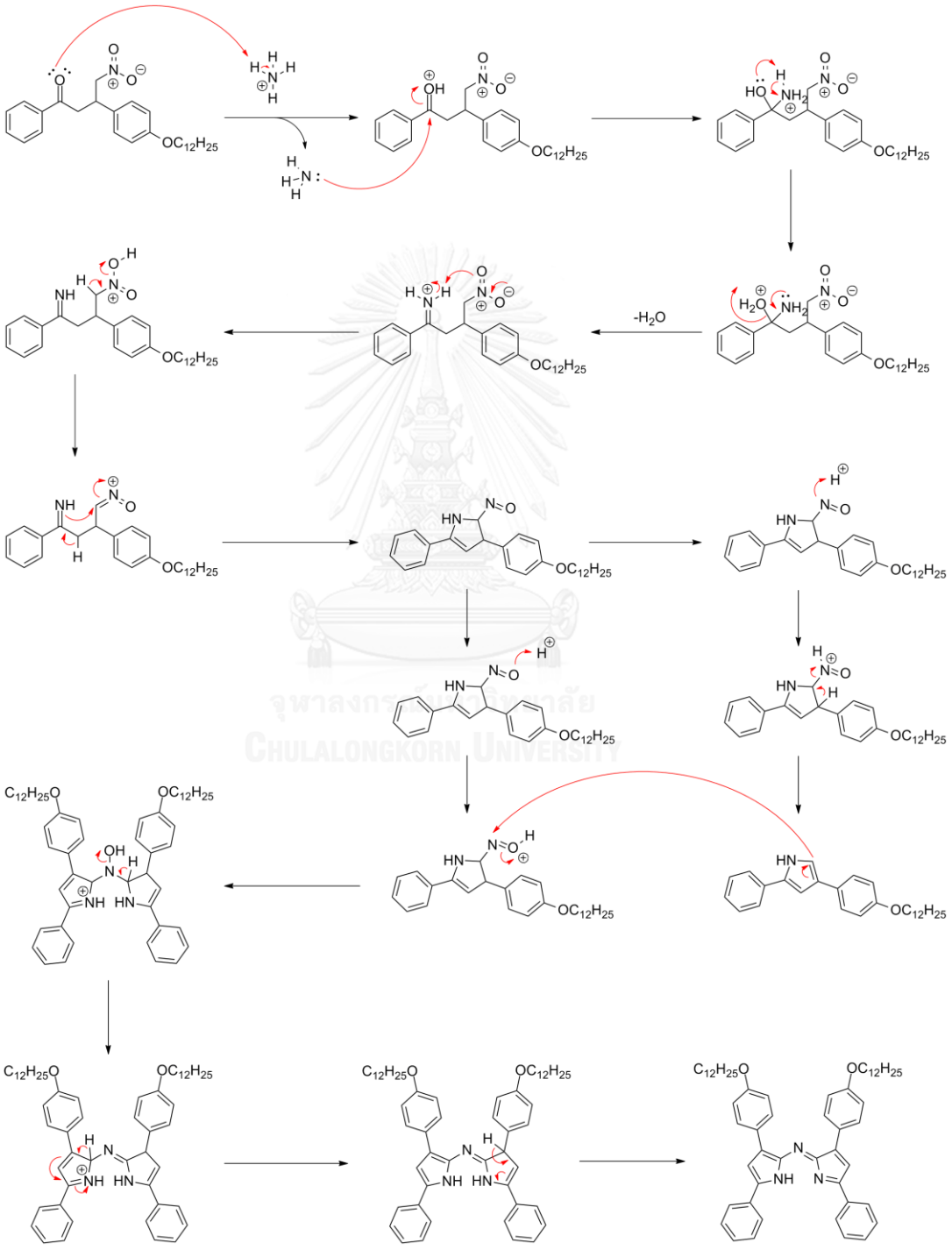


**Figure 3.12** The mechanism of aza-dipyrromethene condensation.

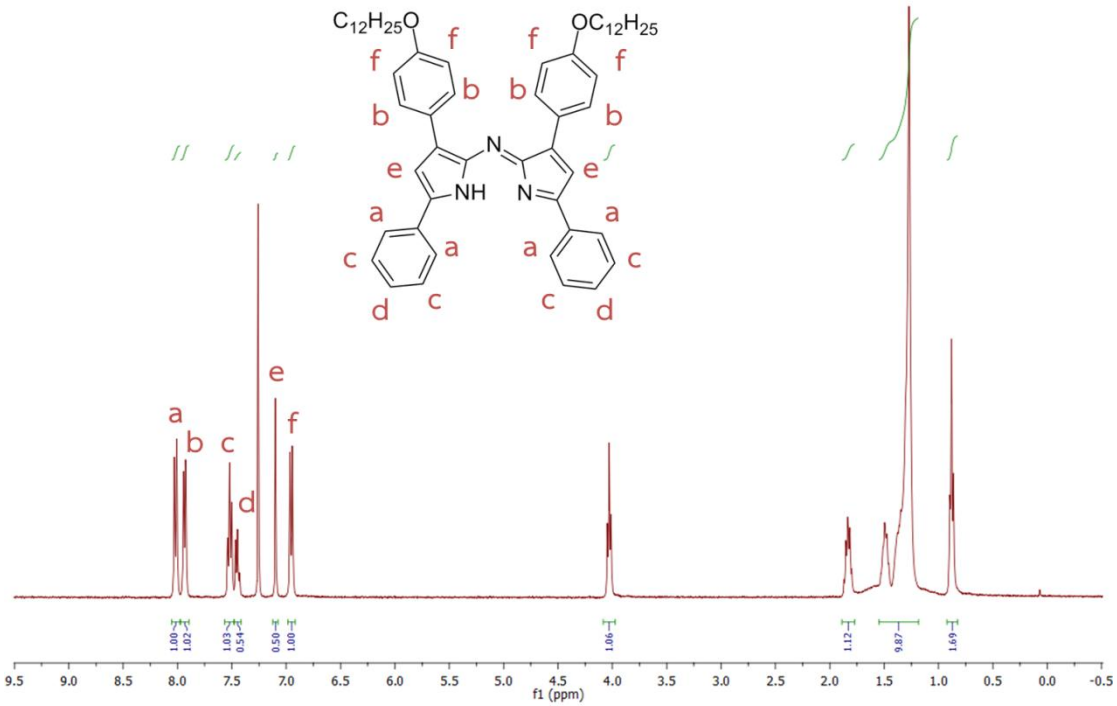


**Figure 3.13** The $^{1}$H NMR spectrum of 3-(4-(dodecyloxy)phenyl)-*N*-(3-(4-(dodecyloxy) phenyl)-5-phenyl-2*H*-pyrrol-2-ylidene)-5-phenyl-1*H*-pyrrol-2-amine (**7**)

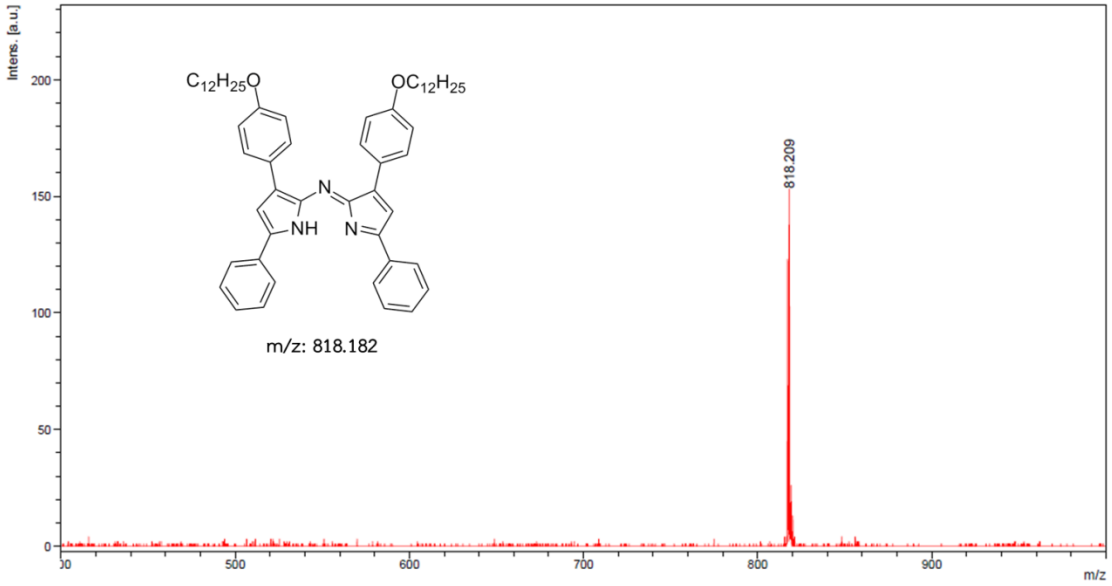


**Figure 3.14** The MALDI-TOF mass spectrum of 3-(4-(dodecyloxy)phenyl)-*N*-(3-(4-(dodecyloxy)phenyl)-5-phenyl-2*H*-pyrrol-2-ylidene)-5-phenyl-1*H*-pyrrol-2-amine (**7**)

In addition, MALDI-TOF mass spectral analysis was also used to confirm the structure of 3-(4-(dodecyloxy)phenyl)-*N*-(3-(4-(dodecyloxy)phenyl)-5-phenyl-2*H*-pyrrol-2-ylidene)-5-phenyl-1*H*-pyrrol-2-amine (**7**). The molecular ion peak was found at 818.209 which was consistent with calculated exact mass of 818.182 (**Figure 3.14**).

### 3.3.5 Synthesis of 4,4-difluoro-1,7-bis(4-dodecyloxyphenyl)-3,5-diphenyl-4-bora-3a,4a,8-triaza-*s*-indacene (8)

Compound **7** was then used as a starting material to prepare the BODIPY core **8**. 4,4-Difluoro-1,7-bis(4-dodecyloxyphenyl)-3,5-diphenyl-4-bora-3a,4a,8-triaza-*s*-indacene (**8**) was synthesized by a reaction of aza-dipyrromethane (**7**) with diisopropylamine (DIPEA) in the presence of boron trifluoride diethyl etherate ($BF_3{\cdot}OEt_2$). The reaction mixture was refluxed until the starting material was completely converted to the corresponding product (checked with TLC). After a workup, the crude product was further purified by silica-gel column chromatography using hexanes:dichloromethane at 3:2 as eluent. Product was obtained in 49% yield.

The $^{1}$H NMR spectrum of 4,4-difluoro-1,7-bis(4-dodecyloxyphenyl)-3,5-diphenyl-4-bora-3a,4a,8-triaza-s-indacene (**8**) showed most of proton signals similar to 3-(4-(dodecyloxy)phenyl)-*N*-(3-(4-(dodecyloxy)phenyl)-5-phenyl-2*H*-pyrrol-2-ylidene)-5-phenyl-1*H*-pyrrol-2-amine (**7**) that a little shield of singlet C-H proton signal at β-positions on aza-dipyrromethane core (**Figure 3.15**). The $^{13}$C NMR spectrum of 4,4-difluoro-1,7-bis(4-dodecyloxyphenyl)-3,5-diphenyl-4-bora-3a,4a,8-triaza-s-indacene (**8**) exhibited 12 carbons of aza-BODIPY and 12 carbons of dodecyloxy group due to aza-BODIPY (**8**) is symmetry (**Figure 3.16**).

The 2D NMR spectrum was used to confirm the structure of 4,4-difluoro-1,7-bis(4-dodecyloxyphenyl)-3,5-diphenyl-4-bora-3a,4a,8-triaza-s-indacene (**8**) with the hsqc spectrum indicated the singlet C-H proton signal at β-positions on aza-dipyrromethane core with peak at 6.90 ppm is bonded to the $^{13}$C with peak at 117.39 ppm (**Figure 3.17**).

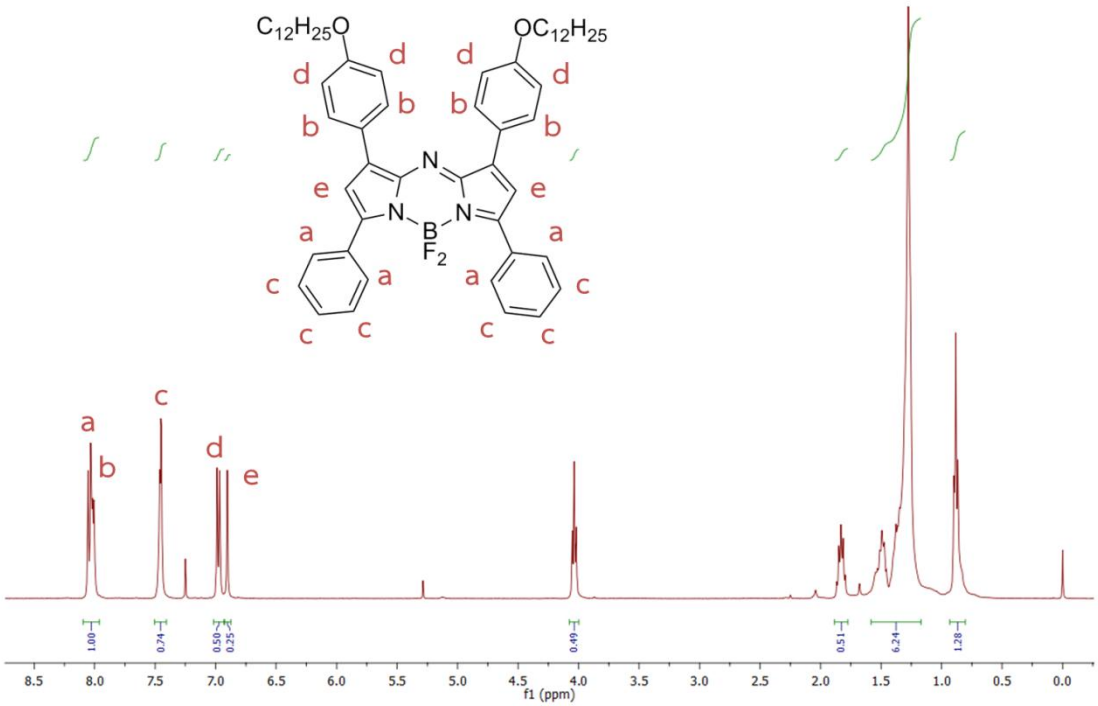


**Figure 3.15** The $^{1}$H NMR spectrum of 4,4-difluoro-1,7-bis(4-dodecyloxyphenyl)-3,5-diphenyl-4-bora-3a,4a,8-triaza-s-indacene (**8**)

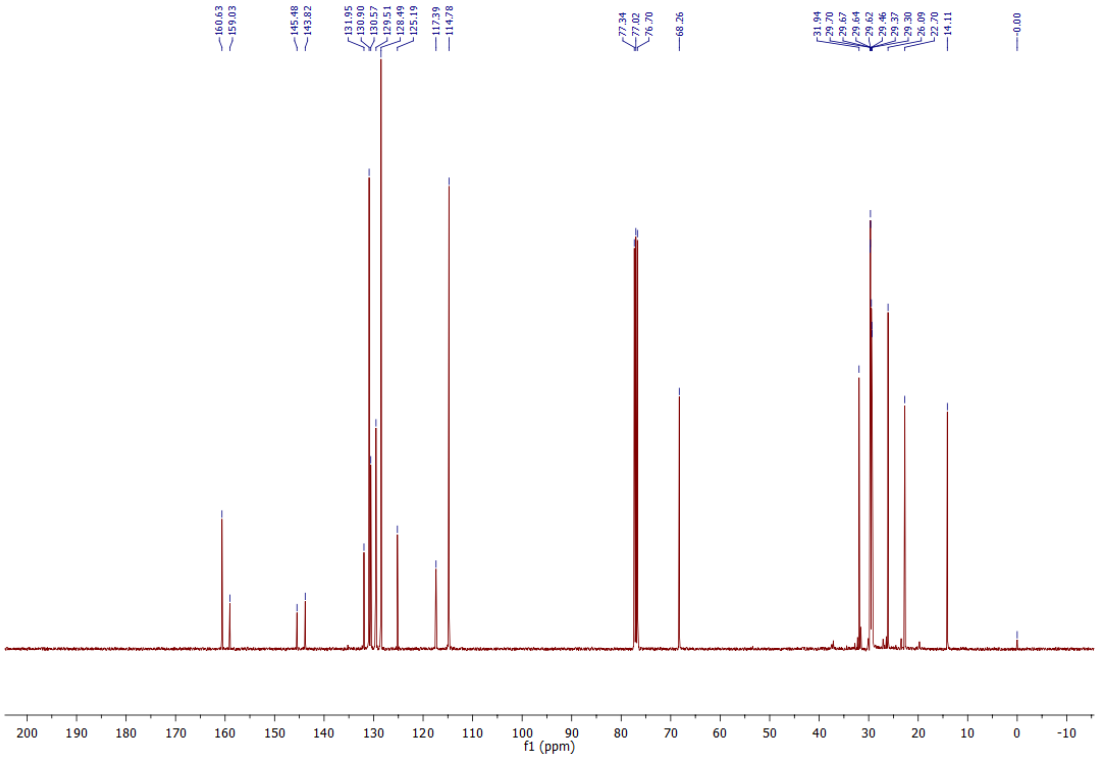


**Figure 3.16** The $^{13}$C NMR spectrum of 4,4-difluoro-1,7-bis(4-dodecyloxyphenyl)-3,5-diphenyl-4-bora-3a,4a,8-triaza-*s*-indacene (**8**)

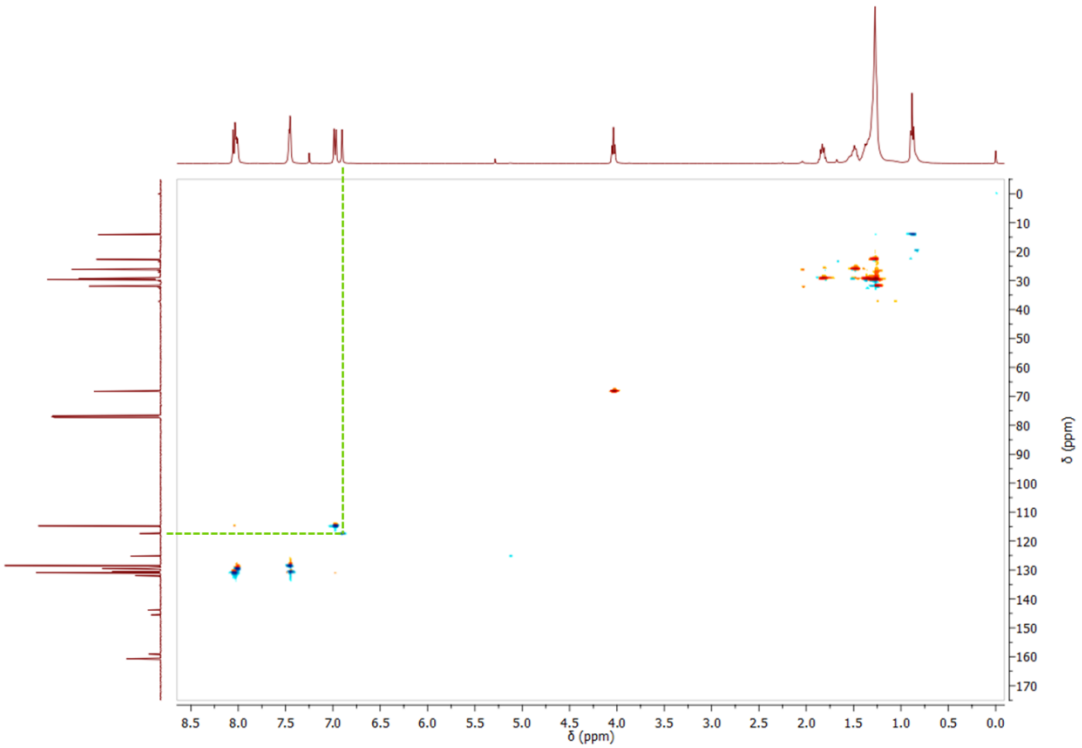


**Figure 3.17** The hsqc spectrum of 4,4-difluoro-1,7-bis(4-dodecyloxyphenyl)-3,5-diphenyl-4-bora-3a,4a,8-triaza-*s*-indacene (**8**)

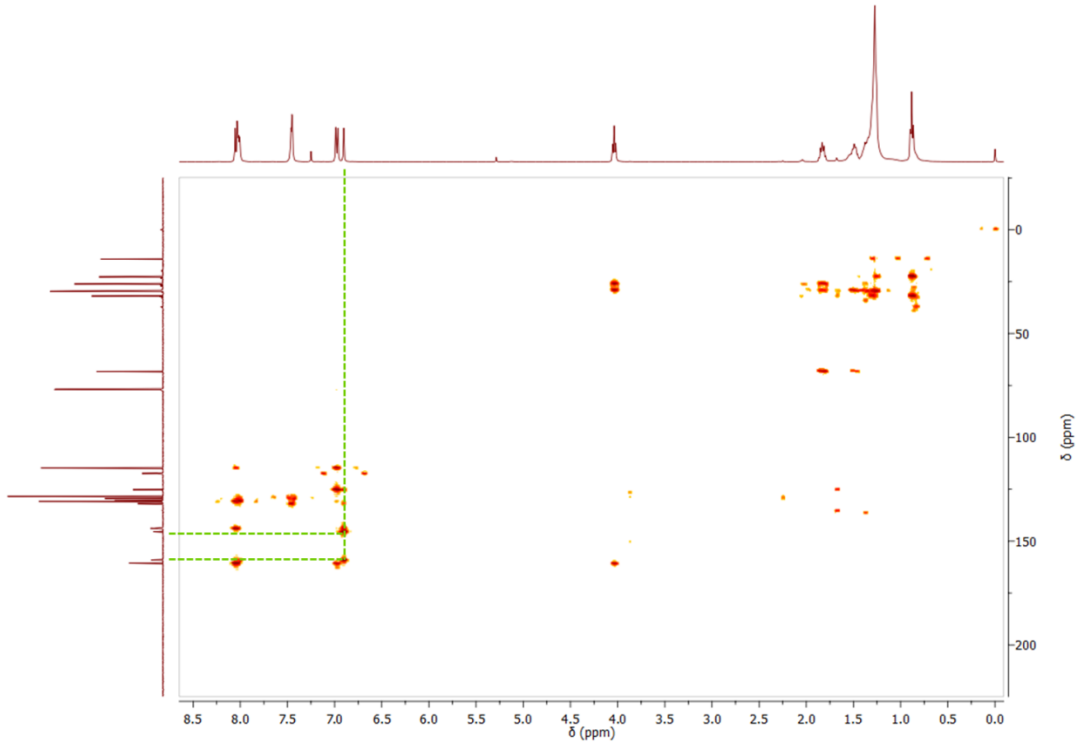


**Figure 3.18** The HMBC spectrum of 4,4-difluoro-1,7-bis(4-dodecyloxyphenyl)-3,5-diphenyl-4-bora-3a,4a,8-triaza-*s*-indacene (**8**)

The HMBC spectrum of 4,4-difluoro-1,7-bis(4-dodecyloxyphenyl)-3,5-diphenyl-4-bora-3a,4a,8-triaza-s-indacene (**8**) was shown in **Figure 3.18** that the singlet C-H proton signal at β- positions on aza-dipyrromethane core coupling with the α, β carbon atom on aza-dipyrromethane core at 145.48 and 159.03 ppm.

### 3.3.6 Synthesis of 2,6-dibromo-4,4-difluoro-1,7-bis(4-dodecyloxyphenyl)-3,5-diphenyl-4-bora-3a,4a,8-triaza-*s*-indacene (9)

In order to prepare a position on the BODIPY core ready to be linked with the alkynyl group of porphyrin **3** through a Sonogashira coupling, a monobromination on one of the BODIPY core is desired. In several attempts to carry out a mono bromination reation on 4,4-difluoro-1,7-bis(4-dodecyloxyphenyl)-3,5-diphenyl-4-bora-3a,4a,8-triaza-*s*-indacene (**8**) with 0.5, 1 or 2 equivalents of *N*-bromosuccinimide at room temperature failed to yield the desired product. Instead, the dibrominated product, 2,6-dibromo-4,4-difluoro-1,7-bis(4-dodecyloxyphenyl)-3,5-diphenyl-4-bora-3a,4a, 8-triaza-*s*-indacene (**9**), was obtained in 68% yield.

The $^{1}$H NMR spectrum of 2,6-dibromo-4,4-difluoro-1,7-bis(4-dodecyloxyphenyl)-3,5-diphenyl-4-bora-3a,4a,8-triaza-*s*-indacene (**9**) was shown in **Figure 3.19**. Most of the proton signals are similar to that of 4,4-difluoro-1,7-bis(4-dodecyloxyphenyl)-3,5-diphenyl-4-bora-3a,4a,8-triaza-*s*-indacene (**8**). No singlet signal of the C-H proton on the aza-dipyrromethane core in the desired product was observed. This confirmed the dibromination had taken place.

The suitable aza-BODIPY to react with the synthesized porphyrin would be the monobrominated product **10**. It was anticipated that changing from a bromine to an iodine would provide an alternative compound to be linked with the prophyrin unit. Therefore, several attempts to synthesize an alternative monoiodinated product based on a literature procedure [40] were carried out in parallel to attempts in bromination. However, none proved successful. The iodination did not occur under this condition and this reaction appeared only starting material (**8**).

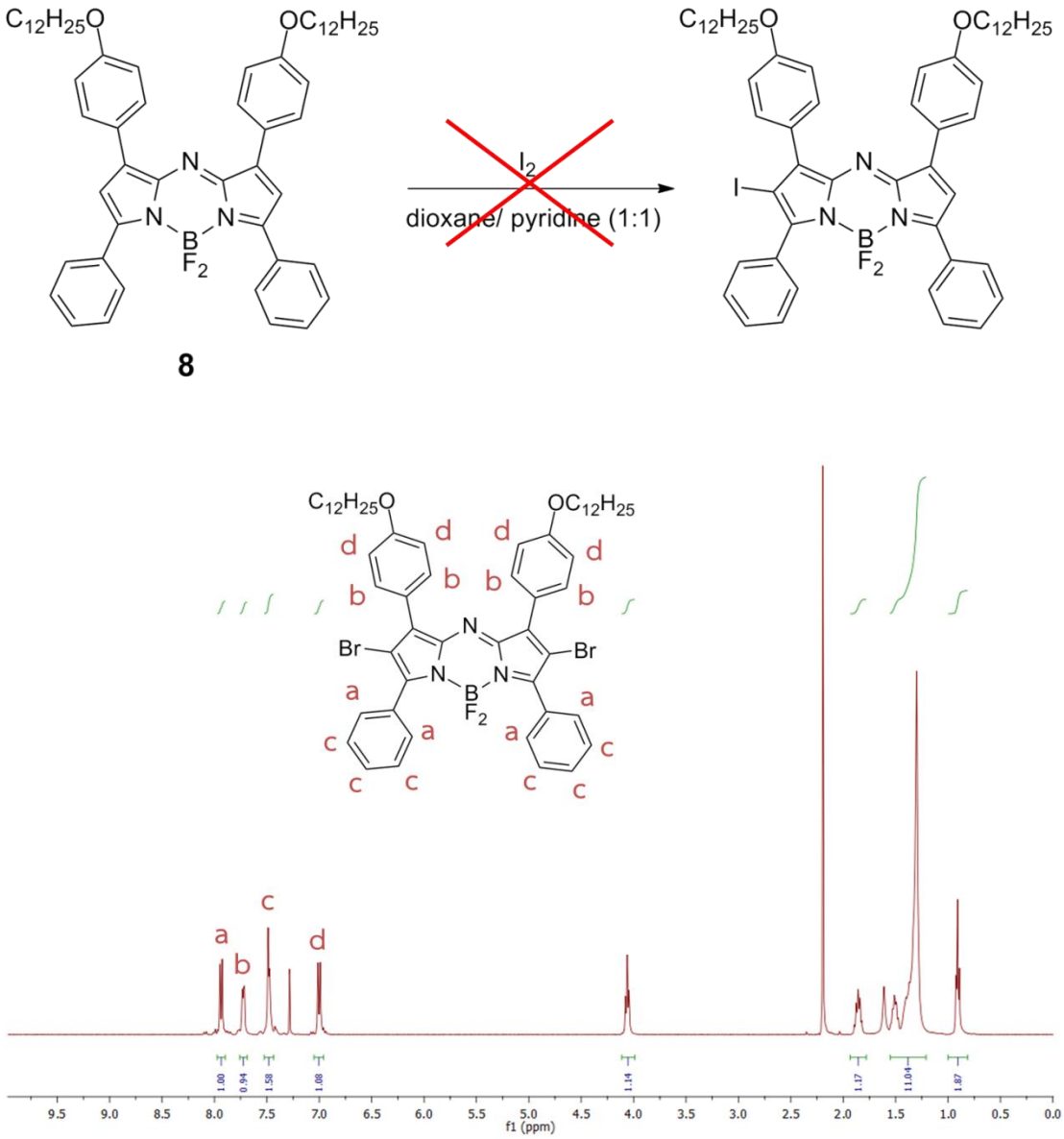


**Figure 3.19** The $^{1}$H NMR spectrum of 2,6-dibromo-4,4-difluoro-1,7-bis(4-dodecyloxy phenyl)-3,5-diphenyl-4-bora-3a,4a,8-triaza-s-indacene (**9**)

### 3.3.7 Synthesis of 2-bromo-4,4-difluoro-1,7-bis(4-dodecyloxyphenyl)-3,5-diphenyl-4-bora-3a,4a,8-triaza-*s*-indacene (10)

The conditions used in attempts to carry out a monobromination may be too harsh resulting in the dibromination instead. Therefore, the reaction temperature has been decreased from room temperature to 0°C. Furthermore, a solution of *N*-bromosuccinimide was added very slowly to a solution of 4,4-difluoro-1,7-bis(4-

dodecyloxyphenyl)-3,5-diphenyl-4-bora-3a,4a,8-triaza-*s*-indacene (**8**). 2-Bromo-4,4-difluoro-1,7-bis(4-dodecyloxyphenyl)-3,5-diphenyl-4-bora-3a,4a,8-triaza-*s*-indacene (**10**) was then successfully synthesized. The reaction was quenched by an addition sodium bicarbonate ($NaHCO_3$) and washed with sodium hydroxide (NaOH) to give the product in a satisfactory 69% yield (the product did not occur dibrominated product) and then characterized by $^1$H NMR spectroscopy and MALDI-TOF mass spectrometry.

The $^1$H NMR spectrum of 2-bromo-4,4-difluoro-1,7-bis(4-dodecyloxyphenyl)-3,5-diphenyl-4-bora-3a,4a,8-triaza-*s*-indacene (**10**) showed most of the proton signals like that of 3-(4-(dodecyloxy)phenyl)-*N*-(3-(4-(dodecyloxy)phenyl)-5-phenyl-2*H*-pyrrol-2-ylidene)-5-phenyl-1*H*-pyrrol-2-amine (**7**). However, since the structure of compound **10** is asymmetric, the proton signals appeared at different position. The peak of the only proton in the aza-BODIPY core was observed because the other proton was replaced by bromine (**Figure 3.20**).

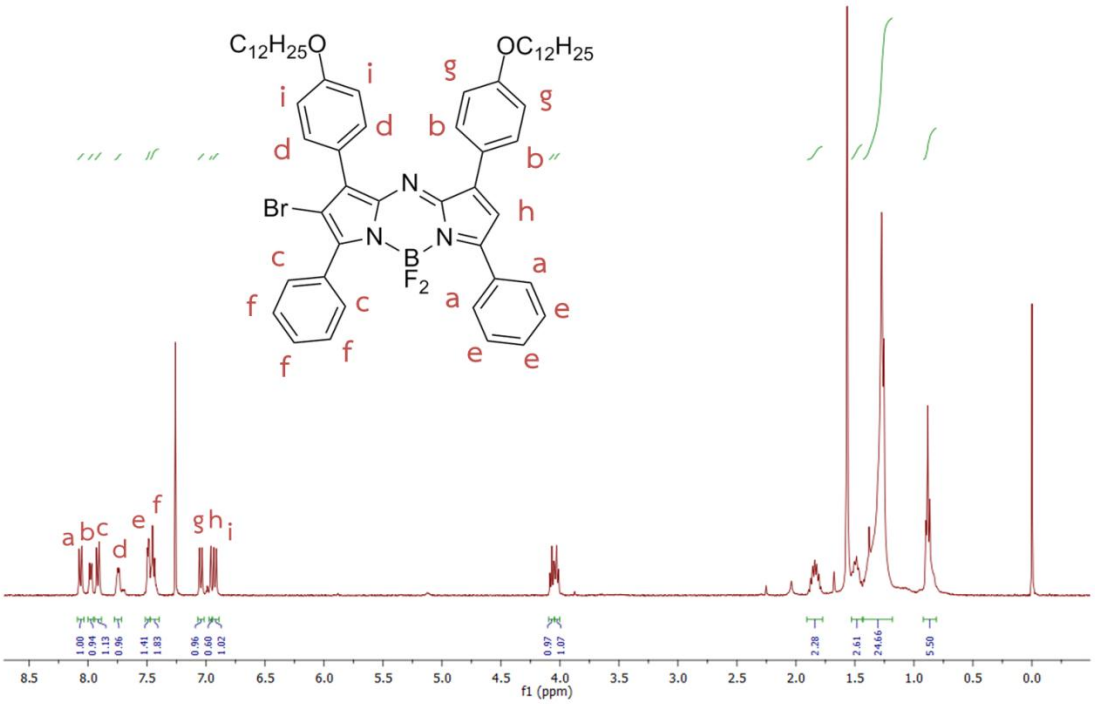


**Figure 3.20** The $^1$H NMR spectrum of 2-bromo-4,4-difluoro-1,7-bis(4-dodecyloxy phenyl)-3,5-diphenyl-4-bora-3a,4a,8-triaza-s-indacene (**10**)

In addition, MALDI-TOF mass analysis was used to confirm the structure of 2-bromo-4,4-difluoro-1,7-bis(4-dodecyloxyphenyl)-3,5-diphenyl-4-bora-3a,4a,8-triaza-*s*-indacene (**10**) with the molecular ion peak found at 944.365 which was consistent with calculated exact mass of 944.878 (**Figure 3.21**).

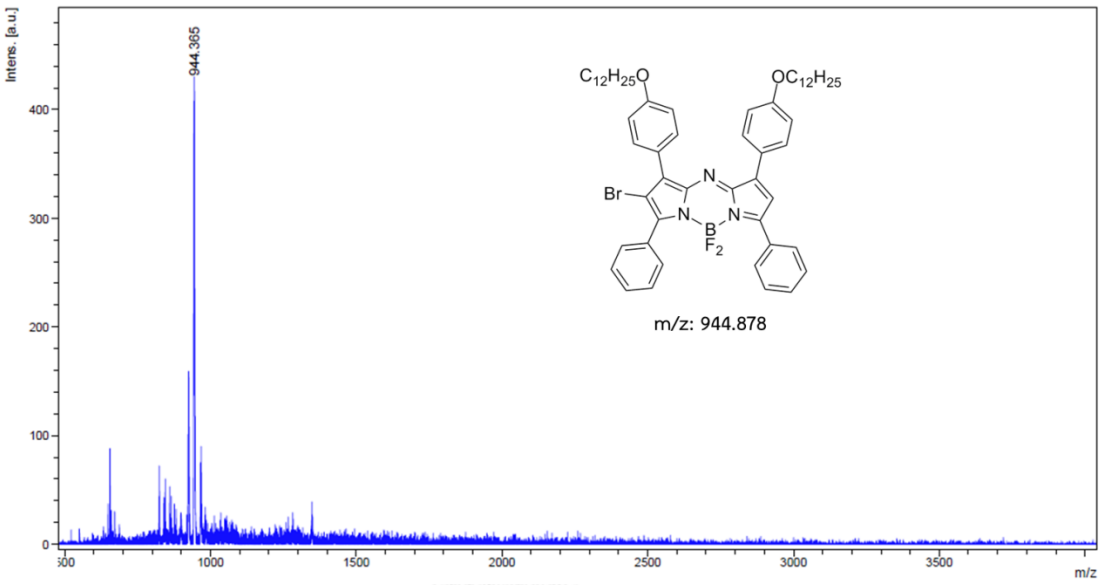


**Figure 3.21** The MALDI-TOF mass spectrum of 2-bromo-4,4-difluoro-1,7-bis(4-dodecyloxyphenyl)-3,5-diphenyl-4-bora-3a,4a,8-triaza-*s*-indacene (**10**)



### 3.4 Synthesis of aza-BODIPY-porphyrin (11)

Aza-BODIPY-porphyrin was synthesized *via* Pd (0) catalyzed Sonogashira coupling in 3 routes (**Scheme 3.4**). First, the synthesis of target molecule *via* Pd (0) catalyzed Sonogashira coupling with 3 equivalent of monobrominated aza-BODIPY (**10**) and 1 equivalent of precursor porphyrin (**3**) and 4-iodobenzoic acid. This route did not occur because the minimal scale of reaction. It's hard to predict the product. Second, the synthesis of target molecule *via* Pd (0) catalyzed Sonogashira coupling with 1 equivalent of precursor porphyrin (**3**) and 1 equivalent 4-iodobenzoic acid. After that, 1 equivalent of monobrominated aza-BODIPY was added. This route is in progress.

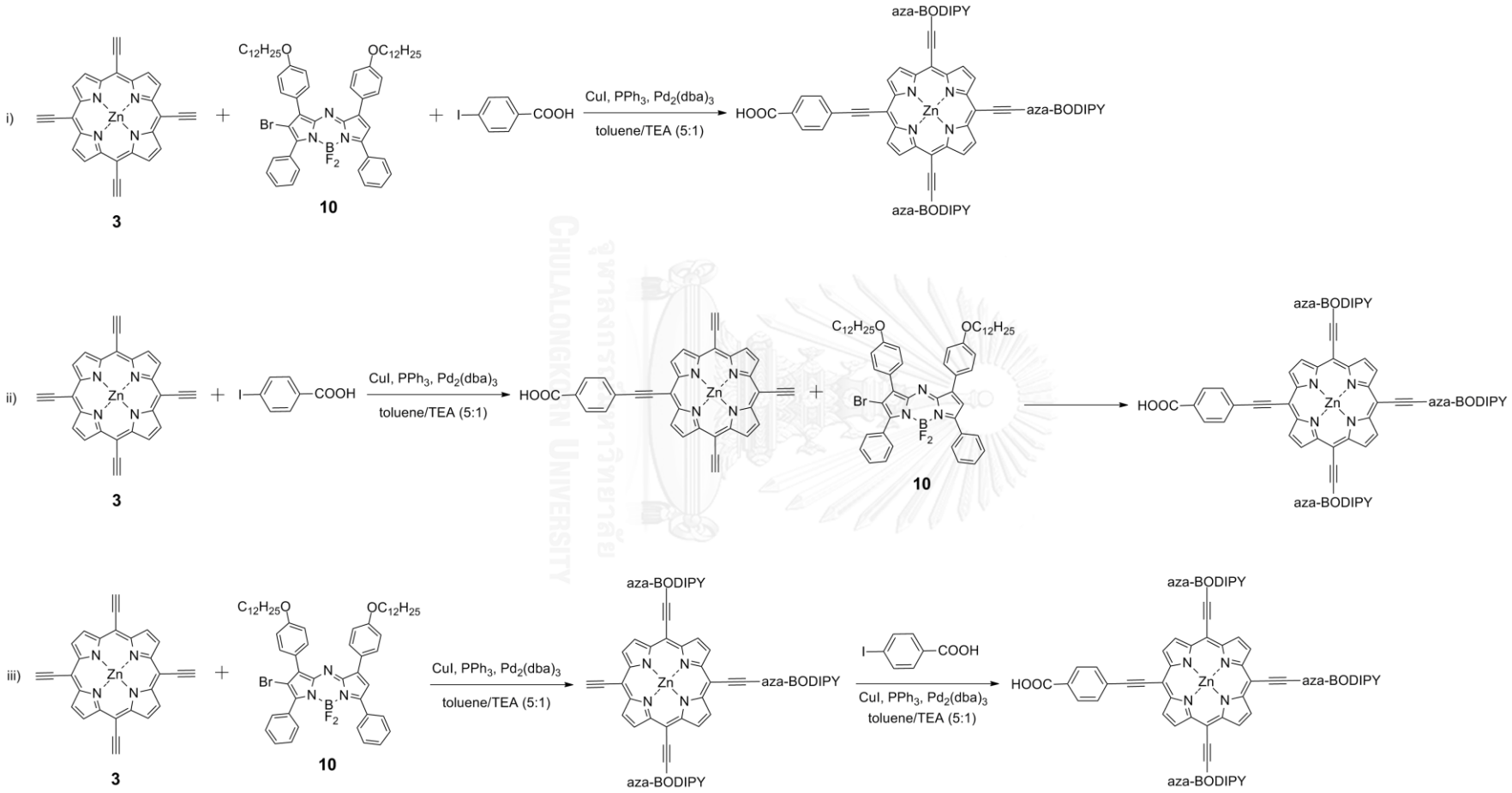


**Scheme 3.4** The propose route to synthesis of aza-BODIPY-porphyrin

Finally, the synthesis of target molecule *via* Pd (0) catalyzed Sonogashira coupling with 3 equivalent of monobrominated aza-BODIPY (**10**) and 1 equivalent of precursor porphyrin (**3**). After a workup, the crude product was further purified by silica-gel column chromatography using hexanes/dichloromethane at 1:1 as an eluent.

The $^{1}$H NMR spectrum of aza-BODIPY-porphyrin (**11**) did not confirm the structure because the minimal scale and impurity of the reaction. It's hard to predict the product.

In addition, the product was analyzed by UV-visible spectroscopy (**Figure 3.22**). The spectrum consist of wavelength maxima at 425, 453, and strong maximum wavelength at 666 nm. The combination of characteristic absorption peaks of [5,10,15,20-ethynylporphinato] zinc(II) (**3**) and 4,4-difluoro-1,7-bis(4-dodecyloxyphenyl)-3,5-diphenyl-4-bora-3a,4a,8-triaza-s-indacene (**8**) but did not confirm the aza-BODIPY-porphyrin conjugated system.

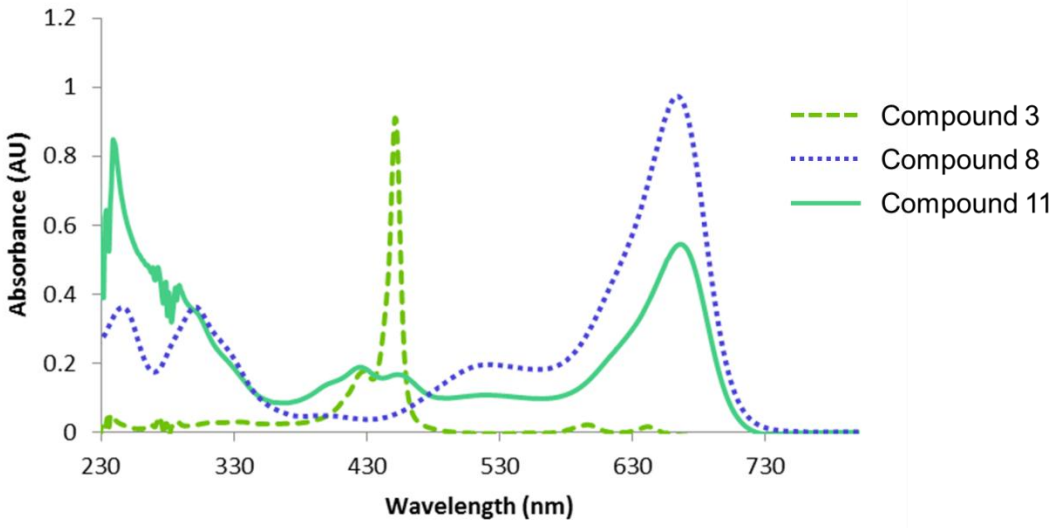


**Figure 3.22** The UV-visible spectrum of [5,10,15,20-ethynylporphinato] zinc(II) (**3**), 4,4-difluoro-1,7-bis(4-dodecyloxyphenyl)-3,5-diphenyl-4-bora-3a,4a,8-triaza-s-indacene (**8**) and aza-BODIPY-porphyrin (**11**).

# CHAPTER IV

# CONCLUSION

The *meso*-alkyne-linked porphyrin zinc complex (**3**) was synthesized in 3 steps (44 %yield) and consisted of a strong absorption (the Soret or B band) at about 451 nm. Another absorption is a weak absorption bands (the Q band) at 596 and 641 nm. Brominated aza-BODIPY (**10**) was synthesized in 6 steps (68 %yield) and can absorb light in the green region (665 nm). Consequently, aza-BODIPY-porphyrin (**11**) was synthesized by Sonogashira coupling reaction of [5,10,15,20-ethynylporphinato] zinc(II) (**3**) with 2-bromo-4,4-difluoro-1,7-bis(4-dodecyloxyphenyl)-3,5-diphenyl-4-bora-3a,4a,8-triaza-*s*-indacene (**10**) can absorb light in the UV-visible region (425, 453, 521 and 666 nm but did not confirmed the aza-BODIPY-porphyrin conjugated system. The aza-BODIPY-porphyrin revealed wide absorption spectrum which can be applied in several applications such as dye sensitized solar cell.

## REFERENCES


[1] Milgrom, L.R. The Colours of Life: An Introduction to the Chemistry of Porphyrins and Related Compounds. Oxford: OUP. 1975.

[2] Thunell, S. Porphyrins, porphyrin metabolism and porphyrias. I. Update. Scandinavian Journal of Clinical and Laboratory Investigation 60(7) (2009): 509-540.

[3] L. Anderson, H. Building molecular wires from the colours of life: conjugated porphyrin oligomers. Chemical Communications (23) (1999): 2323-2330.

[4] Rothemund, P. and Menotti, A.R. Porphyrin Studies. IV.1 The Synthesis of α,β,γ,δ-Tetraphenylporphine. J. Am. Chem. Soc. 63(1) (1941): 267-270.

[5] Rothemund, P. FORMATION OF PORPHYRINS FROM PYRROLE AND ALDEHYDES. J. Am. Chem. Soc. 57(10) (1935): 2010-2011.

[6] Adler, A.D., Longo, F.R., Finarelli, J.D., Goldmacher, J., Assour, J., and Korsakoff, L. A simplified synthesis for meso-tetraphenylporphine. The Journal of Organic Chemistry 32(2) (1967): 476-476.

[7] Lindsey, J.S., Schreiman, I.C., Hsu, H.C., Kearney, P.C., and Marguerettaz, A.M. Rothemund and Adler-Longo reactions revisited: synthesis of tetraphenylporphyrins under equilibrium conditions. The Journal of Organic Chemistry 52(5) (1987): 827-836.

[8] Kennedy, D.P., Kormos, C.M., and Burdette, S.C. FerriBRIGHT: A Rationally Designed Fluorescent Probe for Redox Active Metals. J. Am. Chem. Soc. 131(24) (2009): 8578-8586.

[9] Nierth, A., Kobitski, A.Y., Nienhaus, G.U., and Jäschke, A. Anthracene–BODIPY Dyads as Fluorescent Sensors for Biocatalytic Diels–Alder Reactions. J. Am. Chem. Soc. 132(8) (2010): 2646-2654.

[10] Golovkova, T.A., Kozlov, D.V., and Neckers, D.C. Synthesis and Properties of Novel Fluorescent Switches. The Journal of Organic Chemistry 70(14) (2005): 5545-5549.

[11] Trieflinger, C., Rurack, K., and Daub, J. “Turn ON/OFF your LOV light”: Borondipyrromethene–Flavin Dyads as Biomimetic Switches Derived from the LOV Domain. Angewandte Chemie International Edition 44(15) (2005): 2288-2291.

[12] Sunahara, H., Urano, Y., Kojima, H., and Nagano, T. Design and Synthesis of a Library of BODIPY-Based Environmental Polarity Sensors Utilizing Photoinduced Electron-Transfer-Controlled Fluorescence ON/OFF Switching. J. Am. Chem. Soc. 129(17) (2007): 5597-5604.

[13] Yin, S., Leen, V., Snick, S.V., Boens, N., and Dehaen, W. A highly sensitive, selective, colorimetric and near-infrared fluorescent turn-on chemosensor for Cu2+ based on BODIPY. Chemical Communications 46(34) (2010): 6329-6331.

[14] Kolemen, S., et al. Optimization of distyryl-Bodipy chromophores for efficient panchromatic sensitization in dye sensitized solar cells. Chemical Science 2(5) (2011): 949-954.

[15] Lee, C.Y. and Hupp, J.T. Dye Sensitized Solar Cells: TiO2 Sensitization with a Bodipy-Porphyrin Antenna System. Langmuir 26(5) (2010): 3760-3765.

[16] Treibs, A. and Kreuzer, F.-H. Difluorboryl-Komplexe von Di- und Tripyrrylmethenen. Justus Liebigs Annalen der Chemie 718(1) (1968): 208-223.

[17] Wagner, R.W. and Lindsey, J.S. Boron-dipyrromethene dyes for incorporation in synthetic multi-pigment light-harvesting arrays. in *Pure Appl. Chem.* 1996. 1373.

[18] Gorman, A., Killoran, J., O'Shea, C., Kenna, T., Gallagher, W.M., and O'Shea, D.F. In Vitro Demonstration of the Heavy-Atom Effect for Photodynamic Therapy. J. Am. Chem. Soc. 126(34) (2004): 10619-10631.

[19] Ronny, P., Justin, R.G., Janelle, N.L., Graham, S.-G., and Robert, S.G. Synthesis of Aza-BODIPY Boron Difluoride PDT Agents to Promote Apoptosis in HeLa Cells. Letters in Organic Chemistry 8(6) (2011): 368-373.

[20] Gawley, R.E., Mao, H., Haque, M.M., Thorne, J.B., and Pharr, J.S. Visible Fluorescence Chemosensor for Saxitoxin. The Journal of Organic Chemistry 72(6) (2007): 2187-2191.

[21] Coskun, A., Yilmaz, M.D., and Akkaya, E.U. Bis(2-pyridyl)-Substituted Boratriazaindacene as an NIR-Emitting Chemosensor for Hg(II). Organic Letters 9(4) (2007): 607-609.

[22] Jiang, X.-D., et al. Synthesis of NIR fluorescent thienyl-containing aza-BODIPY and its application for detection of Hg2+: Electron transfer by bonding with Hg2+. Dyes Pigm. 125 (2016): 136-141.

[23] Min, J., et al. Two Similar Near-Infrared (IR) Absorbing Benzannulated Aza-BODIPY Dyes as Near-IR Sensitizers for Ternary Solar Cells. ACS Applied Materials & Interfaces 5(12) (2013): 5609-5616.

[24] Lazarides, T., et al. Promising Fast Energy Transfer System via an Easy Synthesis: Bodipy–Porphyrin Dyads Connected via a Cyanuric Chloride Bridge, Their Synthesis, and Electrochemical and Photophysical Investigations. Inorganic Chemistry 50(18) (2011): 8926-8936.

[25] Kolemen, S., et al. Solid-State Dye-Sensitized Solar Cells Using Red and Near-IR Absorbing Bodipy Sensitizers. Organic Letters 12(17) (2010): 3812-3815.

[26] Sabatini, R.P., McCormick, T.M., Lazarides, T., Wilson, K.C., Eisenberg, R., and McCamant, D.W. Intersystem Crossing in Halogenated Bodipy Chromophores Used for Solar Hydrogen Production. The Journal of Physical Chemistry Letters 2(3) (2011): 223-227.

[27] Rogers, M.A.T. 156. 2 : 4-Diarylpyrroles. Part I. Synthesis of 2 : 4-diarylpyrroles and 2 : 2[prime or minute] : 4 : 4[prime or minute]-tetra-arylazadipyrromethines. Journal of the Chemical Society (Resumed) (0) (1943): 590-596.

[28] Davies, W.H. and Rogers, M.A.T. 46. 2 : 4-Diarylpyrroles. Part IV. The formation of acylated 5-amino-2 : 4-diphenylpyrroles from [small beta]-benzoly-[small alpha]-phenylpropionitrile and some notes on the Leuckart reaction. Journal of the Chemical Society (Resumed) (0) (1944): 126-131.

[29] Knott, E.B. 225. [small beta]-Cycloylpropionitriles. Part II. Conversion into bis-2-(5-cyclylpyrrole)azamethin salts. Journal of the Chemical Society (Resumed) (0) (1947): 1196-1201.

[30] Boyer, J.H., Haag, A.M., Sathyamoorthi, G., Soong, M.-L., Thangaraj, K., and Pavlopoulos, T.G. Pyrromethene–BF2 complexes as laser dyes: 2. Heteroatom Chemistry 4(1) (1993): 39-49.

[31] Tributsch, H. REACTION OF EXCITED CHLOROPHYLL MOLECULES AT ELECTRODES AND IN PHOTOSYNTHESIS*. Photochemistry and Photobiology 16(4) (1972): 261-269.

[32] Vlachopoulos, N., Liska, P., Augustynski, J., and Graetzel, M. Very efficient visible light energy harvesting and conversion by spectral sensitization of high surface area polycrystalline titanium dioxide films. J. Am. Chem. Soc. 110(4) (1988): 1216-1220.

[33] O'Regan, B. and Gratzel, M. A low-cost, high-efficiency solar cell based on dye-sensitized colloidal TiO2 films. Nature 353(6346) (1991): 737-740.

[34] Chen, C.-Y., et al. Highly Efficient Light-Harvesting Ruthenium Sensitizer for Thin-Film Dye-Sensitized Solar Cells. ACS Nano 3(10) (2009): 3103-3109.

[35] Yella, A., et al. Porphyrin-Sensitized Solar Cells with Cobalt (II/III)–Based Redox Electrolyte Exceed 12 Percent Efficiency. Science 334(6056) (2011): 629-634.

[36] Brizet, B., et al. B,B-Diporphyrinbenzyloxy-BODIPY dyes: synthesis and antenna effect. J. Org. Chem. 77(7) (2012): 3646-50.

[37] Whited, M.T., et al. Singlet and Triplet Excitation Management in a Bichromophoric Near-Infrared-Phosphorescent BODIPY-Benzoporphyrin Platinum Complex. J. Am. Chem. Soc. 133(1) (2011): 88-96.

[38] Gresser, R., Hartmann, H., Wrackmeyer, M., Leo, K., and Riede, M. Synthesis of thiophene-substituted aza-BODIPYs and their optical and electrochemical properties. Tetrahedron 67(37) (2011): 7148-7155.

[39] Karatay, A., et al. The effect of heavy atom to two photon absorption properties and intersystem crossing mechanism in aza-boron-dipyrromethene compounds. Dyes Pigm. 122 (2015): 286-294.

[40] Pascal, S., Bucher, L., Desbois, N., Bucher, C., Andraud, C., and Gros, C.P. Synthesis, Electrochemistry, and Photophysics of Aza‐BODIPY Porphyrin Dyes. Chemistry - European Journal 22(14) (2016): 4971-4979.

# APPENDIX

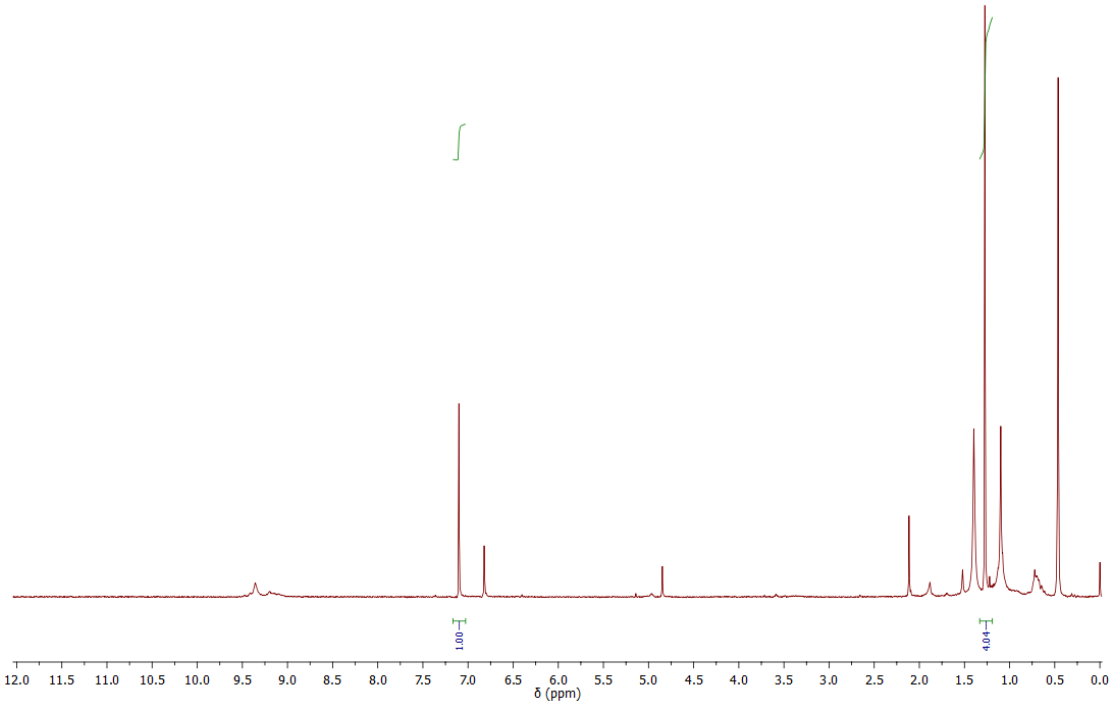


**Figure A-1** The $^{1}$H NMR spectrum of 5,10,15,20-trimethylsilylethynylporphyrin (**1**)

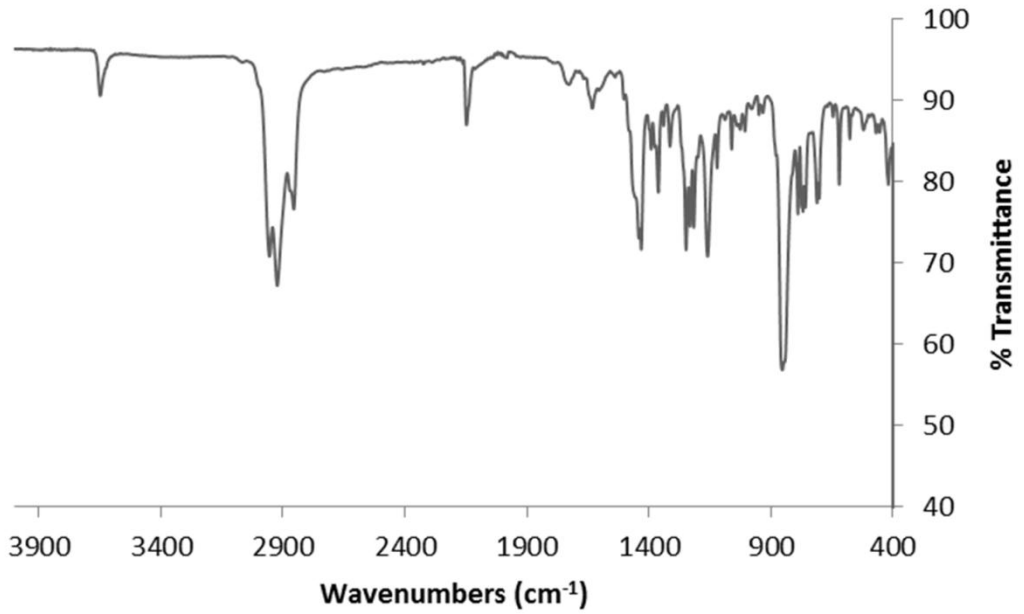


**Figure A-2** The IR spectrum of 5,10,15,20-trimethylsilylethynylporphyrin (**1**)

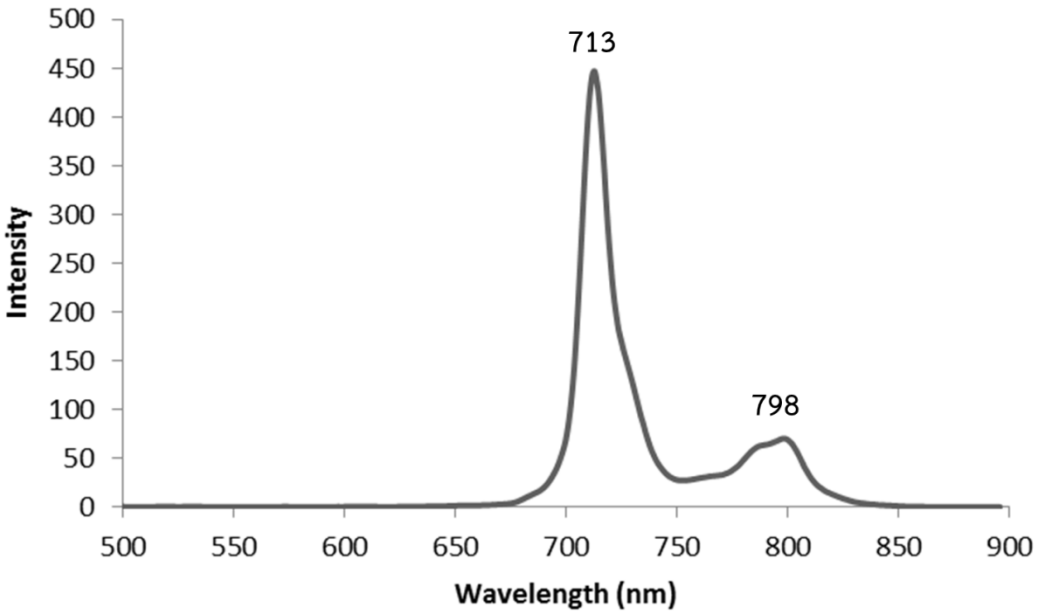


**Figure A-3** The fluorescence spectrum of 5,10,15,20-trimethylsilylethynylporphyrin (**1**)

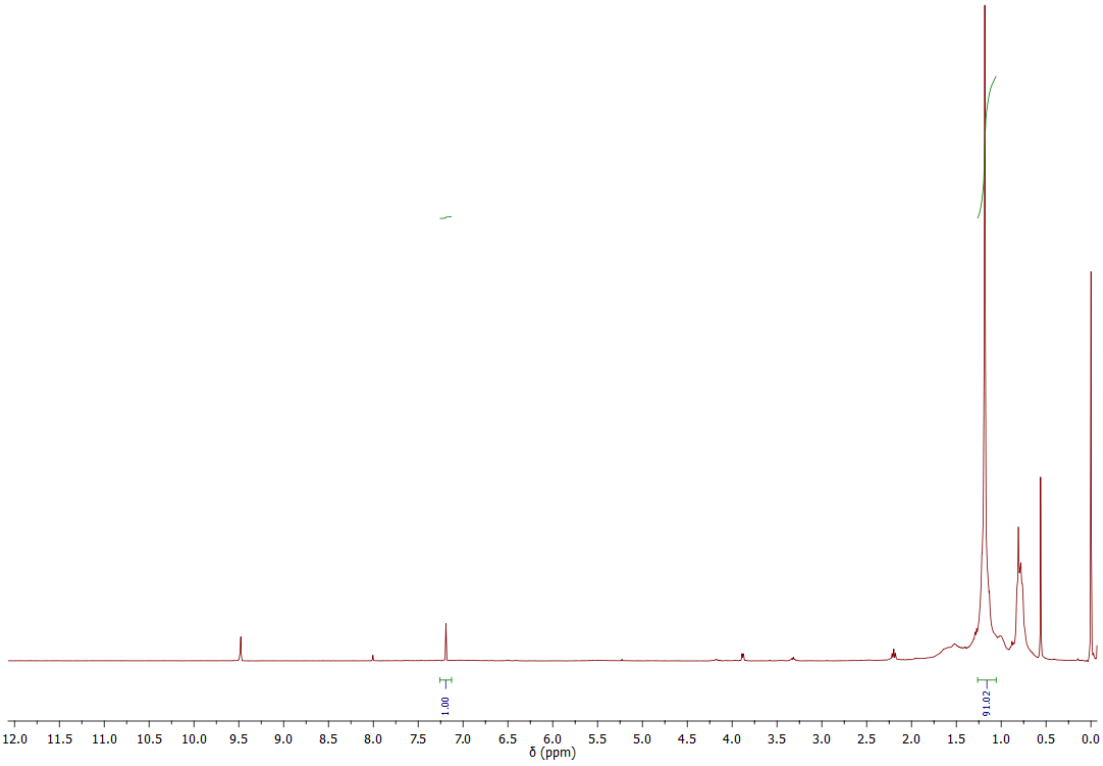


**Figure A-4** The $^{1}$H NMR of spectrum of [5,10,15,20-trimethylsilylethynylporphinato] zinc(II) (**2**)

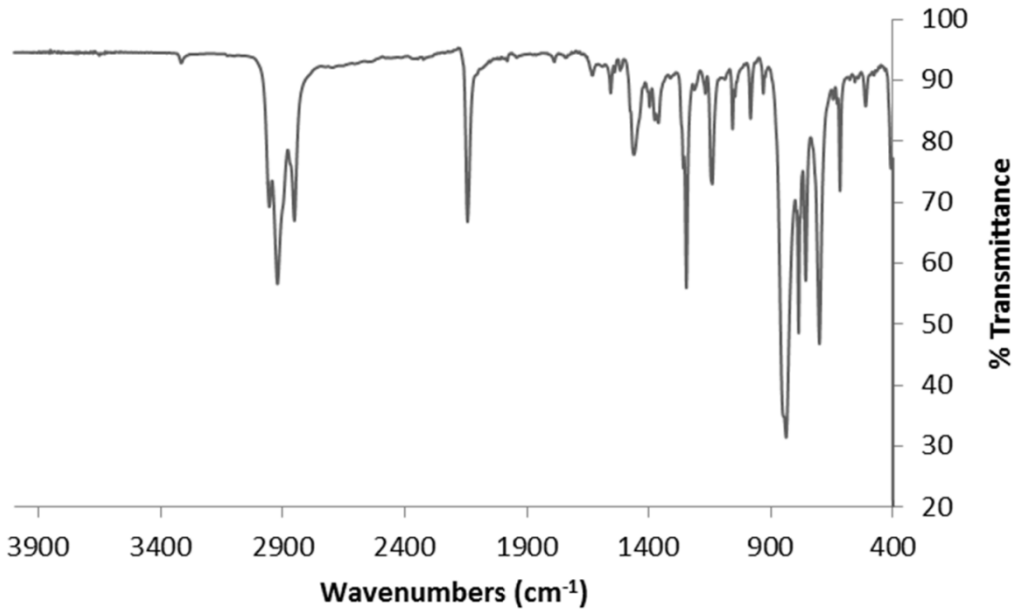


**Figure A-5** The IR spectrum of [5,10,15,20-trimethylsilylethynylporphinato] zinc(II) (**2**)

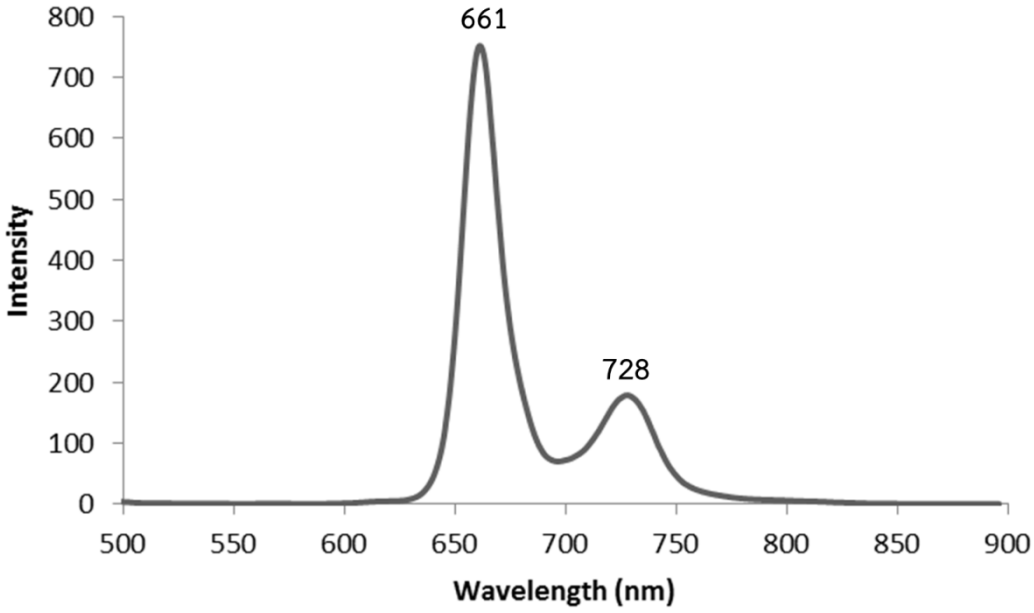


**Figure A-6** The fluorescence spectrum of [5,10,15,20-trimethylsilylethynyl porphinato] zinc(II) (**2**)

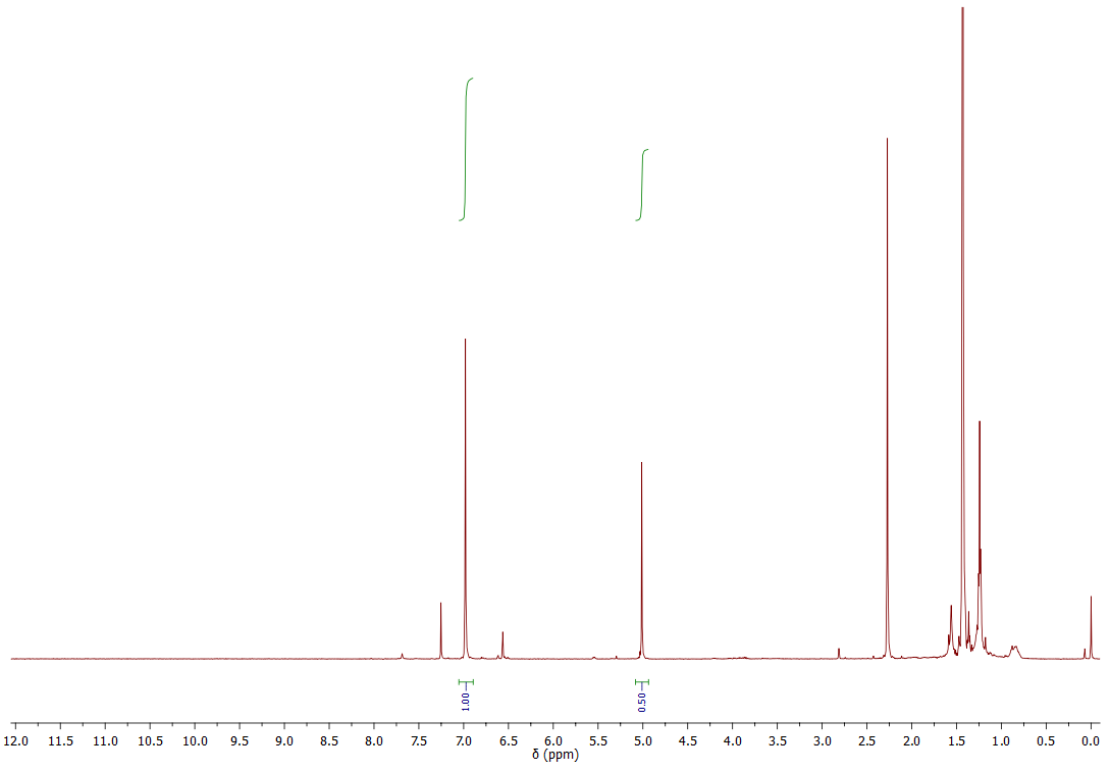


**Figure A-7** The $^{1}$H NMR spectrum of [5,10,15,20-ethynylporphinato] zinc(II) (**3**)

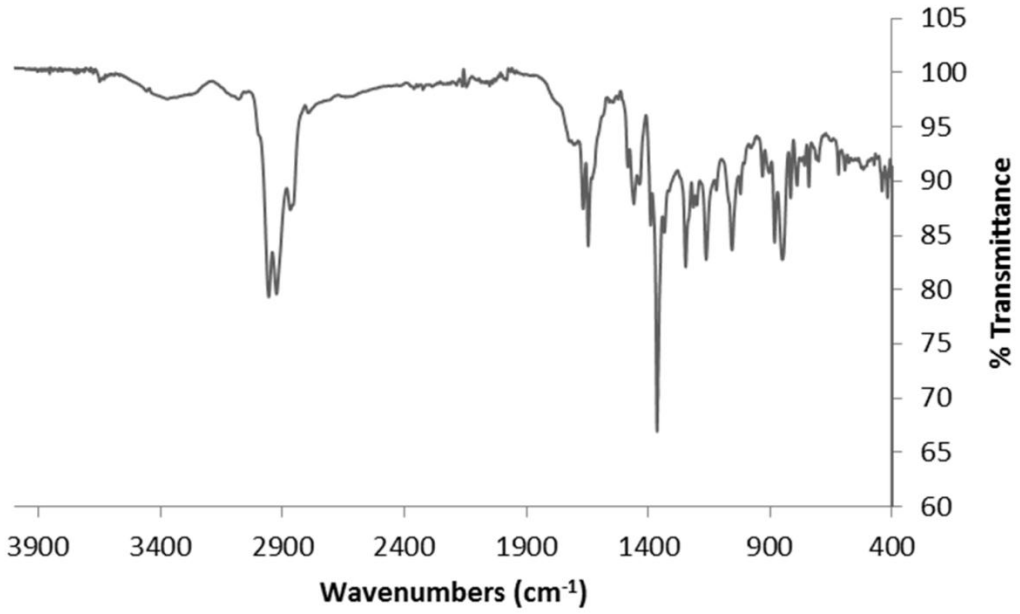


**Figure A-8** The IR spectrum of [5,10,15,20-ethynylporphinato] zinc(II) (**3**)

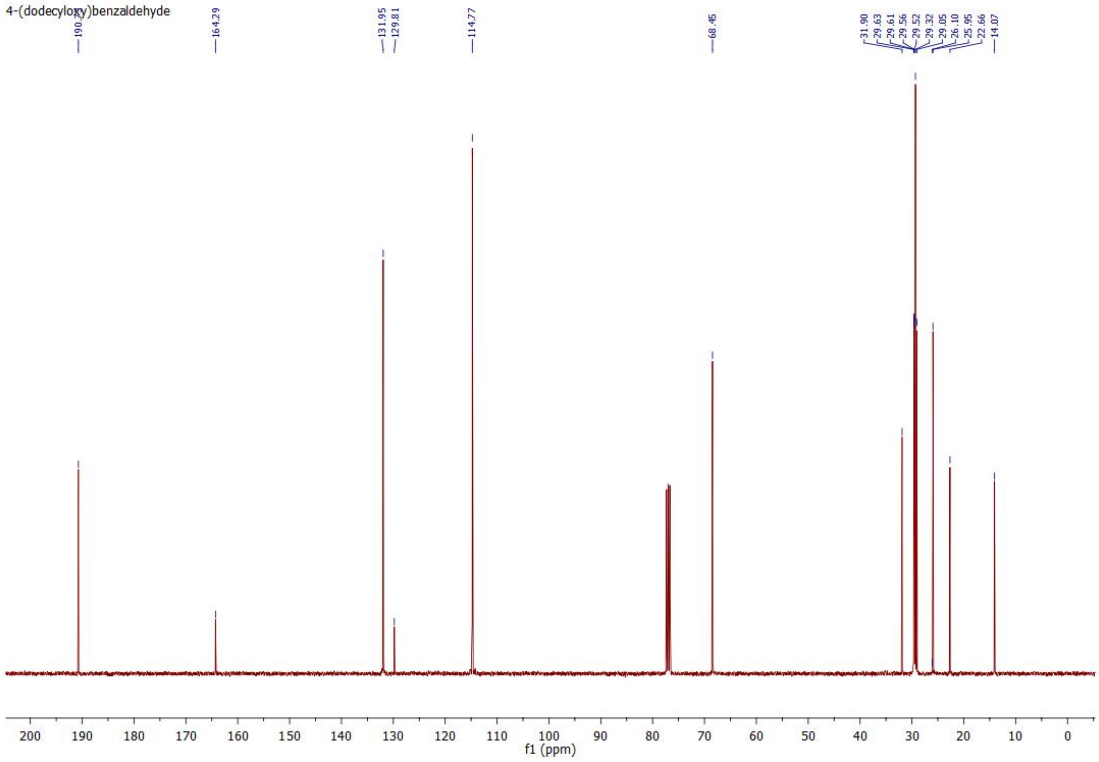


**Figure A-9** The $^{13}$C NMR spectrum of 4-(dodecyloxy)benzaldehyde (**4**)

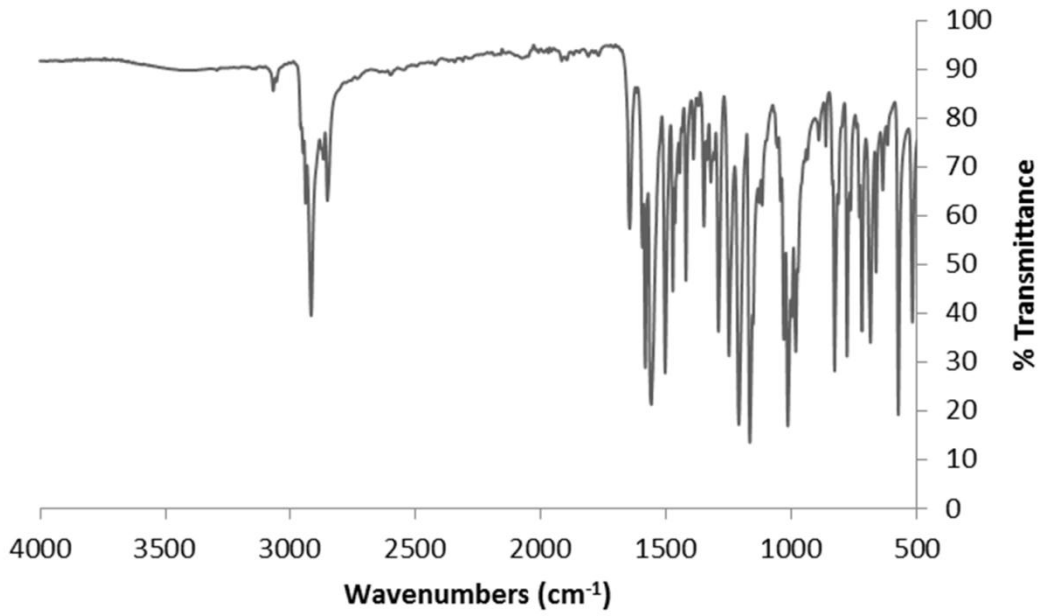


**Figure A-10** The IR spectrum of 4-(dodecyloxy)benzaldehyde (**4**)

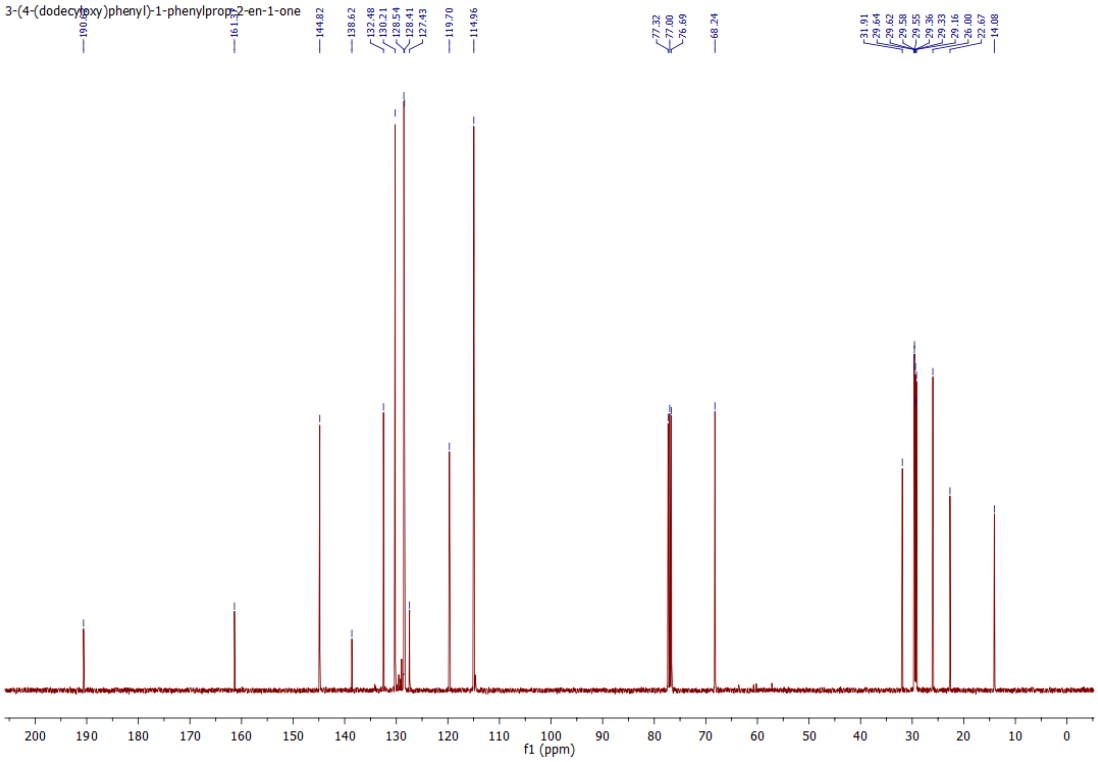


**Figure A-11** The $^{13}$C NMR spectrum of 3-(4-(dodecyloxy)phenyl)-1-phenylprop-2-en-1-one (**5**)

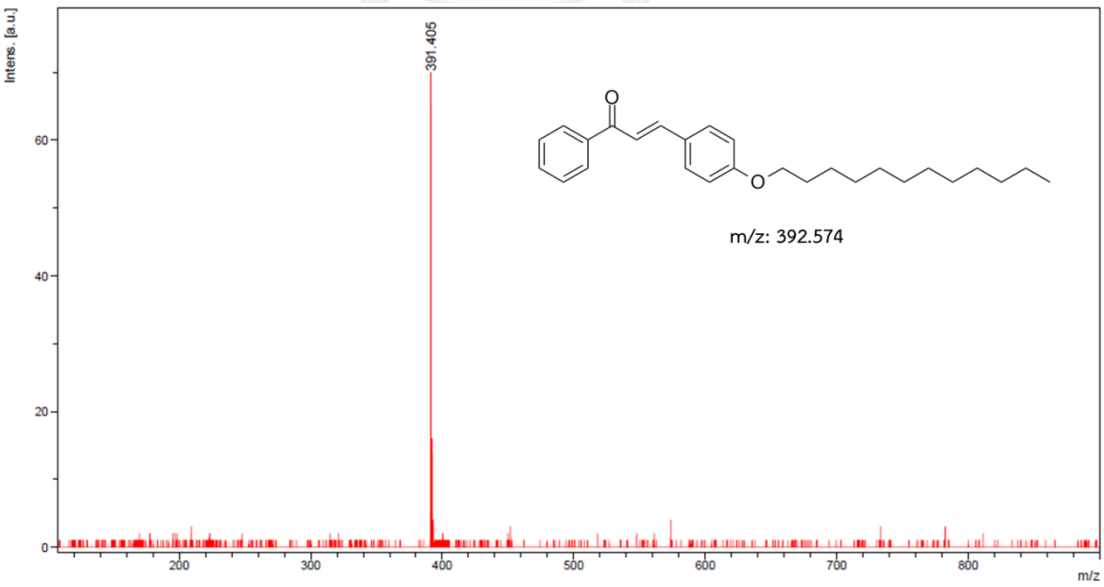


**Figure A-12** The MALDI-TOF mass spectrum of 3-(4-(dodecyloxy)phenyl)-1-phenyl prop-2-en-1-one (**5**)

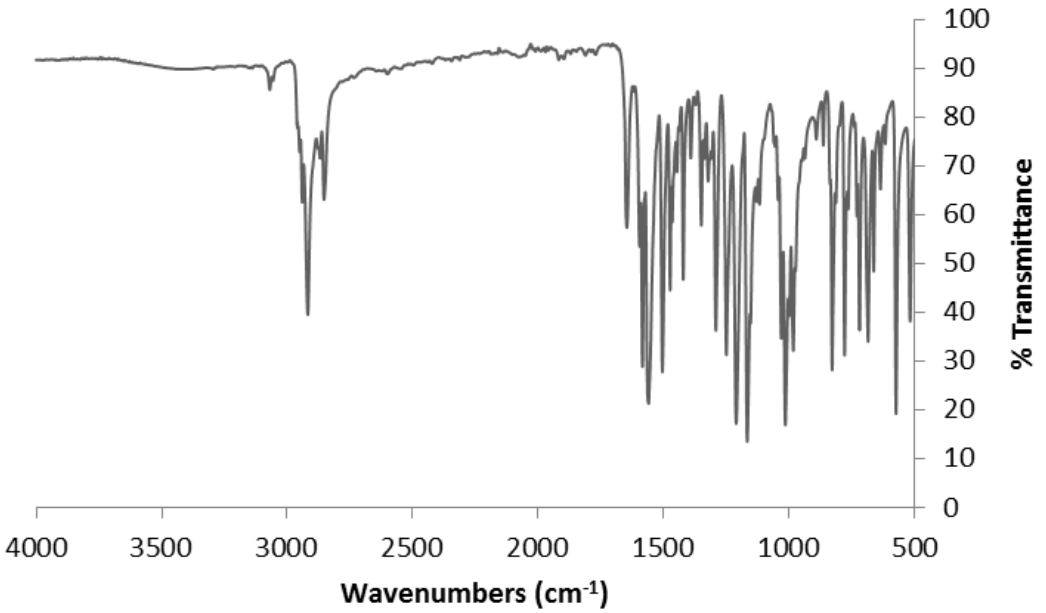


**Figure A-13** The IR spectrum of 3-(4-(dodecyloxy)phenyl)-1-phenylprop-2-en-1-one (**5**)

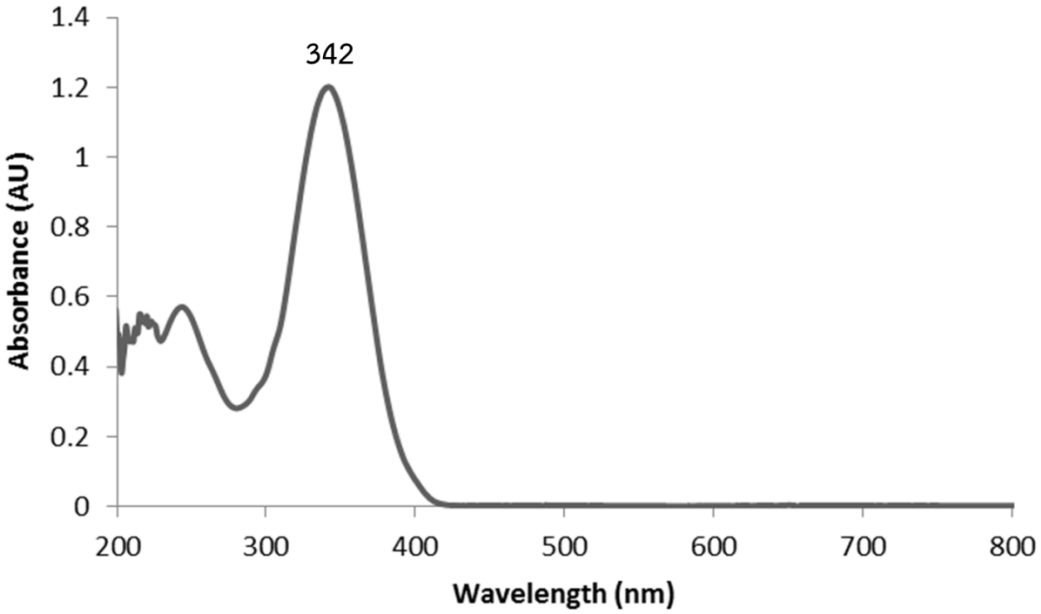


**Figure A-14** The UV-visible spectrum of 3-(4-(dodecyloxy)phenyl)-1-phenylprop-2-en-1-one (**5**)

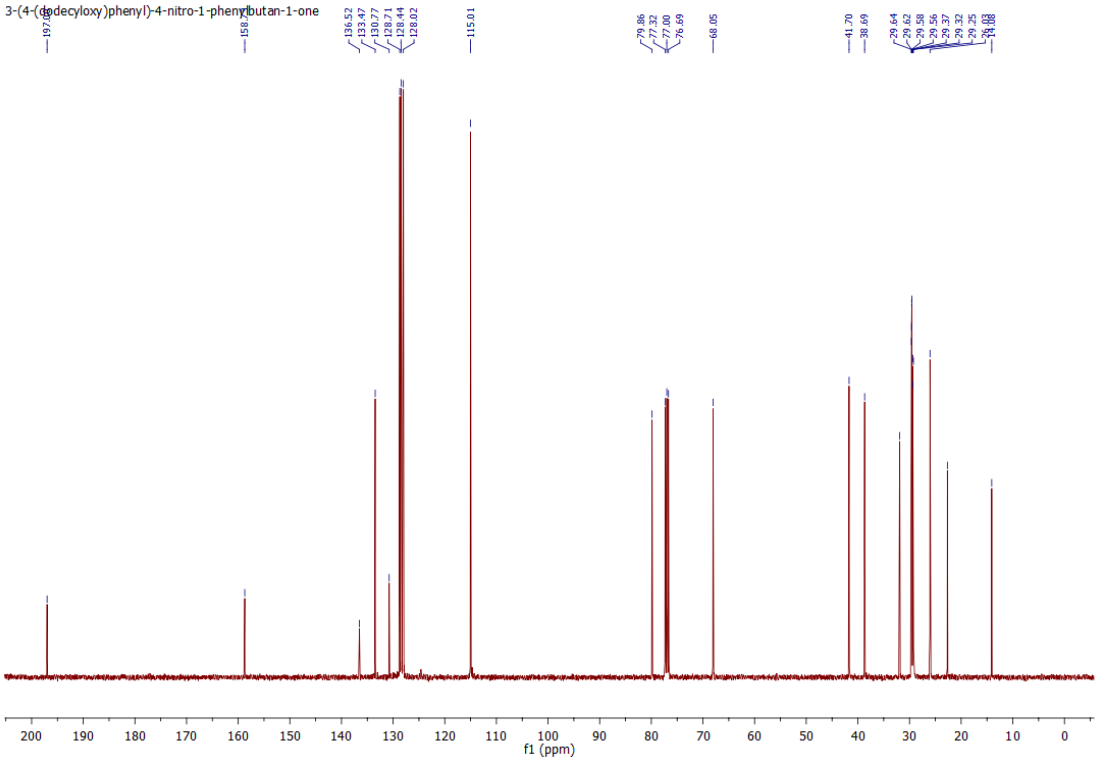


**Figure A-15** The $^{13}$C NMR spectrum of 3-(4-(dodecyloxy)phenyl)-4-nitro-1-phenyl butan-1-one (**6**)

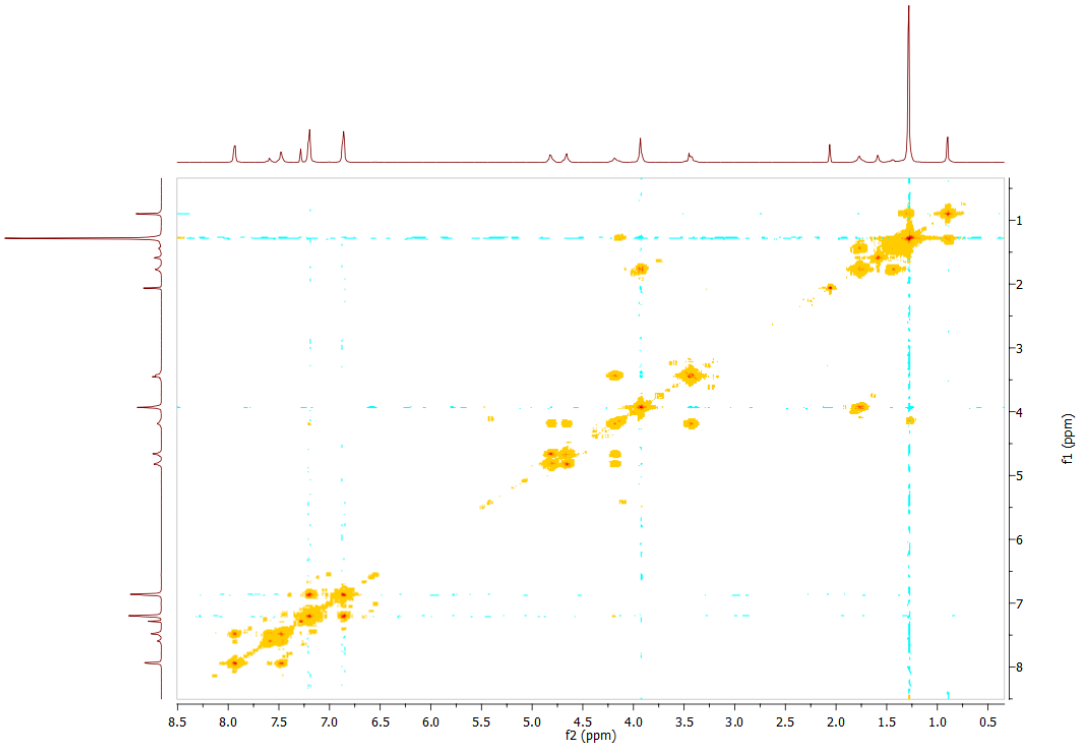


**Figure A-16** The cosy spectrum of 3-(4-(dodecyloxy)phenyl)-4-nitro-1-phenyl butan-1-one (**6**)

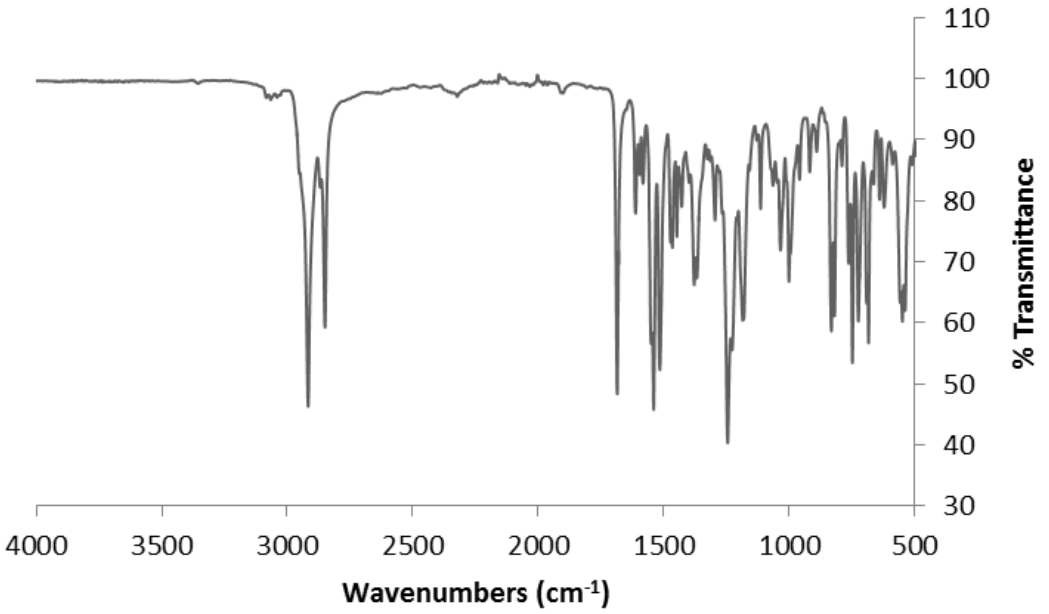


**Figure A-17** The IR spectrum of 3-(4-(dodecyloxy)phenyl)-4-nitro-1-phenyl butan-1-one (**6**)

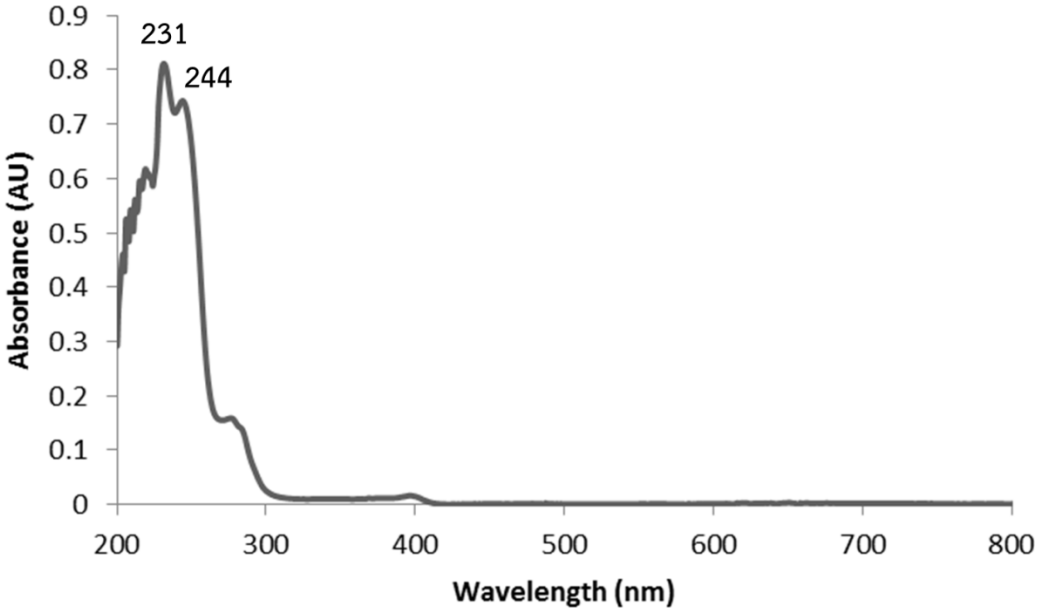


**Figure A-18** The UV-visible spectrum of 3-(4-(dodecyloxy)phenyl)-4-nitro-1-phenyl butan-1-one (**6**)

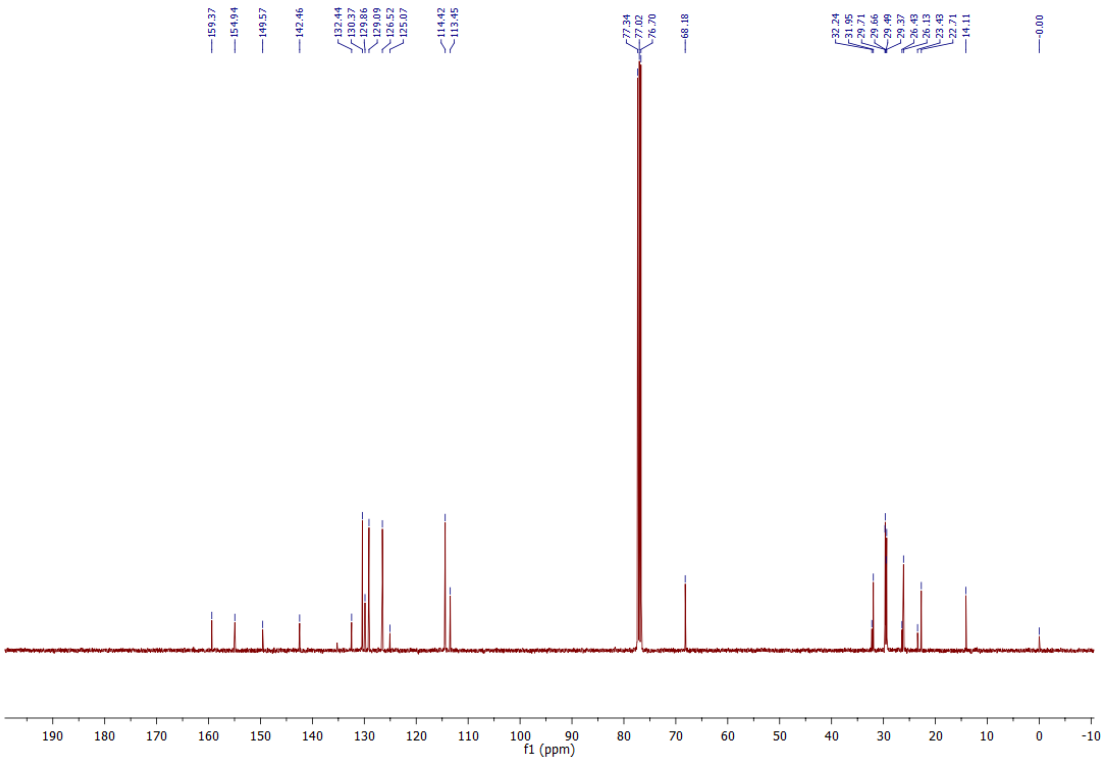


**Figure A-19** The $^{13}$C NMR spectrum of 3-(4-(dodecyloxy)phenyl)-*N*-(3-(4-(dodecyloxy) phenyl)-5-phenyl-*2H*-pyrrol-2-ylidene)-5-phenyl-*1H*-pyrrol-2-amine (**7**)

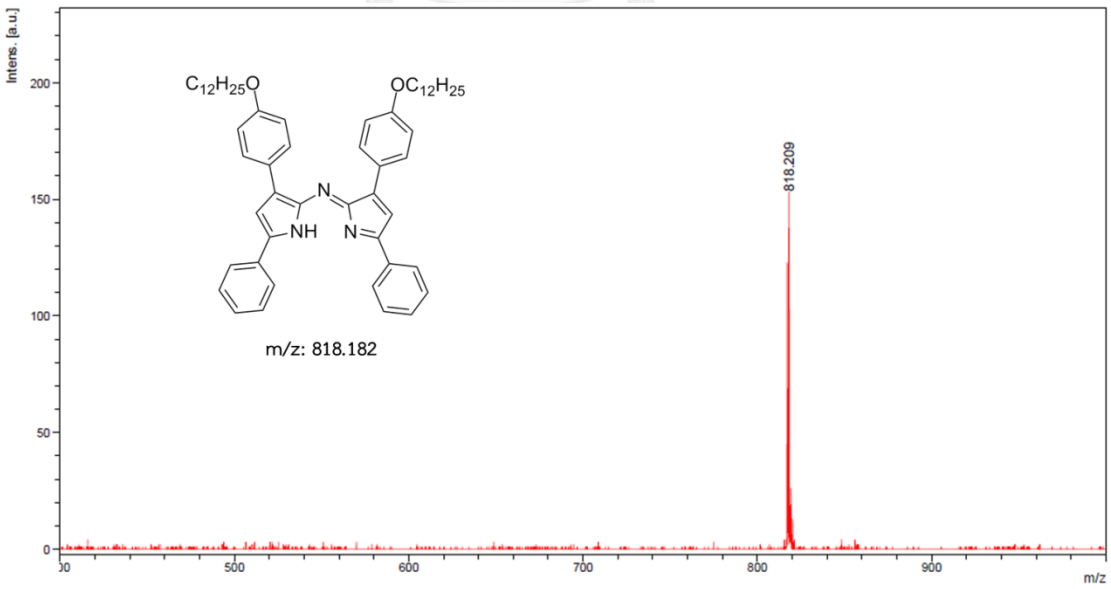


**Figure A-20** The MALDI-TOF mass spectrum of 3-(4-(dodecyloxy)phenyl)-*N*-(3-(4-(dodecyloxy)phenyl)-5-phenyl-*2H*-pyrrol-2-ylidene)-5-phenyl-*1H*-pyrrol-2-amine (**7**)

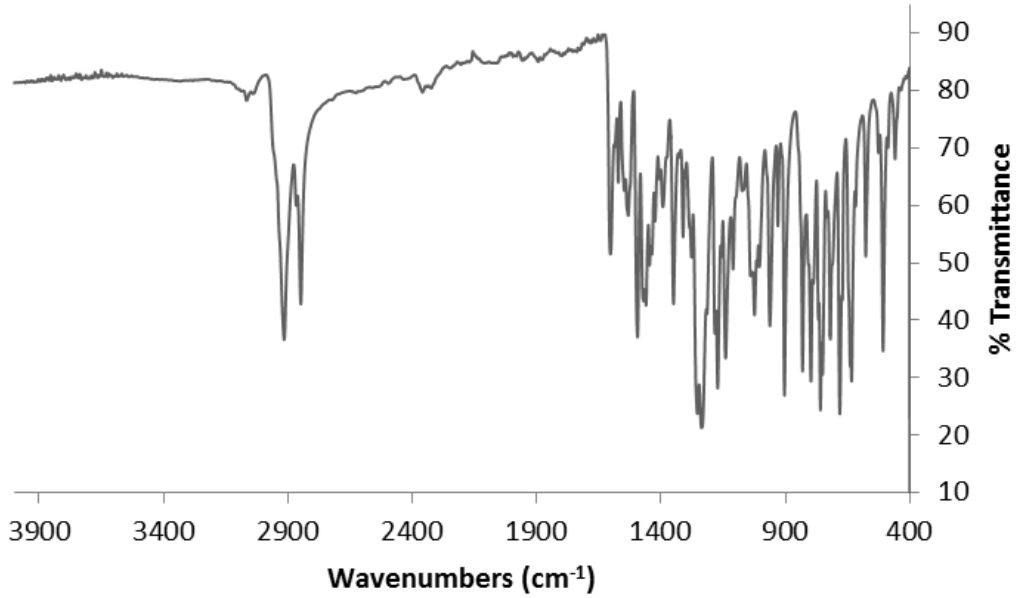


**Figure A-21** The IR spectrum of 3-(4-(dodecyloxy)phenyl)-*N*-(3-(4-(dodecyloxy) phenyl)-5-phenyl-*2H*-pyrrol-2-ylidene)-5-phenyl-*1H*-pyrrol-2-amine (**7**)

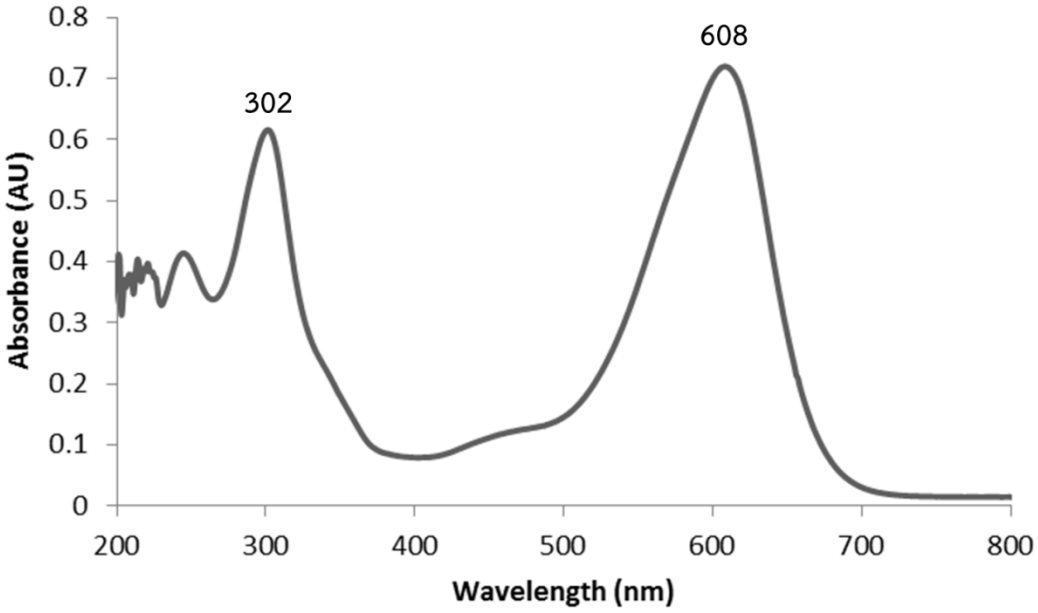


**Figure A-22** The UV-visible spectrum of 3-(4-(dodecyloxy)phenyl)-*N*-(3-(4-(dodecyl oxy)phenyl)-5-phenyl-*2H*-pyrrol-2-ylidene)-5-phenyl-*1H*-pyrrol-2-amine (**7**)

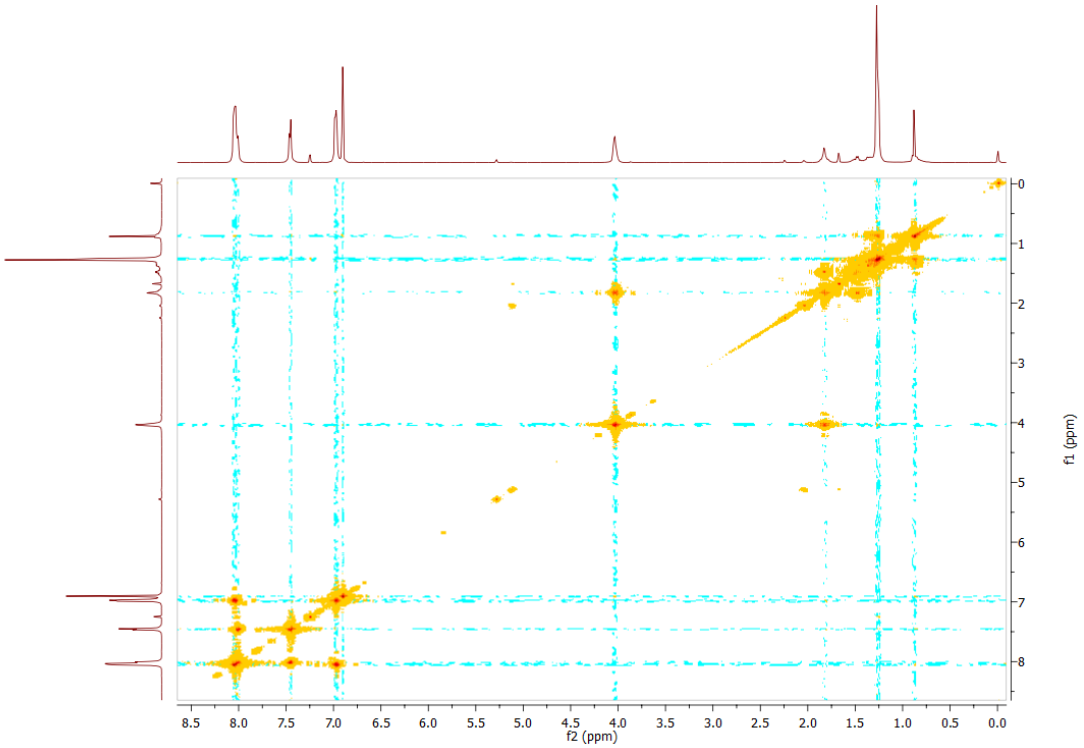


**Figure A-23** The cosy spectrum of 4,4-difluoro-1,7-bis(4-dodecyloxyphenyl)-3,5-diphenyl-4-bora-3a,4a,8-triaza-*s*-indacene (**8**)

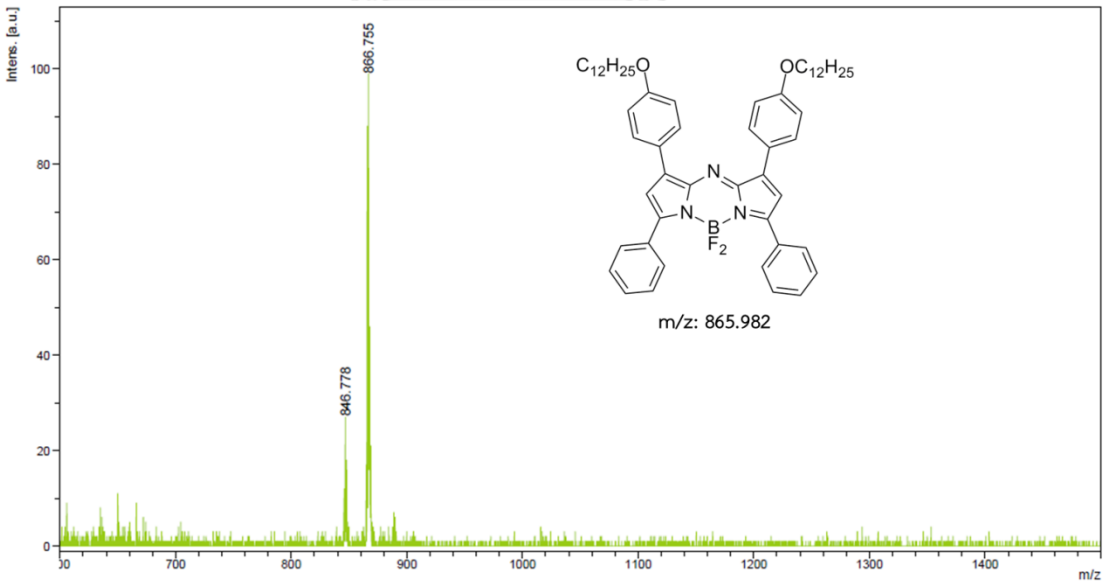


**Figure A-24** The MALDI-TOF mass spectrum of of 4,4-difluoro-1,7-bis(4-dodecyloxy phenyl)-3,5-diphenyl-4-bora-3a,4a,8-triaza-s-indacene (**8**)

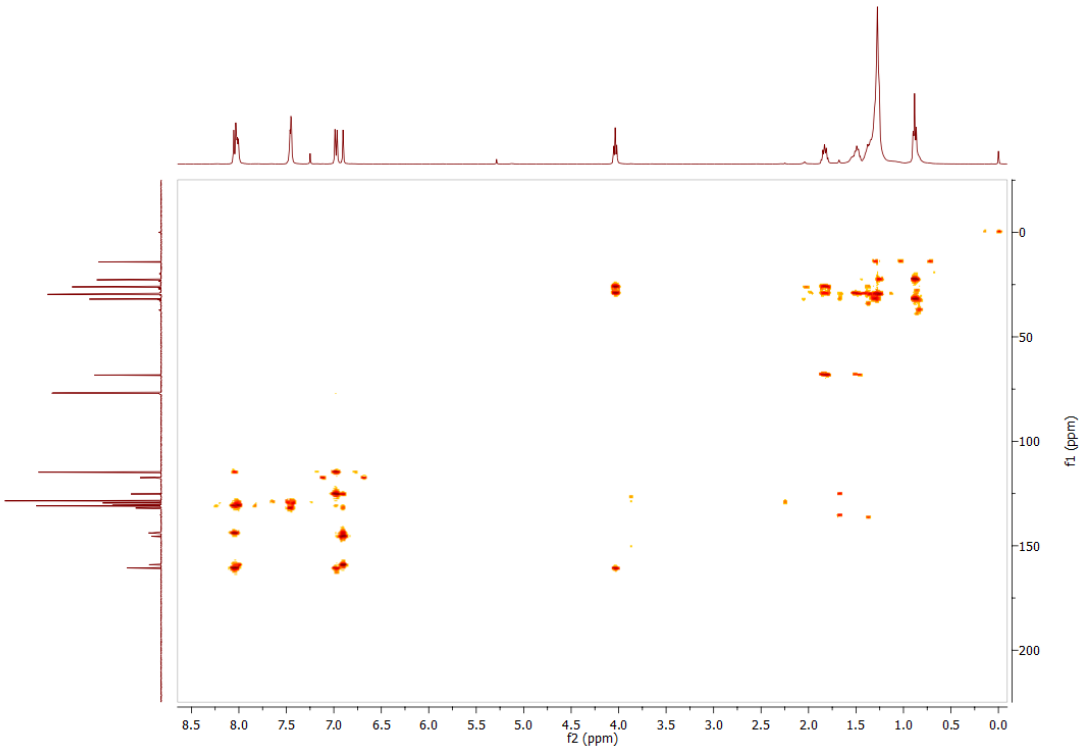


**Figure A-25** The HMBC spectrum of 4,4-difluoro-1,7-bis(4-dodecyloxyphenyl)-3,5-diphenyl-4-bora-3a,4a,8-triaza-*s*-indacene (**8**)

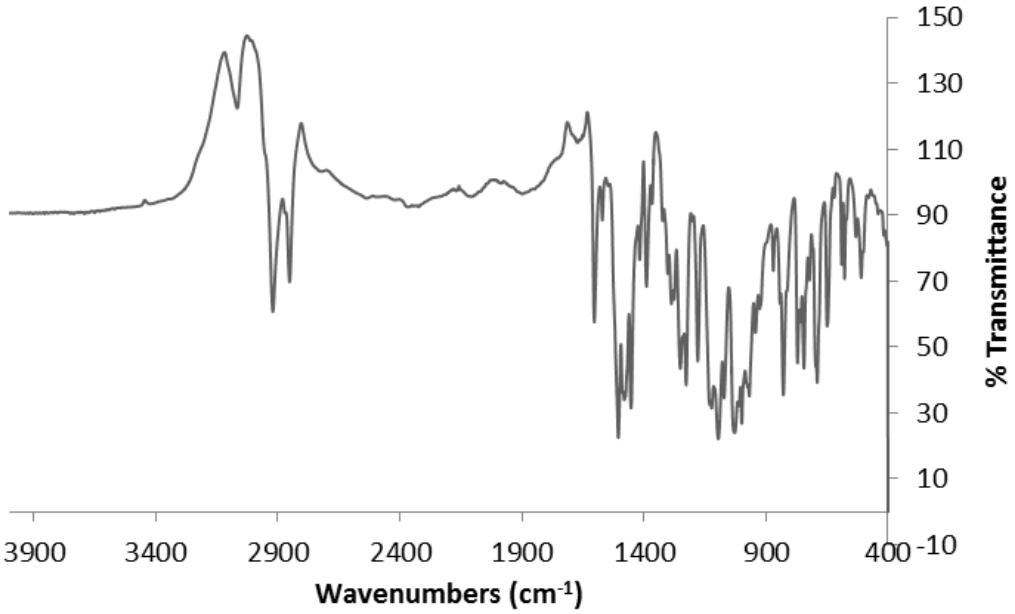


**Figure A-26** The IR spectrum of 4,4-difluoro-1,7-bis(4-dodecyloxy phenyl)-3,5-diphenyl-4-bora-3a,4a,8-triaza-*s*-indacene (**8**)

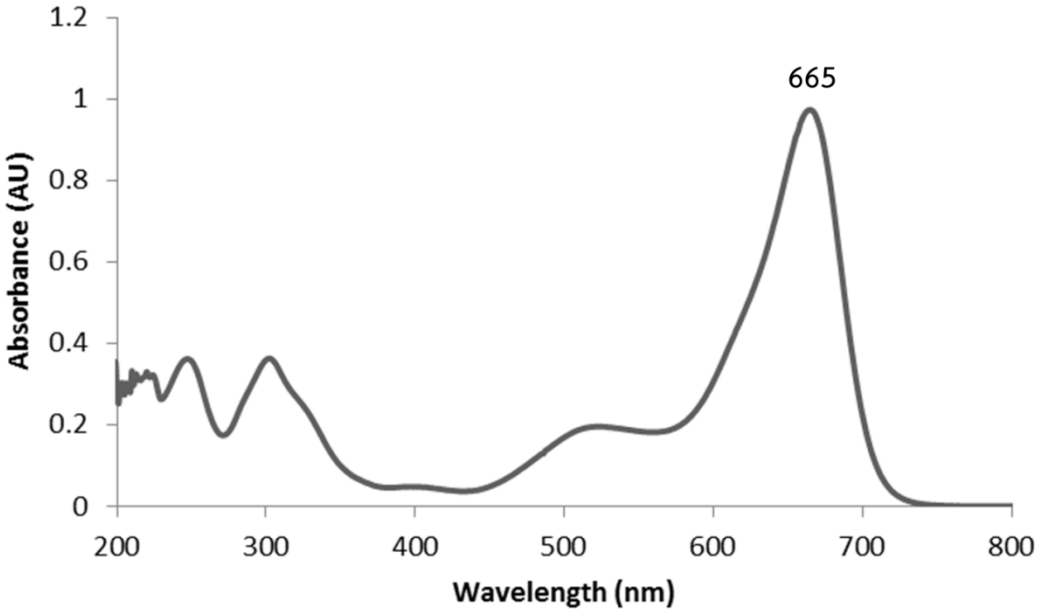


**Figure A-27** The UV-visible spectrum of 4,4-difluoro-1,7-bis(4-dodecyloxy phenyl)-3,5-diphenyl-4-bora-3a,4a,8-triaza-*s*-indacene (**8**)

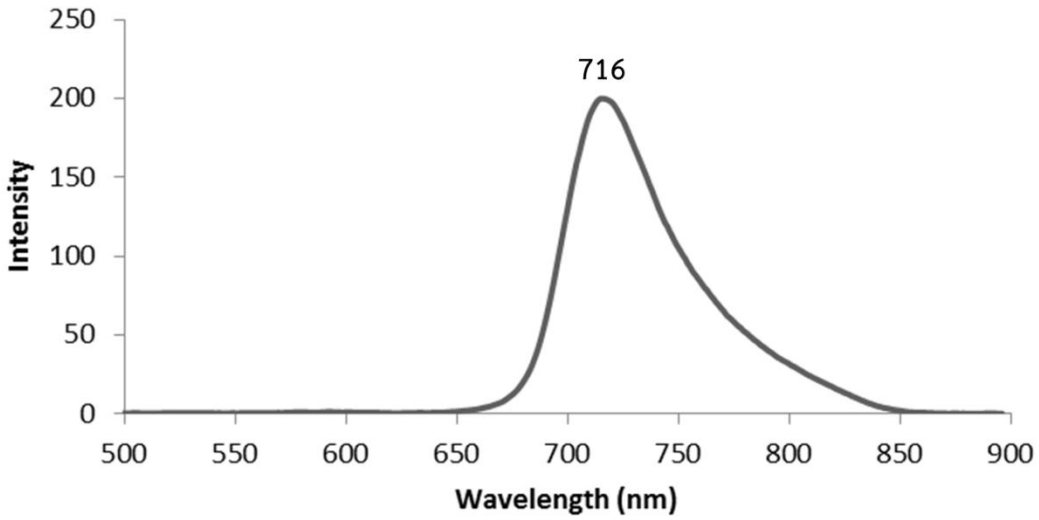


**Figure A-28** The fluorescence spectrum of 4,4-difluoro-1,7-bis(4-dodecyloxy phenyl)-3,5-diphenyl-4-bora-3a,4a,8-triaza-*s*-indacene (**8**)

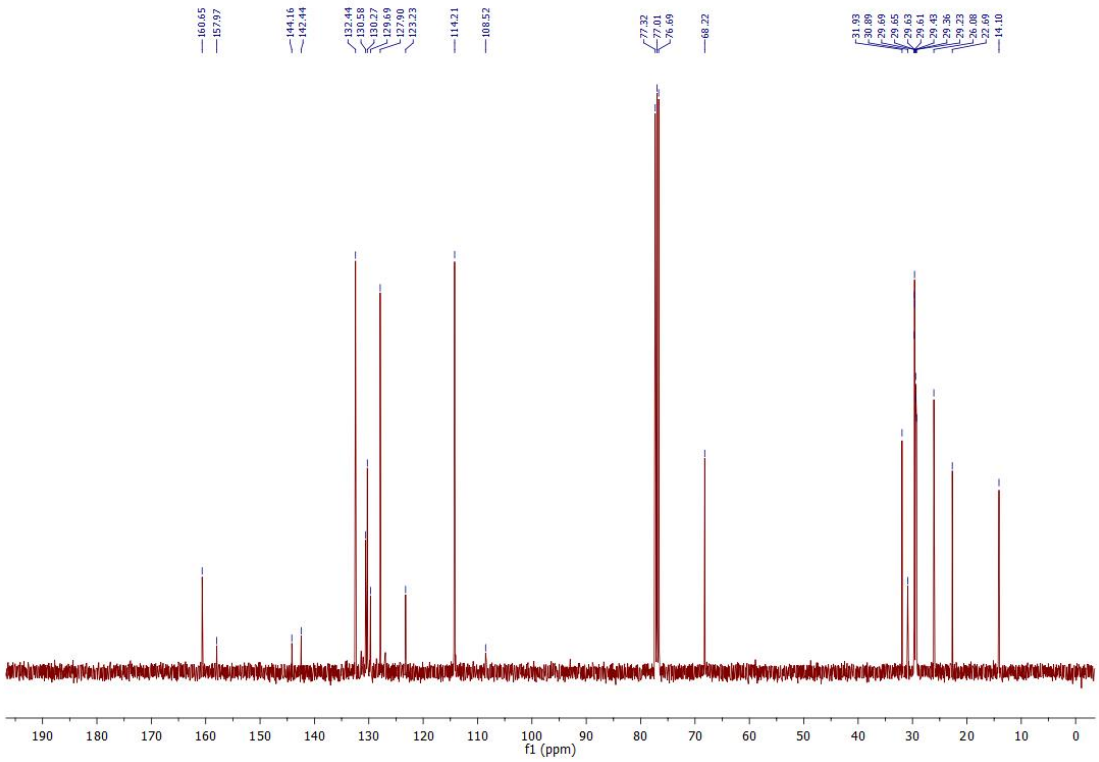


**Figure A-29** The $^{13}$C NMR spectrum of 2,6-dibromo-4,4-difluoro-1,7-bis(4-dodecyloxy phenyl)-3,5-diphenyl-4-bora-3a,4a,8-triaza-*s*-indacene (**9**)

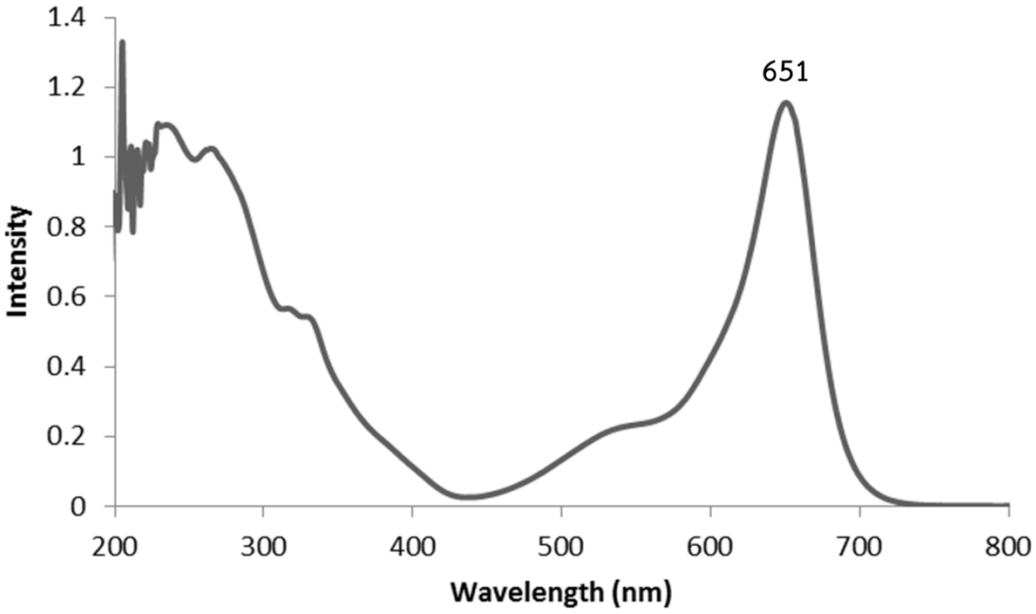


**Figure A-30** The UV-visible spectrum of 2,6-dibromo-4,4-difluoro-1,7-bis(4-dodecyl oxyphenyl)-3,5-diphenyl-4-bora-3a,4a,8-triaza-*s*-indacene (**9**)

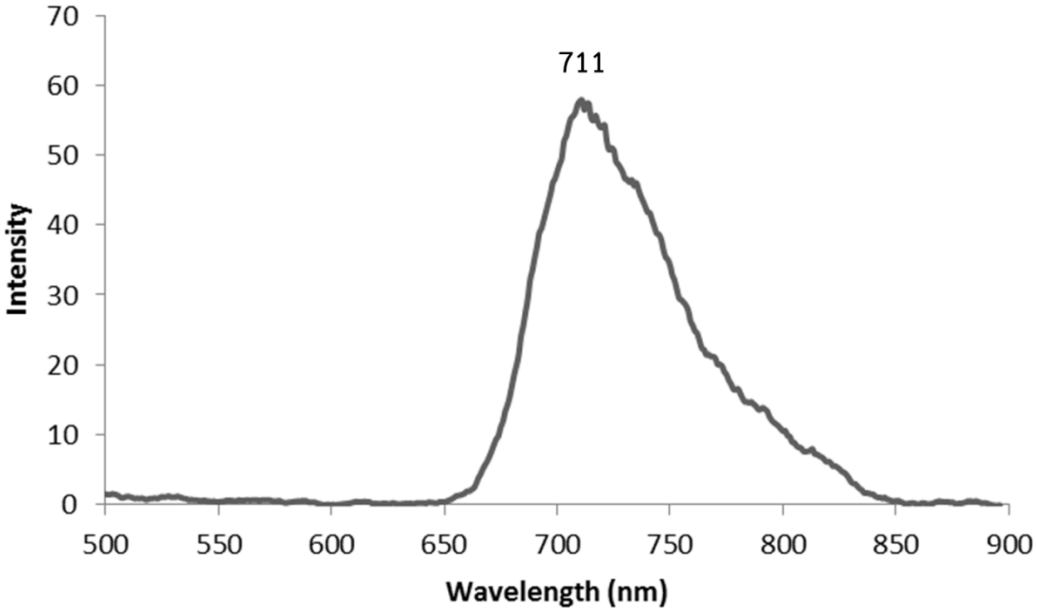


**Figure A-31** The fluorescence spectrum of 2,6-dibromo-4,4-difluoro-1,7-bis(4-dodecyloxyphenyl)-3,5-diphenyl-4-bora-3a,4a,8-triaza-*s*-indacene (**9**)

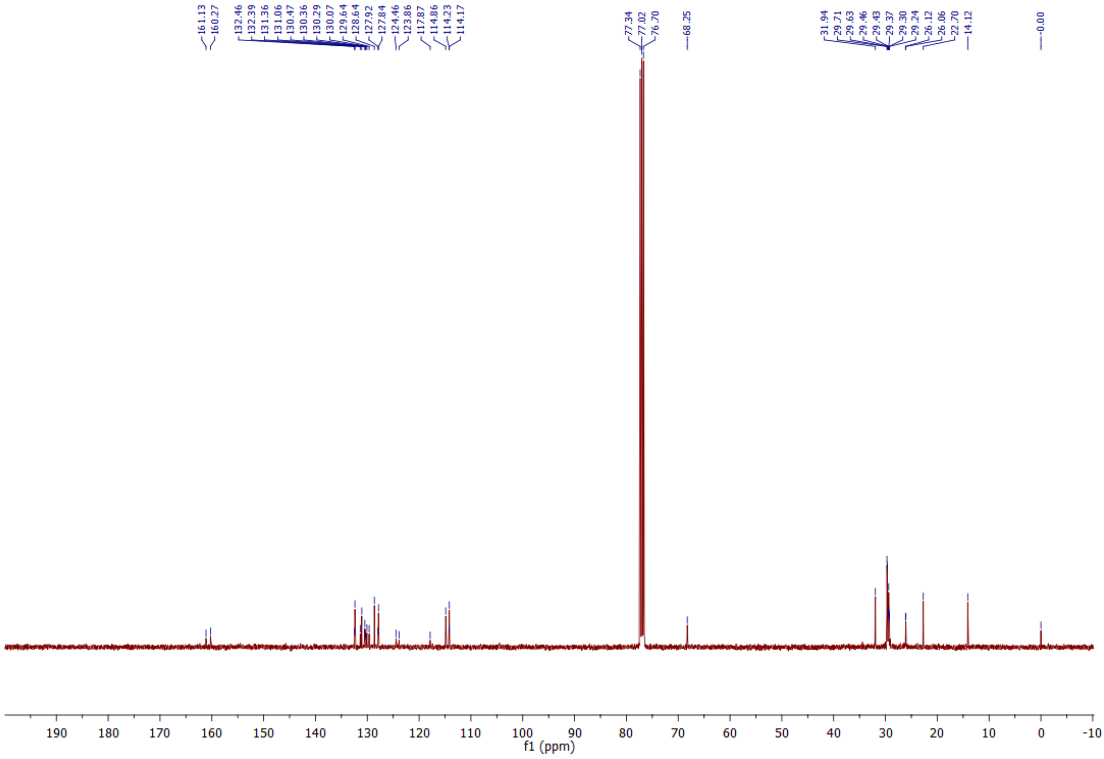


**Figure A-32** The $^{13}$C NMR spectrum of 2-bromo-4,4-difluoro-1,7-bis(4-dodecyloxy phenyl)-3,5-diphenyl-4-bora-3a,4a,8-triaza-*s*-indacene (**10**)

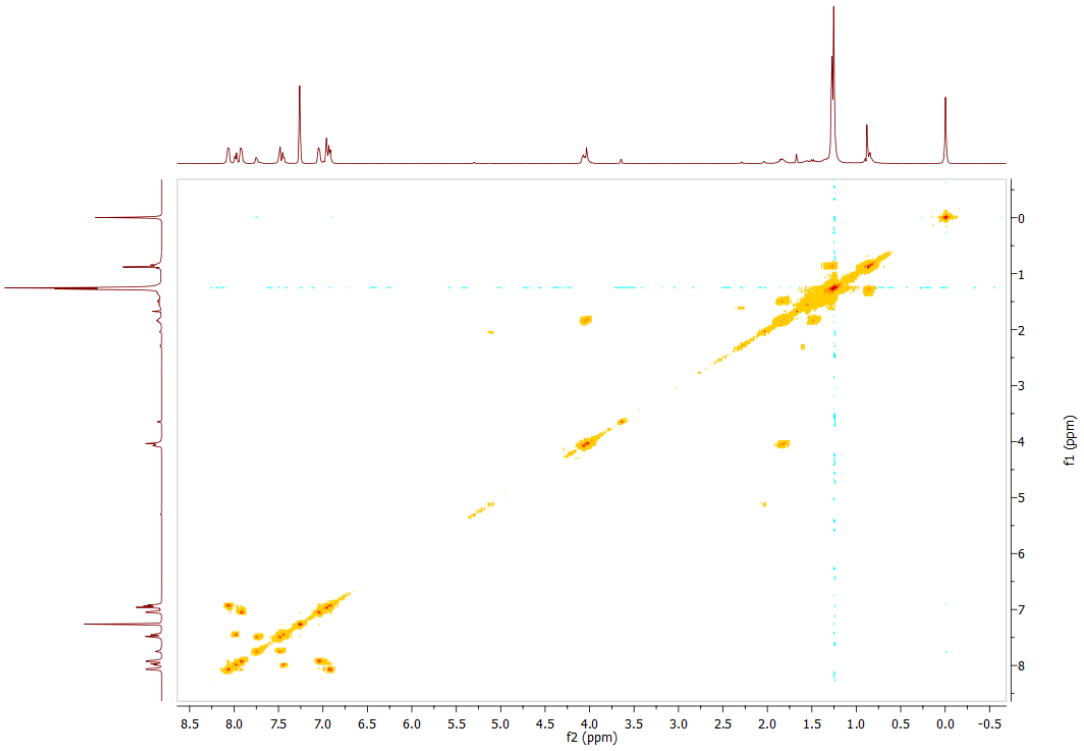


**Figure A-33** The cosy spectrum of 2-bromo-4,4-difluoro-1,7-bis(4-dodecyloxy phenyl)-3,5-diphenyl-4-bora-3a,4a,8-triaza-*s*-indacene (**10**)

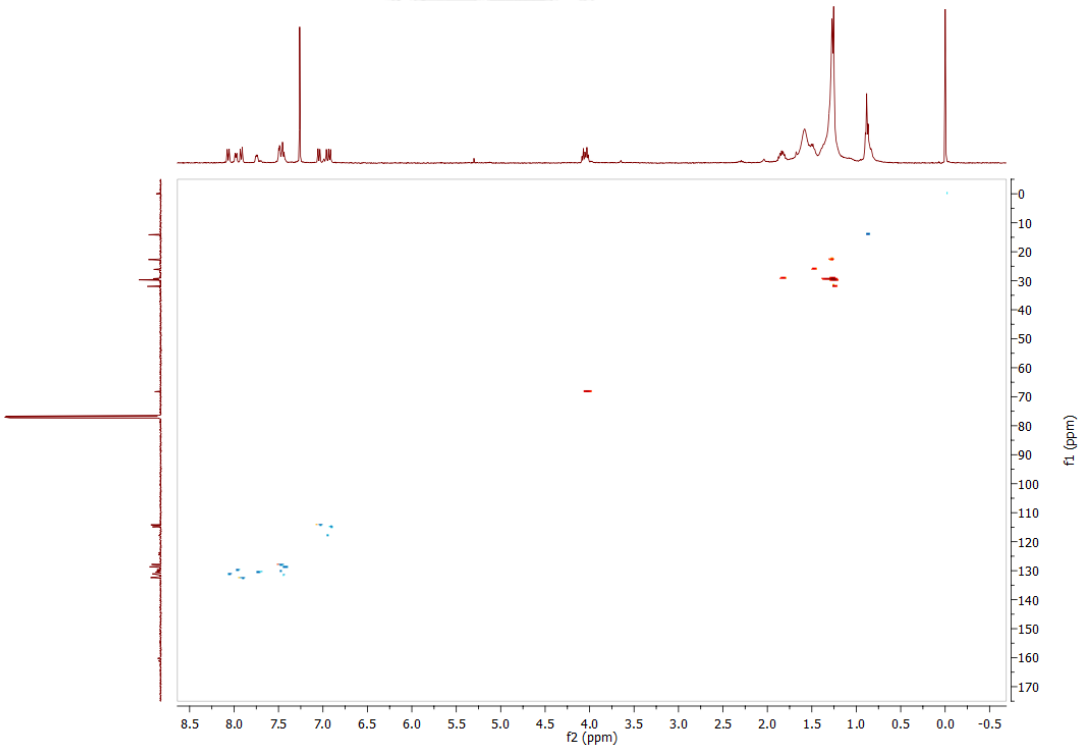


**Figure A-34** The hsqc spectrum of 2-bromo-4,4-difluoro-1,7-bis(4-dodecyloxy phenyl)-3,5-diphenyl-4-bora-3a,4a,8-triaza-*s*-indacene (**10**)

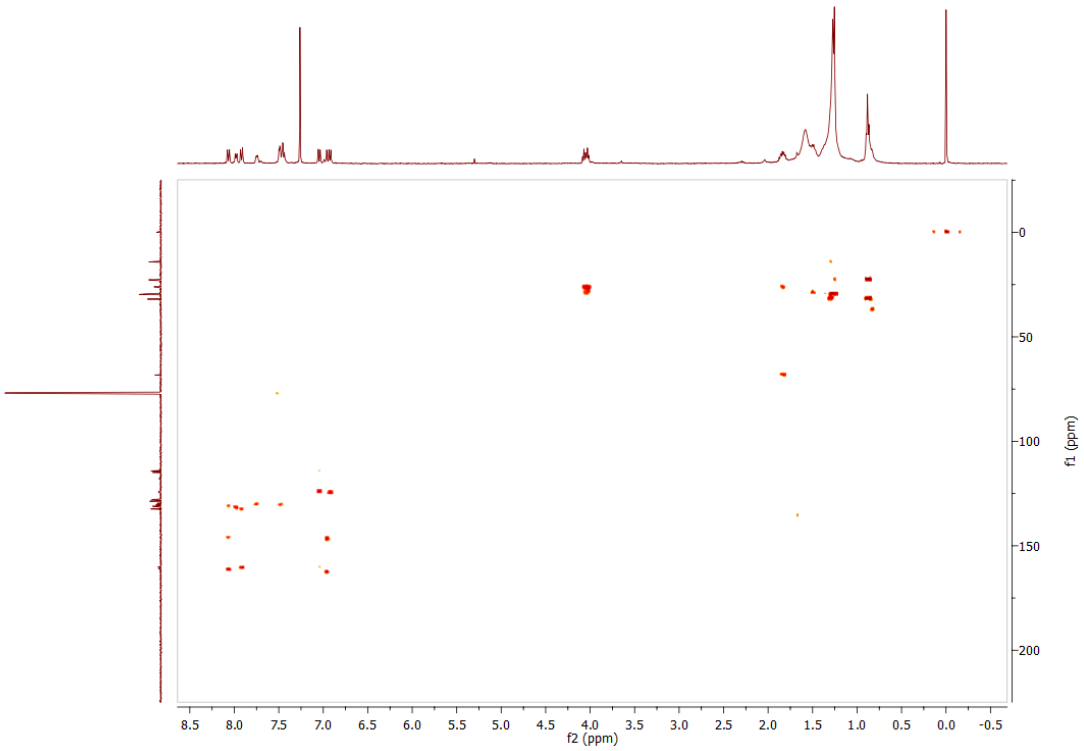


**Figure A-35** The HMBC spectrum of 2-bromo-4,4-difluoro-1,7-bis(4-dodecyloxy phenyl)-3,5-diphenyl-4-bora-3a,4a,8-triaza-*s*-indacene (**10**)

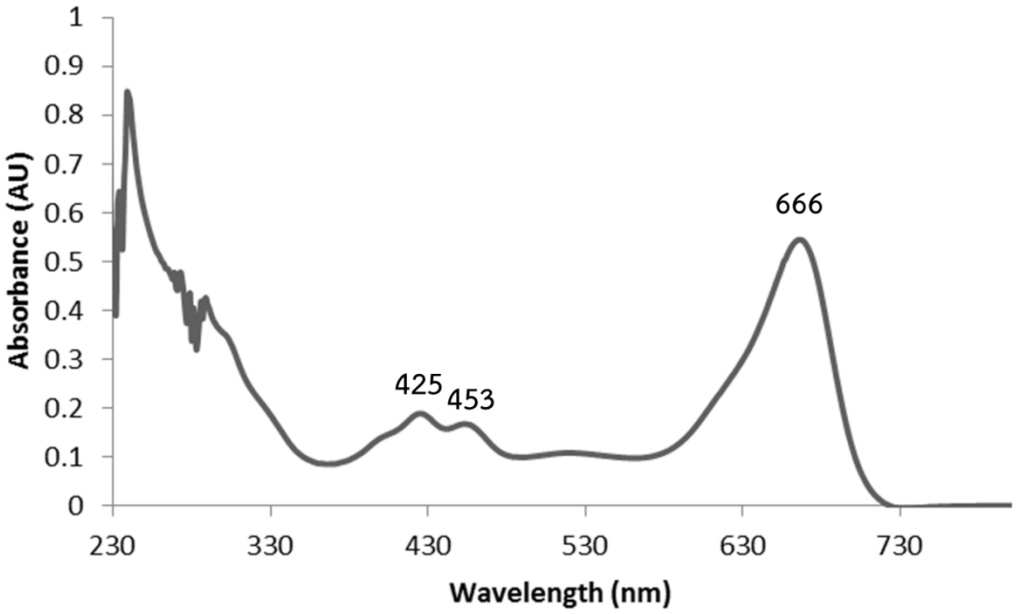


**Figure A-36** The UV-visible spectrum of aza-BODIPY-porphyrin (**11**)

# VITA

Miss Jariya Kayee was born on February 26th, 1991 in Chanthaburi, Thailand. She graduated a Bachelor Degree of Science, majoring in Chemistry from Faculty of Science, Srinakharinwirot University in 2012. Since 2013, she has been a graduate student studying Organic Chemistry as her major course at Department of Chemistry, Faculty of Science, Chulalongkorn University. During her studies towards the Bachelor degree and Master's degree, she was supported by Science Achievement Scholarship of Thailand (SAST).

Her present address is 55/80-81 Village No.5, Phlapphla Sub-district, Muang District, Chanthaburi, Thailand 22000.